

The ER-SURF pathway uses ER-mitochondria contact sites for protein targeting to mitochondria

vom Fachbereich Biologie

der Rheinland-Pfälzischen Technischen Universität Kaiserslautern-Landau

zur Verleihung des akademischen Grades Dr. rer. nat. genehmigte

Dissertation
von

Christian Koch, M.Sc., geb. in Neustadt/Weinstraße

Mündliche Prüfung: 06.12.2023

Dekan:

Prof. Dr. Stefan Kins

Promotionskommissionsvorsitzender:

Prof. Dr. Timo Mühlhaus

Berichterstattende:

Prof. Dr. Johannes M. Herrmann

Prof. Dr. Jan Pielage

EIDESSTATTLICHE ERKLÄRUNG

Hiermit erkläre ich, dass die vorliegende Arbeit ohne unzulässige Hilfe Dritter und ohne Benutzung anderer als der angegebenen Hilfsmittel von mir persönlich angefertigt wurde. Die aus anderen Quellen übernommenen Daten und Konzepte sind unter Angabe der Quelle gekennzeichnet.

Ich habe nicht die entgeltliche Hilfe von Vermittlungs- beziehungsweise Beratungsdiensten in Anspruch genommen. Niemand hat von mir unmittelbar oder mittelbar geldwerte Leistungen für Arbeiten erhalten, die im Zusammenhang mit dem Inhalt der vorgelegten Dissertation stehen.

Die Arbeit wurde bisher weder im In- noch im Ausland in gleicher oder ähnlicher Form einer anderen Prüfungsbehörde vorgelegt.

Die Bestimmungen der Promotionsordnung des Fachbereichs Biologie der Universität Kaiserslautern sind mir bekannt. Insbesondere weiß ich, dass ich vor Vollzug der Promotion zur Führung des Dokortitels nicht berechtigt bin.

Christian Koch

Kaiserslautern, den 02.10.2023

DARLEGUNG DES EIGENANTEILS

Das in Abb.16 A gezeigte Experiment wurde von Anna-Lena Ecker, AG Zellbiologie, RPTU Kaiserslautern, im Rahmen ihrer Bachelorarbeit durchgeführt.

Die Messung aller Massenspektrometrischer Daten (Abb.19-22, 24+25) wurde von Markus Räsche, Center for MS Analytics, RPTU Kaiserslautern, durchgeführt. Die Probenvorbereitung als auch alle statistischen Auswertungen bezüglich dieser Experimente wurden von mir durchgeführt.

Die in Abb.22 A gezeigten elektronenmikroskopischen Aufnahmen wurden von Cristina Prescianotto-Baschong, im Labor von Prof. Dr. Anne Spang, Biozentrum, Universität Basel, durchgeführt.

Die vorliegende Einschätzung über die erbrachte Leistung von Dritten wurde mit den genannten Personen einvernehmlich abgestimmt.

Christian Koch

Prof. Dr. Johannes M. Herrmann

Kaiserslautern, den 02.10.2023

DARLEGUNG ALLER BENUTZTEN HILFSMITTEL UND HILFESTELLUNGEN

Zur Erstellung dieser Arbeit wurde das Microsoft Office 365 Softwarepaket (Word und Excel) genutzt. Das Literaturverzeichnis und Literaturverweise wurden mittels Citavi erstellt. Alle statistischen Analysen erfolgten mittels Microsoft Excel oder R Studio. Alle gezeigten Abbildungen wurden mithilfe der Corel Technical Suite 2020 erstellt. Mikroskopische Aufnahmen wurden mit den Softwarepaketen Fiji und Leica LasX analysiert. Zur Quantifizierung aller Western Blot Experimente wurde die Software ImageQuant genutzt.

Christian Koch

Kaiserslautern, den 02.10.2023

LIST OF PUBLICATIONS

- 2023 Bertgen L., Bökenkamp J., Schneckmann T., **Koch C.**, Räschle M., Storchova Z., Herrmann J.M., Distinct types of intramitochondrial protein aggregates protect mitochondria against proteotoxic stress, *Cell Rep.*, in revision
- 2023 **Koch C.**, Räschle M., Prescianotto-Baschong C., Spang A., Herrmann J.M., The ER-SURF pathway uses ER-mitochondria contact sites for protein targeting to mitochondria, *EMBO Rep.*, in revision
- 2023 Schilling S., Pradhan A., Heesch A., Helbig A., Blennow K., **Koch C.**, Bertgen L., Koo E.H., Brinkmalm G., Zetterberg H., Kins S., Eggert S., Differential effects of familial Alzheimer's disease-causing mutations on amyloid precursor protein (APP) trafficking, proteolytic conversion, and synaptogenic activity, *Acta Neuropathol Commun.*, doi: 10.1186/s40478-023-01577-y.
- 2023 Simakin P*., **Koch C***., Herrmann J.M., A modular cloning (MoClo) toolkit for reliable intracellular protein targeting in the yeast *Saccharomyces cerevisiae*, *Microb Cell.*, doi: 10.15698/mic2023.04.794.
- 2021 **Koch C.**, Schuldiner M., Herrmann J.M., ER-SURF: Riding the Endoplasmic Reticulum Surface to Mitochondria, *Int J Mol Sci.*, doi: 10.3390/ijms22179655.

TABLE OF CONTENTS

Eidesstattliche Erklärung.....	I
Darlegung des Eigenanteils.....	III
Darlegung aller benutzten Hilfsmittel und Hilfestellungen.....	IV
List of Publications.....	V
Table of Contents.....	VII
Summary.....	X
Zusammenfassung.....	XI
1. Introduction.....	1
1.1 ER-mitochondria contact sites.....	1
1.2 Protein targeting.....	3
1.3 The role of chaperones in protein sorting.....	5
1.4 Mitochondrial protein import.....	6
1.5 Protein quality control at the ER and mitochondria.....	7
2. Aim.....	10
3. Results.....	11
3.1 The ERMES contact site is required for the biogenesis of Oxa1.....	11
3.2 Djpl and ERMES act as parallel pathways in the targeting of membrane proteins.....	12
3.3 Proximity between ER and mitochondria is not sufficient for proper ER-SURF targeting.....	15
3.4 Deletion of <i>MDM34</i> is concomitant with suppressor mutations.....	15
3.5 CRISPR interference (CRISPRi) efficiently depletes <i>MDM34</i>	17
3.6 Anhydrotetracycline does not affect mitochondrial translation.....	21
3.7 Knockdown of ERMES affects mitochondrial morphology and function.....	22
3.8 ERMES and Tom70 constitute parallel ER-SURF routes.....	24
3.9 Loss of ER-mitochondria contact sites leads to enrichment of ER in purified mitochondrial fractions.....	27

3.10 Identifying a core set of ER-SURF clients using affinity purification of ER and mitochondria.....	30
3.11 Hydrophobic transmembrane segments determine the contact site dependence of mitochondrial proteins.....	36
4. Discussion	41
4.1 CRISPRi as an effective tool to interrogate the role of MCSs in protein biogenesis.....	41
4.2 ER-SURF is dependent on the presence of ER-mitochondria contact sites.....	42
4.3 Protein trafficking via ER-SURF is independent of lipid transfer at MCSs	45
4.4 The ER as a productive partner in mitochondrial protein biogenesis.....	46
5. Outlook.....	48
6. Materials and Methods	50
6.1 Genetic Methods.....	50
6.1.1 <i>E. coli</i> strains.....	50
6.1.2 Transformation of chemo-competent <i>E. coli</i> cells.....	50
6.1.3 <i>S. cerevisiae</i> strains, plasmids and primers.....	50
6.1.4 <i>S. cerevisiae</i> transformation.....	54
6.2 Molecular Biology Methods.....	54
6.2.1 Isolation of plasmid DNA from <i>E. coli</i>	54
6.2.2 Determination of DNA concentration.....	54
6.2.3 Polymerase Chain Reaction	54
6.2.4 Restriction digest of DNA	57
6.2.5 Ligation of DNA fragments	57
6.2.6 Agarose gel electrophoresis	57
6.2.7 Analysis of mRNA levels by qRT-PCR	58
6.3 Cell Biology Methods.....	58
6.3.1 <i>E. coli</i> – cultivation media	58
6.3.2 <i>S. cerevisiae</i> – cultivation media.....	58
6.3.3. Dropout-Mix	59

6.3.4 Growth Assays	60
6.3.5 YFP reporter assay	60
6.3.6 Isolation of mitochondria	60
6.3.7 Preparation of semi-intact cells.....	61
6.3.8 Fluorescence microscopy	61
6.3.9 Electron microscopy and immuno-electron microscopy	62
6.4 Protein Biochemistry Methods	62
6.4.1 Whole cell lysates	62
6.4.2 SDS-polyacrylamide gel electrophoresis (SDS-PAGE)	62
6.4.3 Transfer of proteins to a nitrocellulose membrane (Western Blot)	63
6.4.4 Protein import into mitochondria.....	64
6.4.5 Import into semi-intact cells	64
6.4.6 Radioactive <i>in vivo</i> labelling of mitochondrial translation products	64
6.4.7 TCA precipitation of proteins	65
6.4.8 Autoradiography	65
6.4.9 Sample preparation and mass-spectrometric identification of proteins.....	65
6.4.10 Analysis of mass spectrometry data.....	68
6.5 Immunology Methods.....	69
6.5.1 Immune decoration of cellulose membranes	69
6.5.2 Antibodies	70
References	71
Abbreviations	87
Acknowledgments.....	91
Curriculum Vitae.....	95

SUMMARY

The vast majority of all mitochondrial proteins are synthesized in the cytosol. These proteins carry characteristic targeting motifs within their sequence, which allows for the binding of chaperones, that in turn usher precursors to the mitochondrial surface for import and assembly. Though, our understanding of these early reactions is still lacking, recent efforts have shown that the ER surface can facilitate the import of mitochondrial proteins (ER-SURF) with the help of the J-protein Djpl. Close cooperation of organelles in form of membrane contact sites is crucial for cellular function. The aim of my work was to investigate whether ER-mitochondria contact sites are critical for the transfer of proteins from the ER to mitochondria.

Several contact sites have been characterized between ER and mitochondria in *S. cerevisiae*. One contact site is called the ER mitochondria encounter structure (ERMES) and another is partly formed by Tom70. Owing to the high propensity of suppressor mutations in ERMES, I employed a knockdown approach to deplete this contact site. Using an inducible CRISPR interference (CRISPRi) system, I could rapidly and efficiently deplete Mdm34, which is a part of ERMES. I could show that depletion of Mdm34 had a synthetic negative effect in combination with a deletion of *TOM70*. Loss of both contact sites led to a strong decrease of many mitochondrial proteins in the whole cell proteome. Using affinity purification of ER and mitochondria in conjunction with mass spectrometry I could demonstrate that a specific set of mitochondrial proteins are enriched on the ER upon loss of Mdm34 and Tom70, which mainly were proteins of the inner membrane e.g., Oxa1 and Cox5A. Moreover, I was able to validate that the import of these proteins was hampered upon loss of both contact sites. Also, *in vivo* the biogenesis of Oxa1 was impeded upon single loss of Mdm34 or Tom70 and strongly impaired if both were lost. Analysis of the maximum hydrophobicity of inner membrane proteins in the ER-SURF set revealed on average a significantly higher peak compared to other inner membrane proteins. I could show that deleting or swapping the transmembrane domain of Cox5A would make it contact site independent or reliant on contact sites respectively, as revealed by an *in vitro* import assay.

In this study I was able to demonstrate the involvement of membrane contact sites in ER-SURF and identify a list of putative clients. Furthermore, I could show that hydrophobicity of the transmembrane segment of inner membrane proteins is one determinant for ER-SURF dependence.

ZUSAMMENFASSUNG

Fast alle mitochondrialen Proteine werden im Zytosol synthetisiert. Diese tragen Zielsequenzen, die mittels Chaperonen, den Transport an die mitochondriale Oberfläche erlauben. Obwohl unser Verständnis dieser frühen Reaktionen noch rudimentär ist, haben jüngste Bemühungen gezeigt, dass die ER-Oberfläche den Import mitochondrialer Proteine mit Hilfe des J-Proteins Djpl ermöglichen kann (ER-SURF). Die Koordination von Organellen in Form von Membrankontaktstellen ist entscheidend für die zelluläre Funktion. Ziel meiner Arbeit war es, zu untersuchen, ob ER-Mitochondrien-Kontaktstellen für den Transfer von Proteinen von der ER-Oberfläche an die Mitochondrien entscheidend sind.

In *S. cerevisiae* gibt es zwei gut charakterisierte Kontaktstellen zwischen ER und Mitochondrien. Eine Kontaktstelle wird als “*ER mitochondria encounter structure*” (ERMES) bezeichnet, die zweite wird teilweise von Tom70 gebildet. Mittels eines induzierbaren Systems, welches die Transkription herunterreguliert (CRISPRi), konnte ich den Verlust von Mdm34, eine Untereinheit von ERMES, und Tom70 gleichzeitig untersuchen. Der Verlust beider Kontaktstellen führte zu einer starken Abnahme vieler mitochondrialer Proteine im Ganzzellproteom. Durch Affinitätsreinigung von ER und Mitochondrien in Verbindung mit Massenspektrometrie konnte ich zeigen, dass eine bestimmte Gruppe mitochondrialer Proteine nach dem Verlust von Mdm34 und Tom70 auf dem ER angereichert wird. Dabei handelte es sich hauptsächlich um Proteine der inneren Membran, z. B. Oxa1 und Cox5A. Darüber hinaus konnte ich nachweisen, dass der Import dieser Proteine durch den Verlust der beiden Kontaktstellen behindert wird. Die Biogenese von Oxa1 wurde durch den alleinigen Verlust von Mdm34 oder Tom70 behindert und stark beeinträchtigt, in Abwesenheit beider. Die Analyse der maximalen Hydrophobizität von Innenmembranproteinen im ER-SURF-Set ergab im Durchschnitt einen deutlich höheren Peak im Vergleich zu anderen Innenmembranproteinen. Ich konnte durch Deletion oder Austausch der Transmembrandomäne von Cox5A die Abhängigkeit des Imports von Kontaktstellen demonstrieren.

In dieser Studie konnte ich die Beteiligung von Membrankontaktstellen an ER-SURF nachweisen und eine Gruppe möglicher Klienten identifizieren. Darüber hinaus konnte ich zeigen, dass die Hydrophobizität eines Transmembransegments von Innenmembranproteinen ein entscheidender Faktor für die ER-SURF-Abhängigkeit ist.

1. INTRODUCTION

One of the hallmarks of a eukaryotic cell is the compartmentalization of biochemical and functional pathways into organelles. DNA replication and transcription, translation, protein sorting and secretion or power generation were separated into the nucleus, cytosol, ER and mitochondria respectively. The ER, as the professional protein folding and delivery organelle, handles roughly one third of the cellular proteome and is a central hub of intracellular communication [1–3]. Whereas mitochondria, a double membrane-bounded organelle, requires roughly 1000 proteins to fulfill its many biosynthetic functions, including, producing the majority of the cellular energy pool in form of ATP [4,5]. The individual biology of ER and mitochondria, as well as their interplay, has been studied extensively using the model *Saccharomyces cerevisiae* (yeast hereafter), which was vital in understanding biosynthetic pathways, mechanism of protein biogenesis and quality control as well as structural aspects [4,6–11].

1.1 ER-mitochondria contact sites

One consequence of compartmentalization is the need to establish means of communication and signaling within the cell, since biochemical pathways span across organelles and need to be regulated according to the cells state as well as environmental cues. Two primary mechanisms were thought to drive this exchange of signals: diffusion and active transport through the cytosol or via vesicular trafficking. However, in recent decades it became apparent that a third mechanism exists: membrane contact sites (MCSs), which hold organellar membranes in close apposition [3]. They are defined by four distinct features: their ability to tether membranes, lack of fusion, they have a specific function and a defined proteome/lipidome. Initially, MCSs were identified between the ER and other organelles, which is reflected in their function in either Ca^{2+} signaling or lipid transport [12]. However, recent systematic studies in yeast revealed contact sites between any pair of two organelles [13,14].

One of the best studied contact sites to date is the ER mitochondria encounter structure (ERMES) which tethers the ER to mitochondria. ERMES is composed of four structural components Mmm1, Mdm12, Mdm34 and Mdm10, which form a chain-like bridge (Fig. 1). It spans a +/- 25 nm gap and roughly 30 complexes make up a singular contact point, of which there are 3 to 6 per cell [15–18].

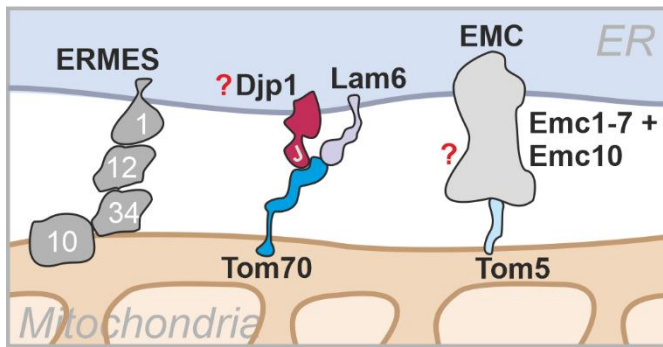


Fig. 1 ER mitochondria contact sites in yeast. Three contact sites are formed between ER and mitochondria. One formed by Mmm1, Mdm12, Mdm34 and Mdm10 (ERMES). A second contact site is formed by the ER resident Lam6 and Tom70. The third contact site is formed by the EMC and Tom5. Question marks indicate putative contact site components.

Additionally, the GTPase Gem1 can associate with ERMES which regulates the lipid flux between ER and mitochondria [17,19]. Another regulatory protein is Tom7, which shuttles Mdm10 from ERMES to the sorting and assembly machinery (SAM) of the outer membrane [20,21]. Owing to its topology, loss of any subunit leads to the disassembly of the whole complex. ERMES was first discovered to play a role in lipid transfer, mainly transporting phosphatidylserine (PS) from the ER to mitochondria [16,22,23]. However, recent work has shown that ERMES plays a key role in a plethora of cellular processes. ERMES promotes the formation of mitochondria-derived compartments (MDCs), defines the position of intra-mitochondrial complexes such as nucleoids, the MICOS (mitochondrial contact site and cristae organizing center) and the enzymes for coenzyme Q synthesis, that are also called the coenzyme Q synthome [24–28].

Besides ERMES, two more tethering complexes connect the ER with mitochondria in yeast: One tether is formed by the ER-resident sterol transporter Lam6 and Tom70. Lam6 was implicated to regulate the extent of contact between organelles [29,30]. The ER resident J-protein Djp1 has also been shown to interact with Tom70 and act along the same protein sorting pathway [31,32]. However, whether Djp1 is part of the same tethering complex as Lam6 and Tom70 is unclear.

The third contact between ER and mitochondria was proposed to be formed by the ER membrane complex (EMC) and Tom5, which is involved in lipid transfer between the two organelles [33]. However, recent efforts demonstrate a primary function of the EMC in protein insertion into the ER membrane [34].

1.2 Protein targeting

The second consequence of compartmentalization is the need to sort proteins to their proper cellular sub-localizations, since the vast majority of all proteins are synthesized in the cytosol, apart from a very small subset which is synthesized in mitochondria.

Many ER proteins carry an N-terminal signal-sequence (SS), which upon translation is first recognized by the signal recognition particle (SRP). This binding in turn stops translation until SRP is bound by the SRP receptor on the ER membrane. Afterwards, the ribosome is positioned onto the Sec61 translocon where translation and subsequent folding can commence (Fig. 2) [9,35].

Separate from the SRP-dependent pathway, proteins can reach the ER in an SRP-independent fashion (SND). During their synthesis, Snd1 binds the translating ribosome and subsequently targets the proteins to Snd2/Snd3. These two proteins are membrane-embedded and associated with the Sec translocon [36–38].

Alternatively, proteins can be bound by Hsp70s in the cytosol and routed towards the ER. Here they are bound by Sec72 which interacts with Sec71 at the translocon to facilitate the import of these precursors [39].

The guided entry of tail-anchored proteins (GET) pathway is responsible for the insertion of proteins into the ER that carry a C-terminal transmembrane segment. During synthesis of TA proteins, they are bound by Get4/Get5. After synthesis is completed, the precursor is transferred onto Get3, which brings them to the insertion machinery formed by Get1/Get2 [40–42]. The EMC complex has also been implicated in the insertion of TA proteins. However, it seems that the criteria that distinguish the client spectrums of the two pathways are the hydrophobicity of the transmembrane domain (TMD) of a TA protein as well as adjacent charges [43]. Nevertheless, loss of either EMC or GET shows only mild phenotypes indicating that one can take over the function of the other [40,44].

The EMC complex can also aid in the biogenesis of polytopic membrane proteins. It can insert the first N-terminal TMD but afterwards needs the Sec61 machinery to fully insert the protein into the membrane [45].

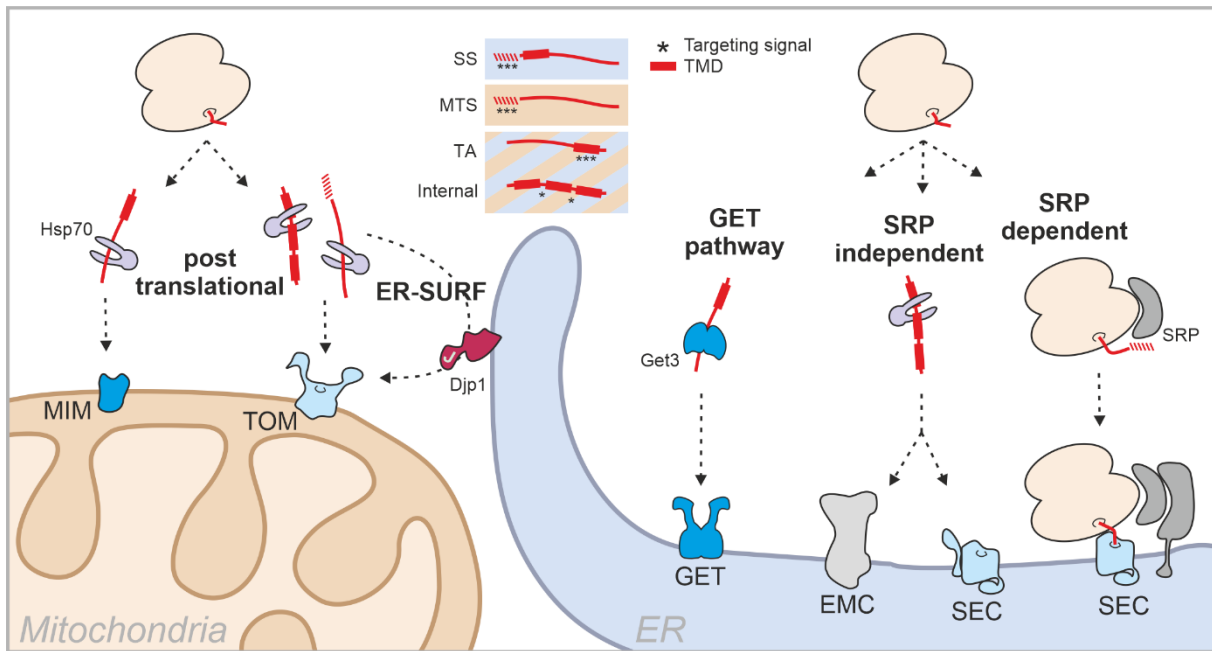


Fig. 2 Targeting of proteins to the ER and mitochondria. Proteins can have an N-terminal targeting signal, signal-sequence (SS) for the ER or mitochondrial targeting signal (MTS) for mitochondria. Tail-anchored proteins (TA) have a C-terminal TMD which encodes the targeting information. Polytopic transmembrane proteins have their targeting information scattered along their sequence. ER proteins are imported in a co-translational manner. The SS is recognized by SRP, bound on the ER membrane by the SRP receptor and afterwards imported. Apart from SRP, ER proteins can be bound by Hsp70s, Sec72 or Snd1 which also targets them to the ER. TA proteins of the ER are bound by Get3 and brought to the GET complex for insertion. Mitochondrial proteins are imported in a post-translational manner. Here Hsp70s play a vital role in keeping precursors unfolded and import competent until they reach either TOM or MIM for their import/insertion. Some precursors can also use the ER surface for their biogenesis. The J-protein Djp1 binds these precursor and hands them over to the TOM complex for their import.

In contrast to the ER, the targeting of mitochondrial proteins is by far less understood. However, like ER proteins, mitochondrial proteins either have an N-terminal mitochondrial targeting signal (MTS), internal targeting information or a single transmembrane domain (e.g., TA proteins) [46,47].

Only a handful of proteins seem to be co translationally targeted/imported into mitochondria. Using a proximity-labeling approach in conjunction with ribosome profiling, it was shown that especially proteins of the inner membrane seem to be synthesized close to the mitochondrial surface [48]. The mRNA of such a protein can be bound by Puf3 and recruited to the outer membrane [49,50]. Moreover, it was shown that Om14, an outer membrane protein with unknown function, can interact with nascent chain-associated complex (NAC) and recruit the ribosome to the outer membrane [51,52]. Nevertheless, if these findings constitute co-translational import is still debated.

The majority of mitochondrial proteins are bound by Hsp70s upon their synthesis and ushered towards the main entry gate of mitochondria the translocase of outer membrane (TOM) complex [53–55].

A small subset of mainly hydrophobic inner membrane proteins can also use the ER surface for their biogenesis (ER-SURF). Precursors that end up on the ER surface can be salvaged with the help of the J-protein Djp1. Once bound by Djp1 the stranded precursor can be handed to Tom70 and afterwards be productively imported [47,56]. The exact mechanism of this transfer remains elusive. In addition, how precursor proteins end up on the ER is still not entirely clear. However, recent efforts have shown that some precursor proteins, like Oxa1 or Psd1, are found among proteins that are bound by SRP indicating that the cell erroneously targets these proteins to the ER [57]. Proximity labeling of translating ribosomes at the ER has also revealed that some mitochondrial proteins are synthesized in the vicinity of the ER [48,58]. Moreover, Get3 was shown to interact with mitochondrial proteins. If there is an accumulation of mitochondrial precursor proteins in the cytosol, Get3 is able to direct some of these towards the ER, which seems to be the case especially for carrier proteins, that in turn pose a high proteotoxic potential for the cytosol [59,60].

1.3 The role of chaperones in protein sorting

Chaperones play a vital role in proof-reading and fine tuning the targeting systems of the cell. Co-translational binders such as NAC and Ssb1/Ssb2, proteins of the Hsp70 class, cooperate with SRP and increase its selection fidelity [57,61]. By the same token, Ssa1/Ssa2, also part of the Hsp70 family, are binders of mitochondrial proteins and help to keep them in an unfolded and import-competent state. Moreover, Hsp70s can directly dock onto Tom70, which is part of the TOM complex, via their EEVD motif and directly hand over substrates for import [55].

Nevertheless, Hsp70s display a broad substrate range and are highly abundant proteins, therefore, it is still not quite clear what determines the substrate specificity. More selective targeting might be provided by Hsp40s which act upstream of Hsp70. Hsp40s also called J-proteins, due to the presence of a J-domain, alter and fine tune the substrate specificity of Hsp70s. The most abundant cytosolic J-protein is Ydj1 [62,63]. It was also shown to localize to the ER as well as mitochondria. It plays a role in targeting proteins to both organelles. In this context it was also shown to cooperate with Hsp70 [64,65]. Moreover, *in vitro* studies demonstrated the binding of Ydj1 to Tom20, one receptor of the TOM complex [66]. Another example is Xdj1. Like Ydj1, it is localized in the cytosol as well as to mitochondria. Xdj1 binds

precursor proteins and ushers them to Tom22 for import [31,63]. Lastly, Sis1 overexpression was shown to suppress the loss of Ydj1. In addition, it can also bind Tom20 as well as precursor proteins, showing a redundant role in mitochondrial targeting to Ydj1 [65–67].

1.4 Mitochondrial protein import

Once proteins are routed towards their proper destination, they need to be imported into the organellar lumen or inserted into a membrane. Most mitochondrial proteins carry a cleavable N-terminal mitochondrial targeting sequence (MTS) [68–70]. This amphipathic helix is first recognized by Tom20 and Tom22, the two major receptors of the translocase of outer membrane (TOM) complex (Fig. 3) [8,71]. They pass precursors in a cooperative fashion to the pore-forming β -barrel protein Tom40, which is the main entry gate for mitochondrial proteins of the matrix, inner membrane, intermembrane space and many outer membrane proteins. After translocation through Tom 40 proteins are sorted into their destined sub-compartment.

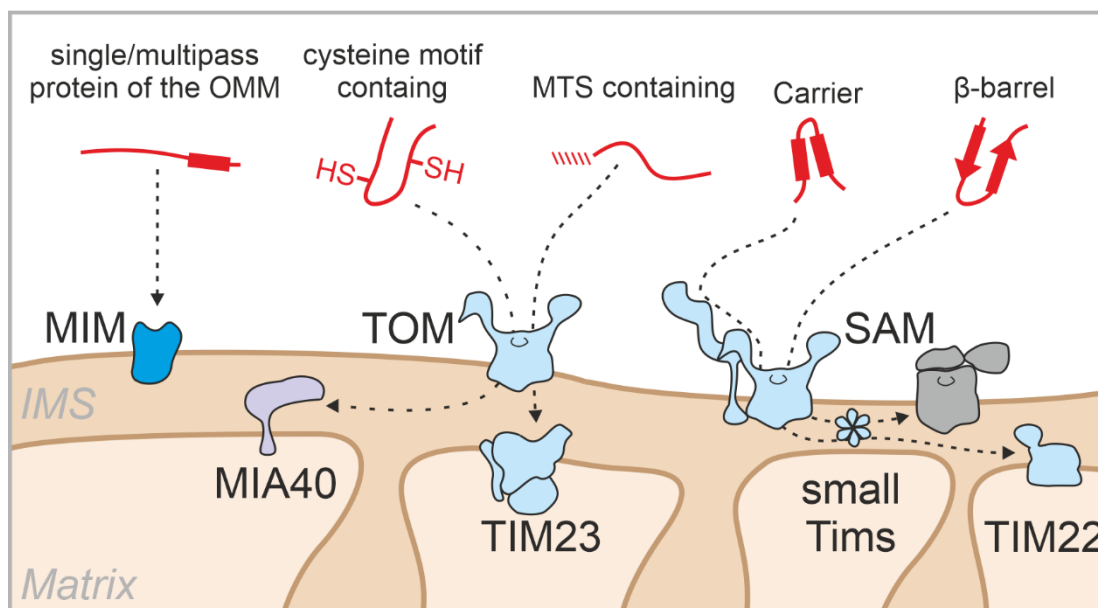


Fig. 3 The five major classes of mitochondrial proteins use different import routes. Proteins of the matrix and many inner membrane proteins are synthesized as precursor proteins with N-terminal matrix targeting signals and imported via the TOM and TIM23 complexes. Metabolite carriers lack presequences and are integrated into the inner membrane by the TIM22 complex. The SAM complex integrates β -barrel proteins into the outer membrane. Many outer membrane proteins with helical transmembrane domains bypass the TOM complex but can be dependent on the MIM complex. IMS, intermembrane space.

Proteins that are destined for the inner membrane or matrix are directed towards the translocase of inner membrane (TIM) complex, which is comprised of the main translocase Tim23, Tim17 and other accessory proteins. The TIM23 machinery threads proteins through the inner membrane, assisted by the membrane potential ($\Delta\Psi$) and the presequence-associated motor (PAM) complex [72,73]. However, Tim17 and Tim23 facilitate local membrane thinning for

protein translocation in contrast to Tom40 [74,75]. After successful translocation the mitochondrial processing peptidase (MPP) cleaves the MTS and the precursor is folded and or assembled [73].

Carrier proteins, with their characteristic 6 transmembrane domain topology, are highly abundant proteins of the IMM. They mediate the transfer of many metabolites including ATP. Unlike MTS-containing proteins the signal information for carriers is scattered across their sequence [76]. They are first recognized on the mitochondrial surface by Tom70, which tightly cooperates with cytosolic chaperones [55,77]. After translocation through TOM, carrier proteins are chaperoned through the IMS with the help of small Tim proteins, which deliver them to the TIM22 complex. Here carrier proteins are inserted into the inner membrane [78,79].

Many proteins of the IMS also lack a classical MTS, but instead carry specific cysteine motifs within their sequence [80]. These motifs are recognized after translocation by the oxidoreductase Mia40, which facilitates their import with the help of the sulfhydryl oxidase Erv1 [81].

β -barrel proteins of the outer membrane form large pores that allow the diffusion of small molecules. Precursors of β -barrel proteins are first recognized at the TOM complex by their β -hairpin motif [82]. Afterwards they are imported through Tom40 and, similar to carrier proteins, chaperoned by small Tim proteins in the IMS. They are brought to the sorting and assembly machinery (SAM), which in it of itself contains a β -barrel protein Sam50, that inserts these precursors into the outer membrane [83–85]. Although Tom40 allows for the entry of many different precursor proteins into mitochondria, MTS-containing proteins pass near one side of the β -barrel, while carrier, IMS proteins and β -barrel precursor pass near the other side of the Tom40 pore [8].

Single- and multi-spanning proteins of the outer membrane form the last class of mitochondrial proteins. Here the insertion mechanisms seem to be quite diverse, however the mitochondrial import (MIM) complex has been implicated to play a role in the insertion of many of these proteins. Nevertheless, a general targeting and insertion mechanism remains elusive [86–89].

1.5 Protein quality control at the ER and mitochondria

Although cells have evolved intricate systems for protein targeting, sorting and import, still some proteins can mis-localize, aggregate, or fail to be imported. Concomitant with all targeting and import machineries cells have evolved mechanisms to proofread these very same systems.

The clearance of proteins from the ER is termed ER-associated degradation (ERAD), which can be further distinguished by the substrate being degraded: Luminal ER proteins (ERAD-L), membrane proteins (ERAD-M) or cytosolic proteins (ERAD-C). The ERAD machinery consists of core components that recognize substrates e.g., Hrd1, components that lead to ubiquitination e.g., Hrd3 and components that extract a given substrate into the cytosol e.g., Cdc48 [10]. Cdc48 is an unfoldase forming a stacked hexameric ring characteristic for AAA+ proteins, which is tethered to the ERAD machinery via Ubx2 [90,91]. Once extracted, the aberrant protein will be degraded by the proteasome (Fig. 4).

The mechanism as well as the structure of the different ERAD machineries have been studied in detail. In contrast, the mechanism of mitochondria-associated degradation (MAD) is by far less understood. However recent efforts demonstrated a pool of Ubx2 that is localized to mitochondria, in particular to the TOM complex. Here it also serves as an adaptor for Cdc48 which facilitates the extraction of stalled import intermediates. This pathway was termed mitochondrial protein translocation-associated degradation (mitoTAD) [92]. Mitochondria also have a second AAA+ protein on the OM, called Msp1, which can also help in clearing aberrant proteins from TOM. In this case it is tethered to the TOM complex via Cis1. This mitochondrial compromised protein import response (mitoCPR) is regulated by the transcription factor Pdr3 [93].

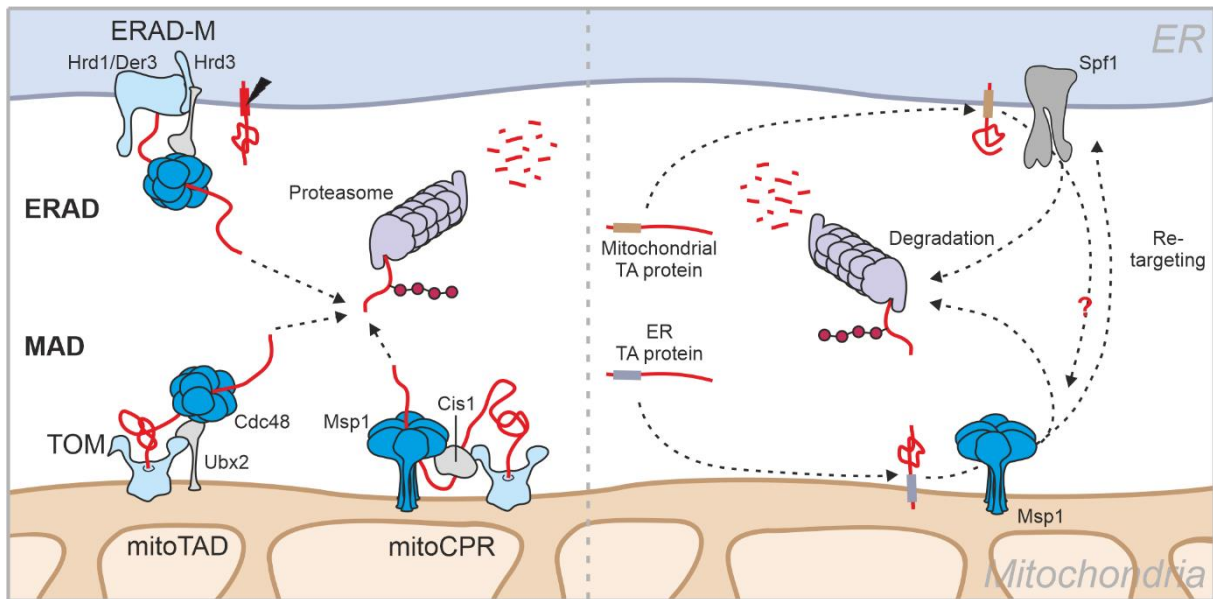


Fig. 4 Surveillance of the mitochondrial outer membrane and the ER by membrane extractors. ER and mitochondrial proteins are released by the AAA proteins Msp1 or Cdc48 into the cytosol to be degraded by the proteasome. Poly-ubiquitin chains serve as degradation signals. Adaptor proteins such as Ubx2 or Cis1 play crucial role in the substrate binding of AAA proteins. Stalled translocation intermediates induce the recruitment of Msp1 to the TOM complex by Cis1 in a process called mitochondrial compromised protein import response (mitoCPR). MAD of translocation intermediates is also referred to as mitochondrial protein translocation-associated degradation (mitoTAD). Msp1 recognizes non-mitochondrial TA proteins as well as translocation intermediates stalled in the TOM complex. It removes these proteins, which then either find their respective target membrane or are degraded, for example via ERAD. An analogous extraction system exists on the ER membrane where Spf1 recognizes and dislocates membrane proteins destined to mitochondria. It is unclear whether such proteins can be re-targeted to mitochondria (indicated with a question mark).

Membrane extractors, such as Msp1, also serve an additional function in clearing mistargeted tail-anchored proteins from the ER or the outer membrane. If Msp1 recognizes an ER tail-anchored protein it extracts the protein, which can subsequently be re-targeted to its cognate membrane or be degraded by the proteasome [94–96]. In a similar fashion, the recently discovered P5A-ATPase Spf1 surveils the ER membrane for mistargeted mitochondrial proteins [97,98]. However, it is unclear whether extracted TA proteins can be rerouted towards mitochondria e.g., via the ER-SURF pathway.

Taken together, it is apparent that mitochondria and ER cooperate closely in the targeting, biogenesis and quality control of their respective proteomes.

2. AIM

Almost all mitochondrial proteins are synthesized in the cytosol and subsequently imported. The mechanistic and structural aspects of the different import routes have been studied extensively [8,73,75,83]. Nevertheless, the early steps of mitochondrial protein sorting and routing are in the process of being unraveled [99,100]. Recent efforts have shown that mitochondrial proteins that strand on the ER can be productively imported with the help of the J-protein Djpl. This pathway was termed ER-SURF. However, the exact molecular mechanism along with other players that might be involved remains unclear. Close cooperation of the two organelles, e.g., in the form of membrane contact sites, seems vital for such a pathway. Moreover, loss of contact site components was previously shown to impede import of mitochondrial proteins [21,101].

The aim of this work was to elucidate the involvement of ER-mitochondria contact sites in the process of ER-SURF. Hence, I needed to establish a system that permits depletion of several contact sites at the same. Furthermore, I wanted to shed light on the client spectrum of ER-SURF as well as identify governing principles. Therefore, I needed to develop or adapt assays that would allow to identify mitochondrial proteins on the ER surface. To address these questions, I employed classical biochemical assays, genetic approaches, *in vitro* imports into semi-intact cells, high-throughput proteomics and fluorescence microscopy.

3. RESULTS

3.1 The ERMES contact site is required for the biogenesis of Oxa1

Djp1 is an established component of the ER-SURF pathway. In conditions where Djp1 is absent and the precursor form of the inner membrane protein Oxa1 is overexpressed, the accumulation of its precursor can be observed [32]. In order to investigate whether ERMES plays a role in ER-SURF routing, I used a deletion strain of *MDM34* as well as *DJP1* and a wild type for reference, overexpressed Oxa1 from a galactose inducible promoter and analyzed the levels of Oxa1 via western blotting.

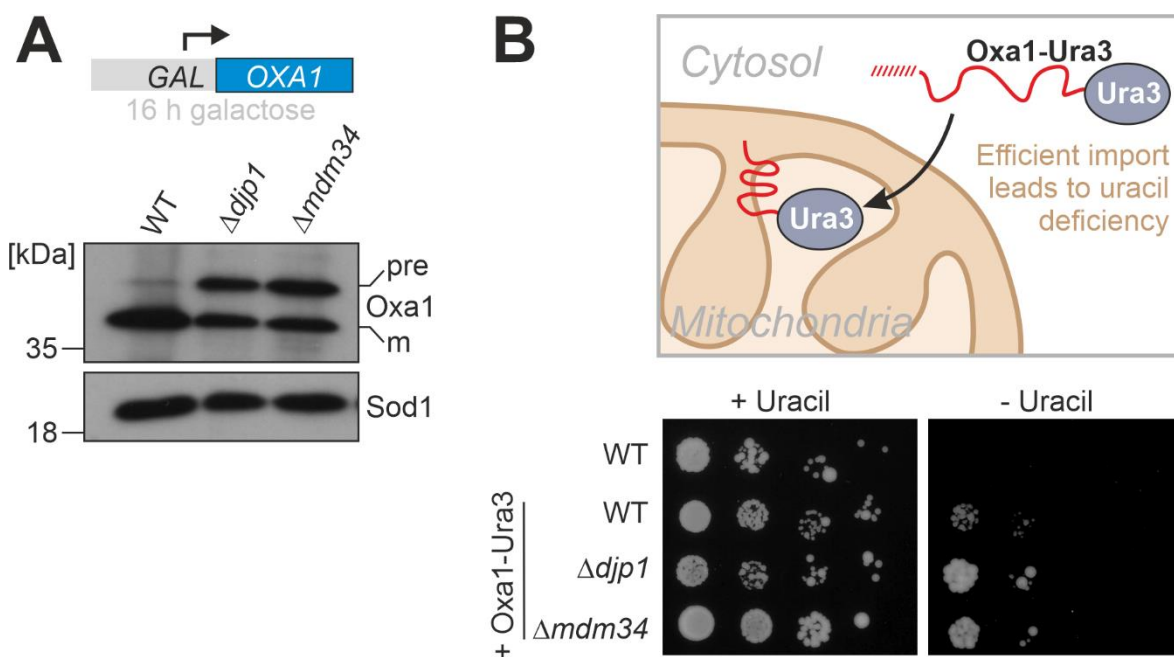


Fig. 5 The ERMES contact site is crucial for the biogenesis of Oxa1. **A.** Western blot analysis of cells carrying an Oxa1 overexpression plasmid. Cells of the indicated strains were grown in lactate medium and shifted to lactate medium that contains 0.5% galactose for 4 hours to induce expression. Cells were harvested, lysed and subjected to SDS-PAGE. The precursor (pre) and mature (m) species of Oxa1 are indicated. **B.** Schematic representation of the Oxa1-Ura3 reporter assay. Normal import of this reporter leads to the depletion of Ura3 from the cytosol and uracil auxotrophy. Impaired import of this reporter restores uracil prototrophy and allows for growth on plates lacking uracil. Cells of the indicated strains were grown to log phase in glucose medium before tenfold serial dilutions were dropped onto plates containing or lacking uracil.

Upon overexpression of Oxa1 precursor accumulation is observed for the deletion of *DJP1*, as previously shown, and a similar accumulation is seen for the deletion of *MDM34* indicative of its possible function in Oxa1 biogenesis (Fig. 5A). To validate this finding, I employed the Oxa1-Ura3 reporter construct, which uses growth on media without uracil or lack thereof as a proxy for efficient targeting of this reporter into mitochondria. Since Ura3 is an enzyme of the cytosol required for uracil biosynthesis, its sequestration into mitochondria will lead to growth deficiency on media lacking uracil. Therefore, I transformed the strains with the Oxa1-Ura3

reporter, grew them in liquid media and spotted tenfold serial dilutions on plates with or without uracil. Dj_p1 and Mdm34 deficient cells showed marked growth on plates without uracil compared to wild type which showed hardly any growth (Fig. 5B), further buttressing the idea that ERMES plays a role in Oxa1 biogenesis and thus in ER-SURF.

To check whether the observed phenotype of Δ *mdm34* is a secondary effect of altered Dj_p1 levels, I analyzed the protein levels of Dj_p1 in all strains via western blotting.

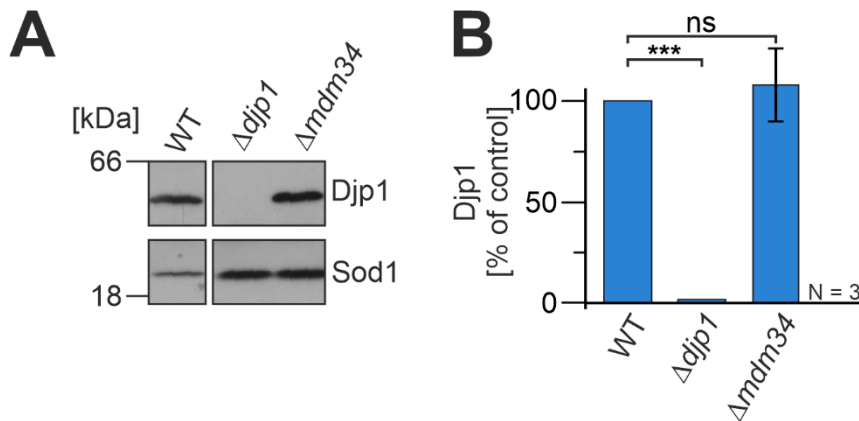


Fig. 6 Dj_p1 levels are unchanged in Δ *mdm34* cells. **A** Western blot analysis of steady-state levels of Dj_p1 and control protein Sod. Cells of the indicated strains were grown to mid log phase, harvested, lysed and subjected to SDS-PAGE. **B** Quantification of Dj_p1 levels normalized to Sod1 in comparison to wild type of three biological replicates (n = 3). Plotted are mean values and standard deviations. Statistical difference was calculated with a student's t-test. Statistical significance was assigned as follows: p-value < 0.005 = ***.

As shown in Fig. 6 the levels of Dj_p1 were unchanged upon deletion of *MDM34*, implying that the previously observed defects are a direct consequence of loss of Mdm34 and therefore ERMES. Taken together these results show that ERMES is involved in ER-SURF in a Dj_p1 independent manner.

I next wanted to elucidate at which step ERMES acts in Oxa1 biogenesis, either in the import or early in the targeting and routing of Oxa1. Furthermore, I wanted to find out whether ERMES acts in concert with Dj_p1 or via a separate axis. Hence, I generated a double knockout of *MDM34* and *DJP1*, which I included in the following analysis.

3.2 Dj_p1 and ERMES act as parallel pathways in the targeting of membrane proteins

Since a classical import assay into isolated mitochondria does not give any indication as to the targeting steps of mitochondrial precursor proteins, I used an *in vitro* import assay using semi-intact cells [32,102]. To prepare semi-intact yeast cells, cells are grown in liquid media, harvested and the cell wall is digested by addition of zymolyase. Afterwards, cells are slowly

frozen over liquid nitrogen to permeabilize the plasma membrane, thereby generating yeast cells that are suitable for an import assay with the cell interior still intact (Fig. 7A). I incubated the generated semi-intact cells with radiolabeled Oxa1 precursor for 5 and 20 minutes and in addition treated them with proteinase K to digest any unimported Oxa1.

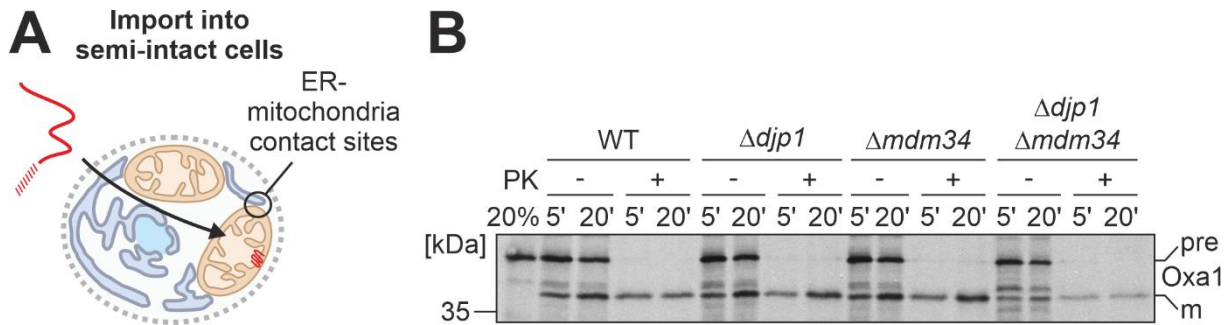


Fig. 7 Import of Oxa1 into semi-intact cells of $\Delta djp1 \Delta mdm34$ is markedly decreased. **A** Schematic depiction of an import reaction into semi-intact yeast cells (SICs). SICs maintain the intracellular and organellar architecture as well as contacts between organelles. **B** Radiolabeled Oxa1 was synthesized in reticulocyte lysate in the presence of ^{35}S methionine and incubated with semi-intact cells obtained from the indicated strains. After 5 and 20 minutes, the cells were isolated, treated without or with proteinase K (PK) for 30 min on ice and subjected to SDS-PAGE, western blotting and autoradiography. 20% of the radioactive protein used per import reaction was loaded for comparison.

The import of Oxa1 was not impeded by the single deletions, however the double mutant showed a strikingly impaired import (Fig. 7B). This implies that indeed ERMES and Djp1 act in parallel and not along the same pathway. Nevertheless, the observed defect might be caused by a mitochondrial defect. Thus, I turned to the classical import assay into isolated mitochondria.

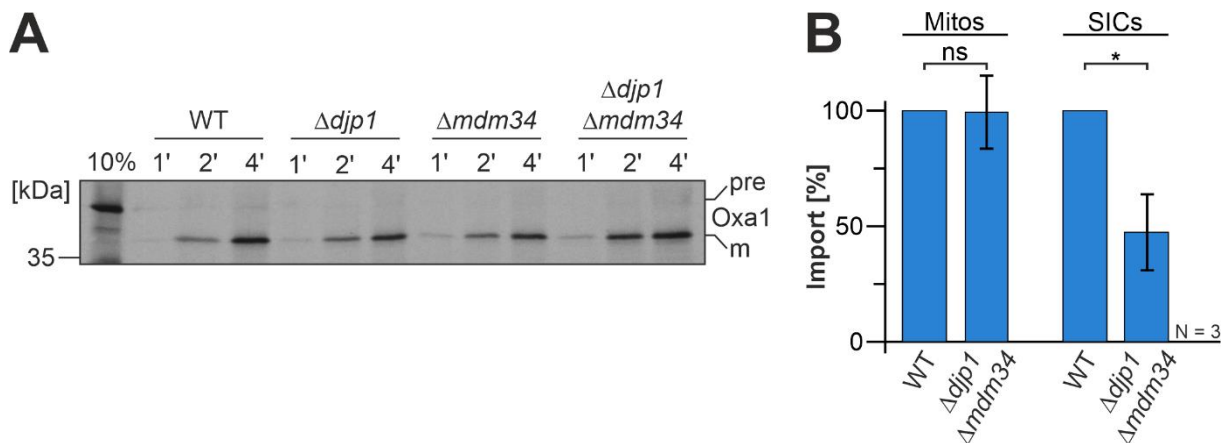


Fig. 8 Loss of Djp1 and ERMES do not affect mitochondrial import capacity. **A** Radiolabeled Oxa1 was imported into isolated mitochondria. After 1, 2 and 4 minutes, mitochondria were isolated, treated with proteinase K (PK) for 30 min on ice and subjected to SDS-PAGE, western blotting and autoradiography. 10% of the radioactive protein used per import reaction was loaded for comparison. **B** Quantification of the import of Oxa1 into semi-intact cells or mitochondria of wild type and $\Delta djp1 \Delta mdm34$ of three biological replicates (n = 3) with semi-intact cells and mitochondria, respectively. Statistical difference was calculated with a student's t-test. Statistical significance was assigned as follows: p-value < 0.05 = *.

As shown by the mitochondrial import neither the single mutants nor the double mutant showed any impairment in Oxa1 import (Fig. 8A). Quantification of the import of Oxa1 into mitochondria and semi-intact cells of wild type and $\Delta djp1\Delta mdm34$ cells revealed efficient import on mitochondrial level. However, the double mutant displayed a marked and consistent import defect into semi-intact cells (Fig. 8B). Taken together these results suggest that firstly ERMES and Djp1 act via separate routes and secondly that ERMES plays a role during the early steps of Oxa1 biogenesis. Moreover, it seems that ER-SURF operates via different mechanism and clients can use one or the other.

To this end I wanted to test whether other substrates would show a similar behavior as Oxa1. Hence, I repeated the import into semi-intact cells this time with Coq2, a hydrophobic inner membrane protein involved in ubiquinone biosynthesis. As controls I imported Hsp60, the chaperonin of the mitochondrial matrix and MrpL15 a small protein and constituent of the mitochondrial ribosome.

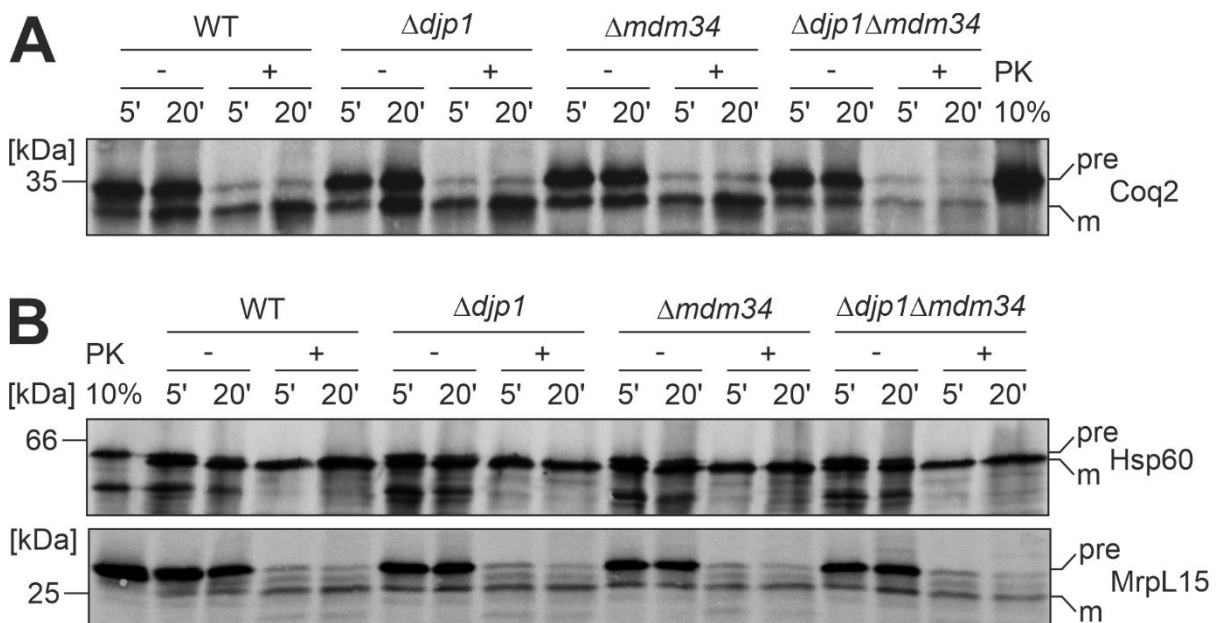


Fig. 9 Coq2 import into semi-intact cells is hampered by loss of Djp1 and Mdm34. **A** Radiolabeled Coq2 was synthesized in reticulocyte lysate in the presence of ^{35}S methionine and incubated with semi-intact cells obtained from the indicated strains. After 5 and 20 minutes, the cells were isolated, treated without or with proteinase K (PK) for 30 min on ice and subjected to SDS-PAGE, western blotting and autoradiography. 20% of the radioactive protein used per import reaction was loaded for comparison. **B** Import of Hsp60 and MrpL15 into semi-intact cells. Samples were treated as described in A.

Like for Oxa1 the import of Coq2 is not affected upon loss of either Djp1 or Mdm34 and similarly the import is strongly decreased if both proteins are lost (Fig. 9A). Nevertheless, the import of Hsp60 and of MrpL15 is not hampered in any condition (Fig. 9B) indicating that the import defect of Coq2 is not a batch effect and that import per se is possible. This finding

together with the Oxa1 import implies that Djp1 and ERMES seem to be relevant for the biogenesis of membrane proteins.

3.3 Proximity between ER and mitochondria is not sufficient for proper ER-SURF targeting

One role that ERMES might play in the routing of precursor proteins via ER-SURF is proximity between ER and mitochondria to allow for efficient transfer between the organelles. This implies that the import defect can be rescued via expression of a synthetic tether that would provide the necessary proximity. Therefore, I used an established tether construct [16] consisting of the Tom70 transmembrane domain, that inserts into mitochondrial outer membrane, fused to GFP and followed by the tail-anchor (TA) sequence of Ubc6, that inserts into the ER membrane, termed Chimera (Fig. 10A). I transformed wild type and the double mutant with either an empty vector or the Chimera construct, prepared semi-intact cells and performed an import reaction with Oxa1.

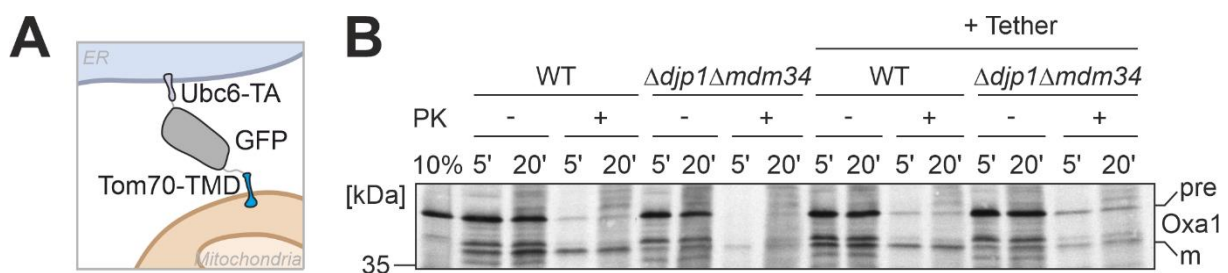


Fig. 10 Expression of Chimera cannot suppress the import defect in the $\Delta dj1\Delta mdm34$ cells **A** Schematic depiction of the Chimera tether. This tether is built by the Tom70 transmembrane domain fused to GFP fused to the tail anchor of Ubc6 thereby connecting ER and mitochondria [16]. **B** Radiolabeled Oxa1 was synthesized in reticulocyte lysate in the presence of ^{35}S methionine and incubated with semi-intact cells obtained from the indicated strains. After 5 and 20 minutes, the cells were isolated, treated without or with proteinase K (PK) for 30 min on ice and subjected to SDS-PAGE, western blotting and autoradiography. 20% of the radioactive protein used per import reaction was loaded for comparison.

The double mutant again demonstrated an import defect, which is not rescued by expression of the Chimera tether. The small variation in signal intensity between double mutant with or without tether might be explained by sample-to-sample variation. This finding suggests that mere proximity is not sufficient for the transfer of proteins from the ER to mitochondria and that ERMES might play an active role in precursor transfer. However, it is also conceivable that ERMES might provide a platform for other, yet unknown, ER-SURF components to assemble.

3.4 Deletion of *MDM34* is concomitant with suppressor mutations

The deletion of ERMES subunits such as Mdm34 severely impairs growth on no-fermentable carbon sources [16,103–105], however mutant cells can quickly adapt and accumulate

suppressor mutations and compensate the growth defect [106]. To test if the $\Delta mdm34$ bears a suppressor mutation I performed a growth assay in liquid media. I grew wild type and $\Delta mdm34$ cells in galactose-containing media and afterwards diluted them into media containing fermentable and non-fermentable carbon sources in a 96-well plate format. The OD₆₀₀ was measured in a 96-well plate reader every 10 minutes for 72 hours while shaking continuously.

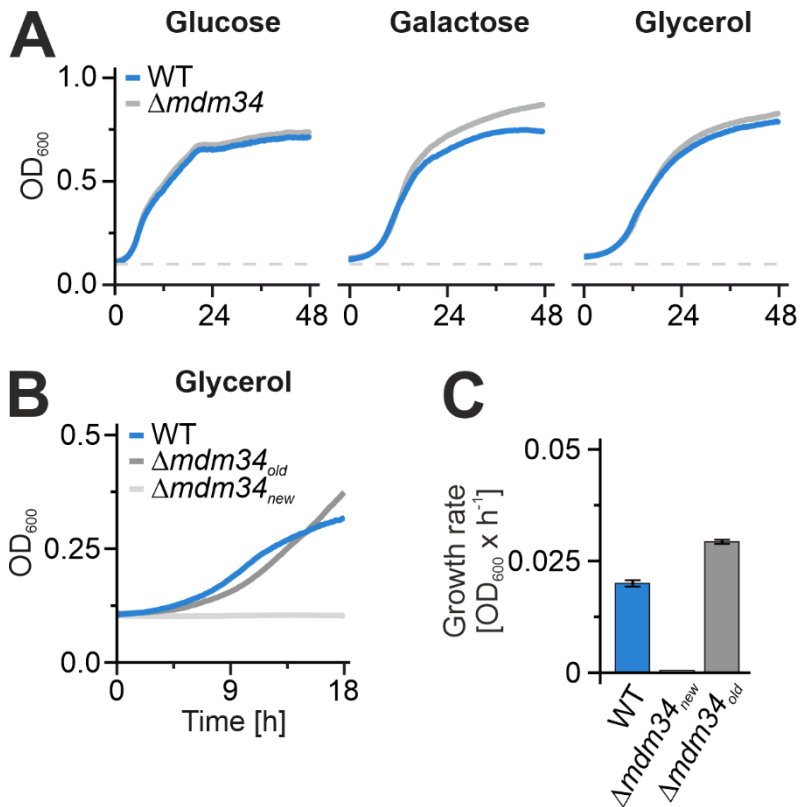


Fig. 11 Deletion of *MDM34* quickly leads to suppressor mutations. **A** The indicated strains were grown in galactose medium to log phase and used to inoculate cultures with the carbon sources indicated. Cells were grown at 30°C under constant agitation. Cell growth was continuously monitored. The graphs show mean values of three technical replicates. **B** Growth curve analysis comparing a fresh and an old knockout of *MDM34* compared to wild type. Cells were treated as described in A. **C** Growth rates were determined by calculation of the slope of the curve in log phase. The graphs show mean values of three technical replicates.

The growth curve revealed that the *MDM34* deletion strain grew like wild type even on the non-fermentable carbon source glycerol (Fig. 11A). I concluded that the mutant must carry a suppressor mutation. Hence, I created a fresh deletion of *MDM34* and repeated the growth curve analysis and indeed the fresh deletion strain exhibited a strong growth defect on glycerol (Fig. 11B-C). Since deletion of any ERMES component poses the possibility of suppressor mutations and could thereby mask any effect on the ER-SURF pathway I decided to use a conditional mutant.

3.5 CRISPR interference (CRISPRi) efficiently depletes *MDM34*

To circumvent the problem of suppressor mutants I decided to switch to an inducible CRISPR interference approach, which quickly would deplete Mdm34 from the cells and allow me to study the immediate effects upon loss of ERMES without generating suppressor mutations. Hence, I used an established system, which constitutively expresses catalytically dead Cas9 (dCas9) fused to the transcriptional repressor Mxi1 and expresses the gene specific gRNA from a tetracycline regulatable promoter (Fig. 12A) [77,107]. I first cloned several guide RNA sequences into the CRISPRi plasmid and transformed them into wild type (from here on referred to as *MDM34*↓). Afterwards I grew the cells in glucose media and added anhydrotetracycline (ATc) to induce expression. Then I harvested the cells extracted RNA and tested the guide efficiency by quantitative real time PCR (RT qPCR) with primers specific for *MDM34* (data not shown). The most efficient guide was selected and used for all further experiments. In order to see how fast and how persistent the knockdown would be I induced depletion of *MDM34* and took samples every 2 hours for up to 8 hours.

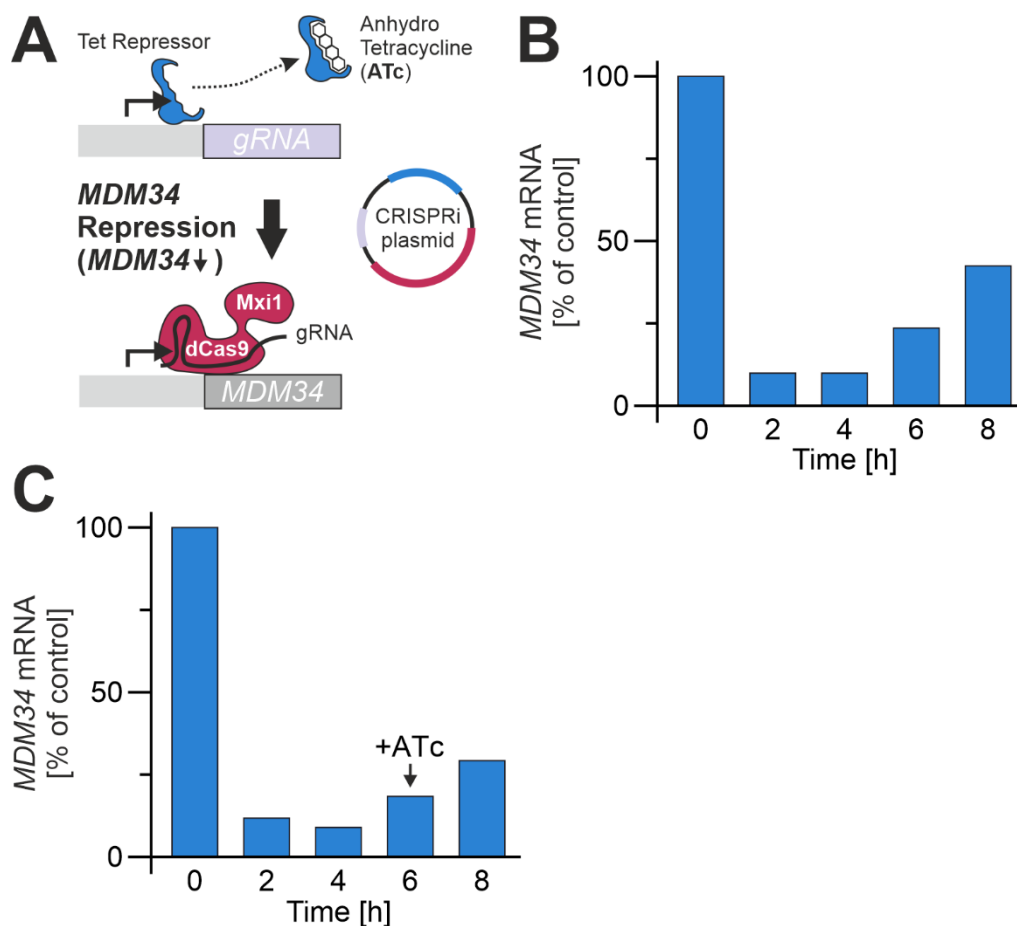


Fig. 12 Addition of ATc rapidly induces knockdown of *MDM34*. **A** Schematic representation of the *MDM34* depletion by CRISPR interference (CRISPRi). ATc-induced inhibition of the Tet repressor leads to the expression of a gRNA that recruits the dCas9-Mxi1 fusion to the *MDM34* promoter thereby blocking transcription of the *MDM34* gene [107]. **B** The *MDM34* \downarrow plasmid was transformed into wild type cells. Cells were grown to early log phase induced with 240 ng/ml ATc. Samples were taken after the indicated timepoints. The mRNA levels of *MDM34* as well as control transcripts were quantified by qPCR before and after induction. **C** Cells were treated as described in B but additional ATc was supplemented after 6 hours of induction.

Analysis of the time course experiment revealed that the mRNA of *MDM34* was depleted to ~12% already after 2 hours of induction. Nevertheless, the knockdown was not persistent as the mRNA levels started to recover after 6 hours (Fig. 12B). Hence, I repeated the experiment this time adding additional ATc after 6 hours of induction assuming that the amount of ATc might be the limiting factor. However, this did not change the onset of recovery after 6 hours (Fig. 12C), indicating that there might be an active counter regulation to the knockdown of *MDM34*.

Yeast cells undertake major changes in their metabolic networks upon a shift from fermentation to respirations in conditions where glucose availability is limiting, and ethanol concentrations are increasing. During this so-called diauxic shift the yeast proteome is significantly altered [108,109]. I assumed that the recovery of the mRNA levels might be due to the changes yeast cells undertake during the diauxic shift. Thus, I wanted to test how different growth stages, as a proxy for the metabolic program, would affect the knockdown efficiency. To this end I

induced the knockdown of *MDM34* for 8 hours in three different cultures, each one diluted to a point that within the given time would either still be in exponential phase ($OD_{600} = 1$), be at the end of exponential phase ($OD_{600} = 2$) or be in the diauxic shift ($OD_{600} = 3$).

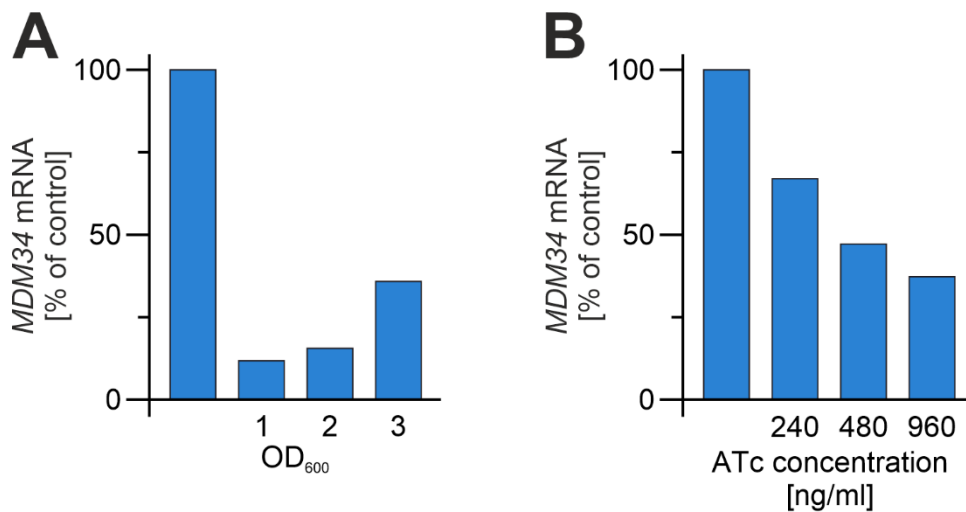


Fig. 13 A higher ATc concentration yields better knockdown efficiency of MDM34. The *MDM34* \downarrow plasmid was transformed into wild type cells. Cells were grown to early log phase induced with 240 ng/ml ATc and diluted to reach the indicated OD after 8 hours of growth. The mRNA levels of *MDM34* as well as control transcripts were quantified by qPCR before and after induction. **C** Cells were grown to early log phase induced with the ATc concentrations indicated for 16 hours. mRNA levels were analyzed as described in A.

Indeed, the qPCR results showed a decrease in knockdown efficiency when yeast cells are grown to a higher density (Fig. 13A) and confirming the idea that yeast cells counteract the knockdown concomitant with the metabolic reprogramming during diauxic shift. To try and prevent this problem and to accommodate longer induction times I reasoned that increasing the ATc concentration to a high enough level might suppress the recovery.

Therefore, I grew cells in the presence of varying concentrations of tetracycline. I induced the knockdown for 16 hours to see what effect the increasing ATc concentration would have on the maximum recovery. Cells that were grown with 960 ng/ml for 16 hours showed the smallest recovery of knockdown efficiency (Fig. 13B) and thus I chose this concentration for all further experiments.

To see whether the carbon source was relevant for depletion efficiency I depleted *MDM34* for 2 hours this time with either glucose, galactose or glycerol as a carbon source.

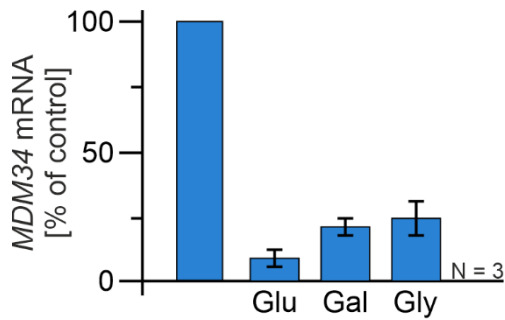


Fig. 14 *MDM34* is efficiently depleted on all carbon sources. The *MDM34*↓ plasmid was transformed into wild type cells. Cells were grown to early log phase in medium containing the indicated carbon sources before 960 ng/ml ATc was added. The mRNA levels of *MDM34* as well as control transcripts were quantified by qPCR before and 2 hours after induction. Shown are mean values and standard deviations of three biological replicates (n = 3).

The qPCR analysis revealed that depletion of the *MDM34* efficiently works on all carbon sources, however there was a minor difference between glucose and galactose/glycerol (Fig. 14). This is most likely due to the slower growth rates on these carbon sources and therefore dilution of the still present mRNA through division is not as prominent, since the abundance of Mdm34 is comparable on all three carbon sources [5].

To further validate the system, I wanted to check how fast the protein Mdm34 is depleted. To this end, I genomically tagged Mdm34 with an HA tag and transformed it with the *MDM34*↓ plasmid. I grew the cells in liquid media and induced repression by addition of ATc. After 0, 4 and 8 hours, I collected samples and analyzed the levels of Mdm34 (HA) via western blotting.

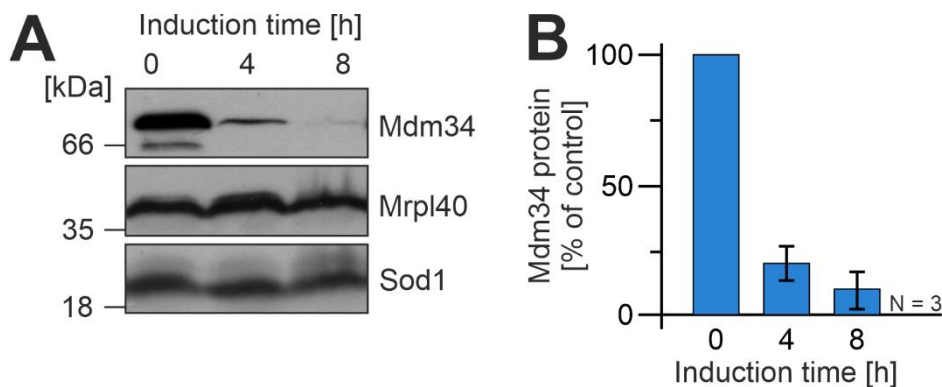


Fig. 15 Mdm34-HA is quickly lost upon induction of CRISPRi. **A** Western blot analysis of steady-state levels of Mdm34 and control proteins Sod1 and MrpL40. Wild type cells with a genomic HA tagged *MDM34* harboring the *MDM34*↓ plasmid were induced by addition of 960 ng/ml ATc. After the indicated timepoints cells were harvested, lysed and subjected to SDS-PAGE. **B** Quantification of Mdm34 levels normalized to Sod1 in comparison to 0 hours of induction of three biological replicates (n = 3). Plotted are mean values and standard deviations.

The levels of Mdm34 dropped to ~25 % already after 4 hours of induction and to ~12 % after 8 hours showing that also on protein level CRISPRi rapidly depletes Mdm34 (Fig. 15A-B).

All in all, Mdm34 was rapidly and efficiently depleted by CRISPRi. However, the knockdown was not persistent and an increase in the amount of tetracycline was required to increase knockdown efficiency over longer periods of time.

3.6 Anhydrotetracycline does not affect mitochondrial translation

Tetracyclines are potent antibiotics [110,111] that inhibit bacterial translation. Since mitochondria are of bacterial origin, an effect of tetracyclines has also been observed for mitochondrial translation [112,113]. Therefore, I wanted to test whether the amount of tetracycline I was using would already have an effect on mitochondrial translation or on growth on non-fermentative carbon sources indicative of mitochondrial fitness. Thus, I grew wild type cells with the *MDM34*↓ plasmid or with an empty vector in the presence or absence of ATc. I isolated the cells, treated them with cycloheximide to stop cytosolic translation, and radiolabeled mitochondrial translation products with ³⁵S-methionine. Afterwards I collected samples, subjected them to SDS-PAGE and western blotting.



Fig. 16 Anhydrotetracycline does not affect mitochondrial translation or mitochondrial fitness. **A** Analysis of mitochondrial translation products. Indicated strains were grown in galactose medium and depletion of Mdm34 was induced by addition of ATc for 16 hours. Mitochondrial translation products were radiolabeled for 15 min with ³⁵S-methionine in the presence of cycloheximide to inhibit cytosolic translation. Radiolabeled proteins were visualized by SDS-PAGE and autoradiography. **B** Growth curve analysis of wild type with increasing amounts of ATc. The indicated strains were grown in galactose medium to log phase and used to inoculate cultures with the carbon sources indicated. Cells were grown at 30°C under constant agitation. Cell growth was continuously monitored. The graphs show mean values of three technical replicates.

Addition of tetracycline or simultaneous depletion of *MDM34* did not alter mitochondrial translation since all 8 mitochondrial translation products are expressed to a similar degree in all conditions. (Fig. 16A). In order to test for effects on mitochondrial fitness I employed a simple growth assay in liquid culture, as described above, and subjected wild type cells to increasing amounts of ATc. The growth curve analysis demonstrated that there was no observable growth

defect in any condition (Fig. 16B). Two conclusions can be drawn from these results, first that the ATc concentration used does not produce any major side effects and second that depletion of *MDM34* does not lead to loss of mtDNA (ρ^0), since mitochondrial translation is unaffected, contrary to the deletion mutant [105], further demonstrating the advantage of the depletion model.

3.7 Knockdown of ERMES affects mitochondrial morphology and function

Next, I wanted to verify that the depletion model would show similar defects to the deletion strain. Hence, I performed a growth analysis in liquid media with wild type bearing an empty plasmid or the *MDM34*↓ plasmid. Depletion of ERMES did not show an effect on glucose, however a marked growth reduction was observed for galactose and glycerol (Fig. 17A).

One hallmark upon loss of any ERMES subunit is the collapse of the mitochondrial network [103–105,114,115]. To test whether this was true for the depletion model I employed timelapse microscopy. To this end, I transformed the strains with a matrix targeted mNeonGreen, grew them in liquid culture, harvested them and seeded cells on a glass slide with an agarose pad with minimal galactose-containing media supplemented with ATc. Images were taken automatically every 5 minutes (Fig. 17B).

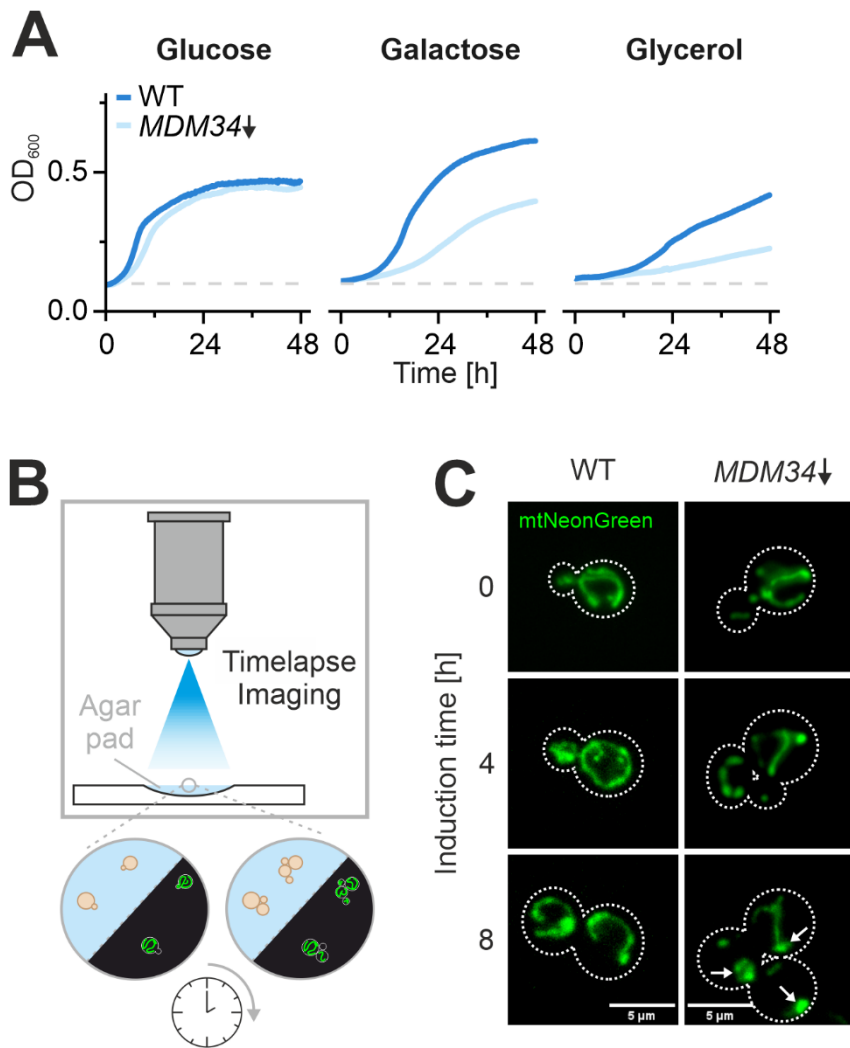


Fig. 17 Loss of Mdm34 leads to impaired growth and collapse of the mitochondrial network. **B** Growth curve analysis of wild type with an empty vector or the *MDM34*↓ plasmid. The indicated strains were grown in galactose medium to log phase and used to inoculate cultures with the carbon sources indicated. Cells were grown at 30°C under constant agitation. Cell growth was continuously monitored. The graphs show mean values of three technical replicates. **B, C** Wild type cells were transformed with the *MDM34*↓ plasmid or an empty vector and additionally with a plasmid for the expression of a mitochondria-targeted mNeonGreen protein. The indicated strains were grown in galactose medium to log phase, harvested and seeded onto an agar pad containing ATc to induce repression. Images of bright field and the mNeonGreen channel were acquired automatically every 5 minutes with a Leica 100x objective in a Dmi8 Thunder Imager.

Wild type cells displayed a normal mitochondrial network over the imaging period, whereas the *Mdm34* depleted cells showed a collapse of the mitochondrial network after ~8 hours (Fig. 17C). Moreover, a growth arrest at the end of the imaging time was observed for *MDM34*↓ cells (data not shown) further corroborating the results obtained from the previous growth assay (Fig. 17A)

The depletion model shows similar defects upon loss of ERMES as deletion strains without causing secondary effects like loss of mtDNA or accumulation of suppressor mutations. Thus,

depletion *MDM34* is a well-suited approach to study the immediate and direct consequences of loss of the ERMES contact site.

3.8 ERMES and Tom70 constitute parallel ER-SURF routes

The second contact site between ER and mitochondria in yeast is composed of Tom70 and Lam 6 [29,30]. Moreover Tom70 also interacts with Djp1 in the transfer of precursors during their import into mitochondria and finally Tom70 was also implicated as a receptor for proteins rerouted from the ER to mitochondria [31,32]. This suggest that Djp1 together with Tom70 and Lam6 form one contact site, and one axis of ER-SURF while ERMES forms a second axis of ER-SURF. It has been shown previously that simultaneous deletion of *MDM34* and *TOM70* is not possible and even suppressor mutants for ERMES have a strong synthetic negative defect in combination with *TOM70* knockouts [77,116].

Thus, I wanted to investigate the consequence of loss of ERMES, using the depletion system I established, in deletion backgrounds of *DJP1*, *LAM6* and *TOM70*. In order to address this question, I transformed wild type cells as well as the deletion mutants with an empty vector or the *MDM34*↓ plasmid. I grew the cells in minimal galactose media supplemented with ATc for Mdm34 depletion and spotted ten-fold serial dilutions on plates with fermentable and non-fermentable carbon sources.

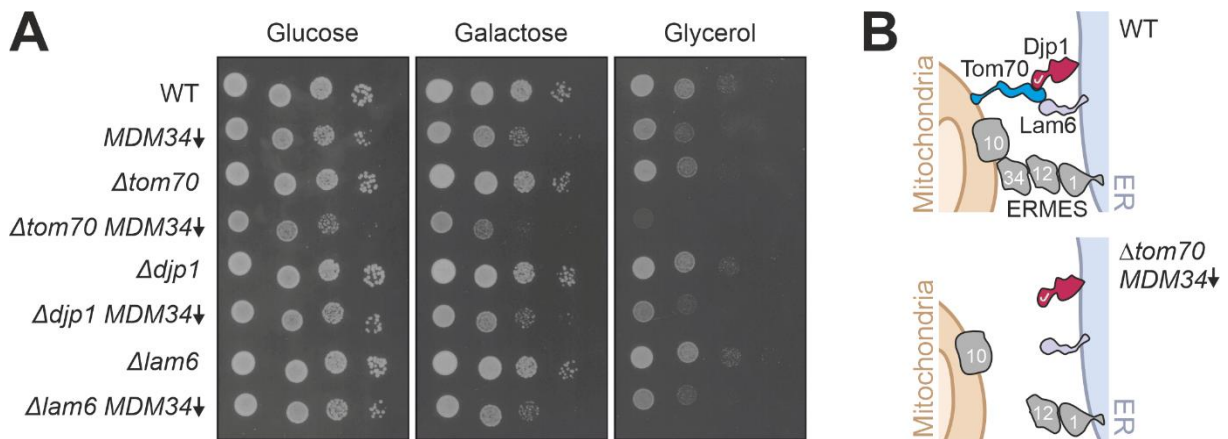


Fig. 18 Knockdown of *MDM34* is synthetically lethal in $\Delta tom70$ cells. **A** Cells of the indicated strains were grown to log phase in galactose medium. Afterwards, knockdown of *MDM34* was induced for 6 hours by addition of ATc. Then cells were harvested and tenfold serial dilutions were dropped onto plates with the indicated carbon sources. **B** Schematic model of the two ER mitochondria contact sites in yeast. One contact site is formed by Mdm10, Mdm34, Mdm12 and Mmm1. The second contact is formed by Tom70 with Djp1 and Lam6 on the ER surface.

As shown in Fig. 18A loss of ERMES leads to a minor growth inhibition on galactose in wild type, $\Delta djp1$ and $\Delta lam6$, which is more pronounced on glycerol. However, depletion of Mdm34 in the *TOM70* knockout strain showed a synthetic negative defect on galactose and even

synthetic lethality on glycerol. I reasoned that depletion of ERMES in either $\Delta djp1$ and $\Delta lam6$ would leave the second contact site still intact, since one of the binding partners of Tom70 is still present on the ER whereas in a $\Delta tom70$ context, both contact sites would be lost and thus give rise to the deleterious effect (Fig. 18B).

I concluded that the depletion of ERMES in a deletion background of *TOM70* is a well-suited model to study the general involvement of contact sites in the ER-SURF pathway. Thus, I wanted to investigate the changes in the cellular proteome under these conditions. To this end I transformed wild type and $\Delta tom70$ with an empty vector or the *MDM34* \downarrow plasmid. I grew the cells in liquid media and treated them with or without ATc for 8 and 24 hours. After each time point the cells were collected and lysed. Afterwards, proteins were tryptically digested, labeled with isobaric tandem mass tags (TMT), multiplexed and subjected to LC-MS/MS (Fig. 19A).

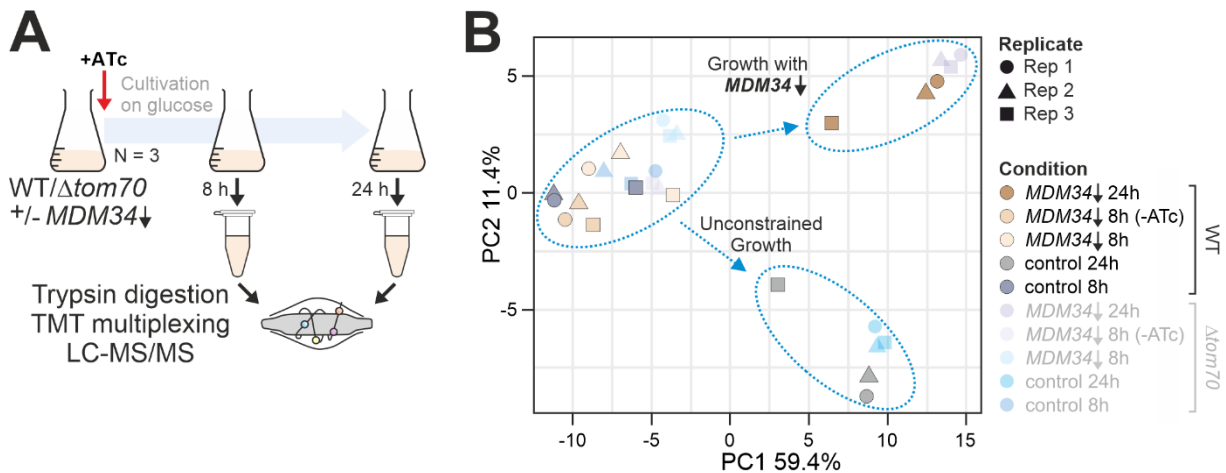


Fig. 19 Loss of the ERMES contact site leaves a characteristic footprint on the cellular proteome. A. Schematic workflow of the proteomic analysis of wild type and $\Delta tom70$ cells with an empty vector or the *MDM34* \downarrow plasmid. **B.** Principal component analysis of all samples measured in the data set.

Principal Component Analysis revealed that on one hand knockdown of *MDM34* for 8 hours hardly altered the proteome in wild type or $\Delta tom70$ respectively. On the other hand, knockdown for a prolonged period led to drastic changes in the cellular proteome upon loss of one or both contact sites (Fig. 19B). Further analysis of the data showed a striking effect on mitochondrial proteins in the absence of ERMES as compared to wild type, many of which were decreased in abundance (Fig. 20A).

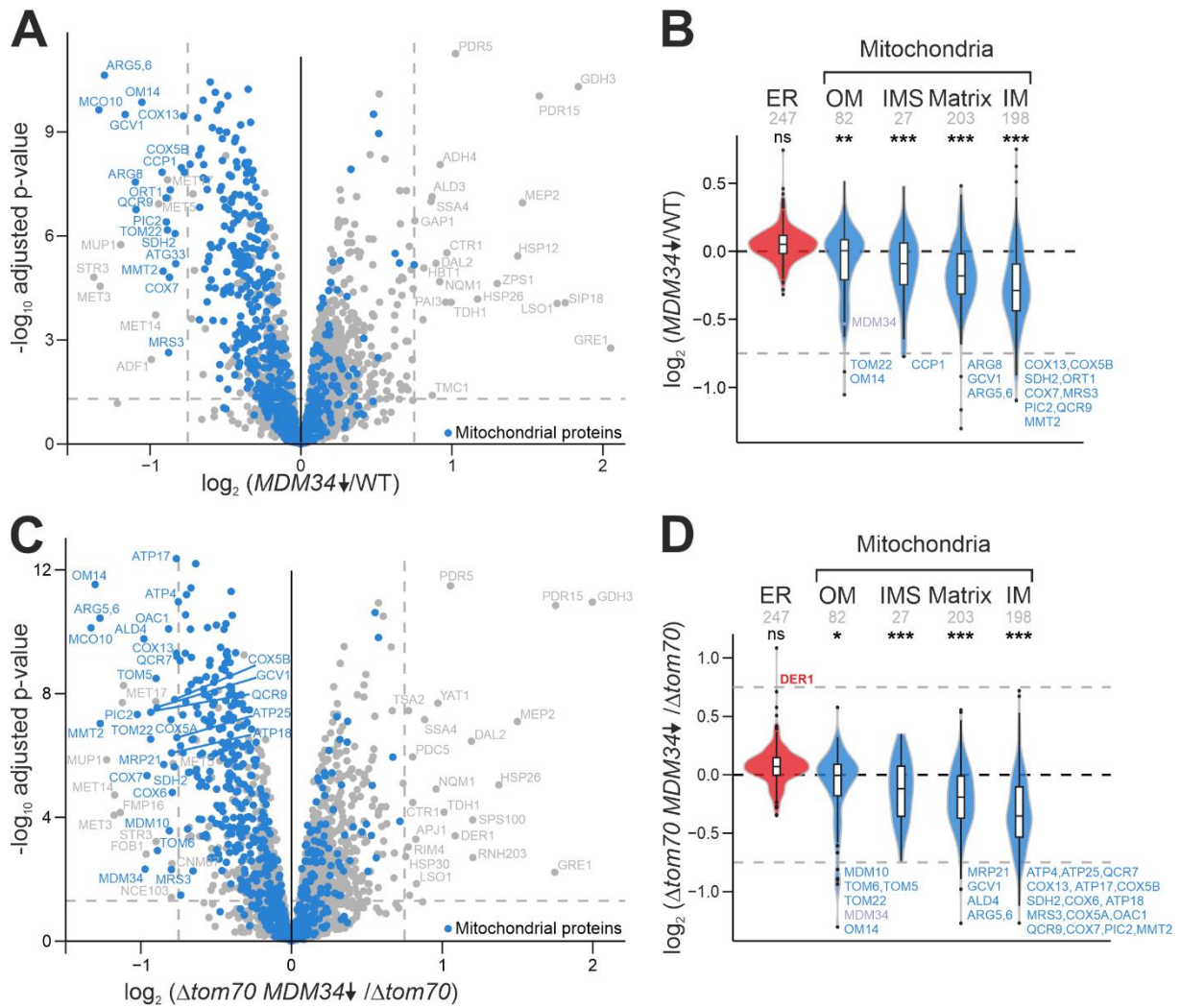


Fig. 20 Depletion of ER-mitochondria contact sites leads to a specific reduction of mitochondrial inner membrane proteins. **A.** Comparison of the proteomes of wild type cells with Mdm34-depleted cells 24 hours after ATc addition. Mitochondrial proteins [5] were indicated in blue. **B.** The violin plot shows the distribution of protein abundances (\log_2 -fold change) in wild type cells relative to Mdm34-depleted cells of the indicated subpopulation. Statistical difference was calculated with a Kolmogorov-Smirnov test comparing the indicated subpopulations with all other proteins. Statistical significance was assigned as follows: p -value $< 0.05 = *$, p -value $< 0.01 = **$, p -value $< 0.005 = ***$. **C.** Comparison of the proteomes of $\Delta tom70$ cells with $\Delta tom70$ Mdm34-depleted cells 24 hours after ATc addition. **D.** violin plot corresponding to the comparison in C. Statistical analysis was carried out as mentioned in B.

Looking closer at the decreased abundance fraction I wanted to investigate if there is a bias towards any mitochondrial sub-compartment. Indeed, all mitochondrial proteins showed a significant shift towards decreased abundance, however, the most striking difference was observed for proteins for the inner membrane (Fig. 20B). By the same token ER proteins did not show a significant shift in their distribution in either direction. These findings held true for the double mutant although to a more severe extent (Fig. 20C-D). This indicates that ER-mitochondria contact sites play a crucial role in the biogenesis or stability of many mitochondrial proteins, in particular those of the inner membrane. Moreover, these findings

corroborate the initial postulate that ER-SURF is especially relevant for hydrophobic inner membrane proteins [32].

3.9 Loss of ER-mitochondria contact sites leads to enrichment of ER in purified mitochondrial fractions

To better understand the changes in the mitochondrial proteome I used the aforementioned strains, induced the depletion of *MDM34* for 16 hours, isolated crude mitochondria and via a sucrose cushion obtained highly purified mitochondria which were subjected to LC-MS/MS (Fig. 21A).

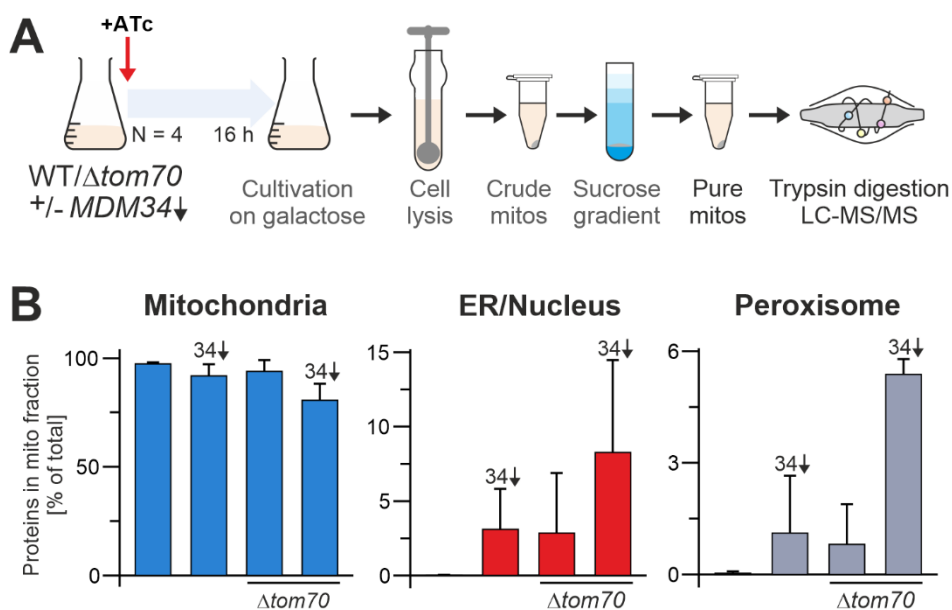


Fig. 21 Loss of ER-mitochondria contact sites is accompanied by strong enrichment of organellar membranes in highly purified mitochondria. **A.** Schematic workflow of the proteomic analysis of wild type and $\Delta tom70$ cells with an empty vector or the *MDM34*↓ plasmid. **B.** The relative intensities measured of mitochondrial proteins [5], ER/Nuclear proteins and peroxisomal proteins [117] was calculated relative to all proteins measured. Shown are mean values and standard deviations of three ($\Delta tom70$) and four (WT) biological replicates. Note that standard deviations are only shown in one direction.

The mitochondrial fractions obtained for all strains were constituted to a large extent of peptides and proteins from mitochondria indicative of a highly purified fraction and in line with previous findings [5,118]. Nevertheless, a striking observation was the consistent accumulation of ‘contaminant’ membranes from ER/Nucleus and Peroxisomes in the single mutants and to an even larger extend in the double mutant (Fig. 21B). This is a counterintuitive observation, since one would expect if contacts between ER and mitochondria are lost the obtained fraction should in turn be ‘purer’. This could either imply a defect in protein sorting in these mutants or, although not mutually exclusive, a change in the physiochemical properties of the different organelles and in turn different running behavior in the sucrose cushion.

Due to these findings, I wanted to test if there are any major changes in the different organelles upon loss of either ERMES, Tom70 or both using transmission-electron-microscopy. Therefore, the strains were grown in minimal galactose media and induced with ATc for 16h. Afterwards, the cells were harvested, fixed and thin sections were prepared for EM imaging.

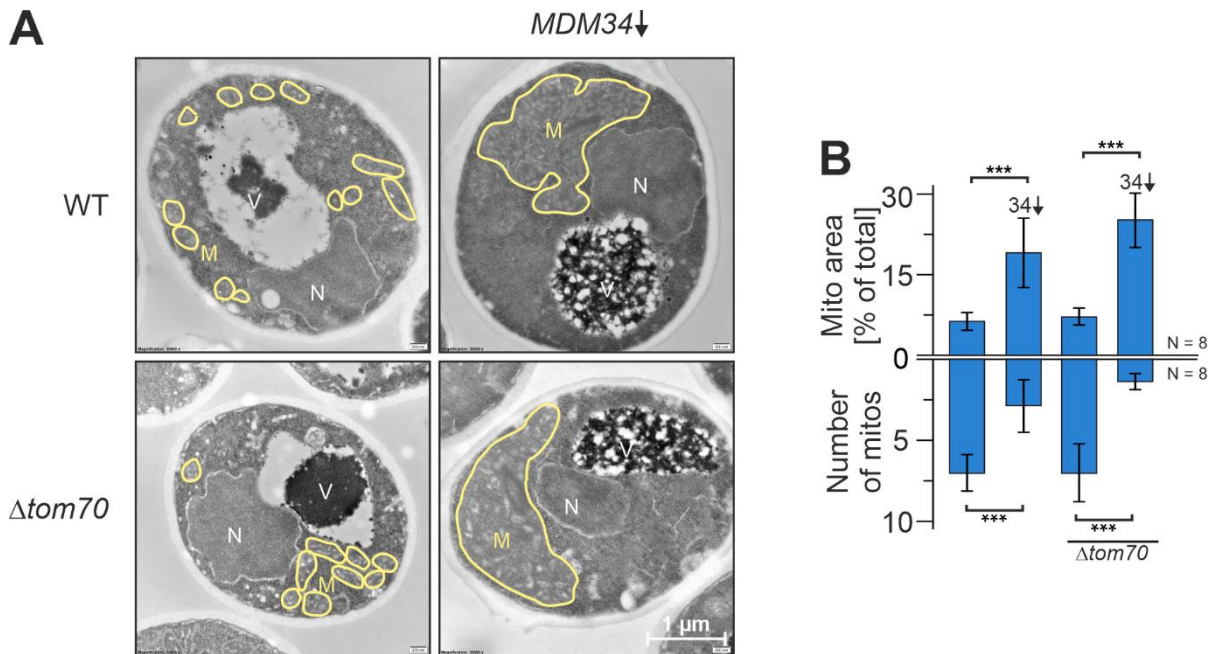


Fig. 22 ERMES is crucial for mitochondrial division. **A** The indicated strains were grown to log phase in galactose media and depletion was induced for 16 hours. Afterwards, cells were embedded, cut into thin slices and imaged by transmission electron microscopy. Mitochondrial membranes are indicated in yellow. Organelles were labeled as follows: M for mitochondria, N for nucleus and V for vacuole. **B** the number and relative area of mitochondria in the section was quantified. Shown are mean values and standard deviations of eight samples. Statistical difference was calculated with a student's t-test. Statistical significance was assigned as follows: p-value < 0.05 = *, p-value < 0.01 = **, p-value < 0.005 = ***.

Wild type and $\Delta tom70$ cells showed a similar cellular architecture as well as similar number, size and shape of mitochondria. However, upon loss of ERMES cells displayed a bloated mitochondrial phenotype. Resulting in much larger mitochondria but fewer sections per cell (Fig. 22A-B). This underpins previous work showing the role of ERMES in mitochondrial division [104,114,115].

I reasoned that these severe structural rearrangements could be accompanied by retrograde signaling or induction of stress response pathways. Insult of mitochondrial dysfunction has been linked to induction of the heat shock response, activation of proteasome associated control elements and induction of the pleiotropic drug response pathway [93,119,120]. Moreover a recent study demonstrated that a massive accumulation of mitochondria precursor proteins on the ER triggers the unfolded protein response [121]. To address this question I used a YFP reporter assay, which uses a modified *CYC1* promoter that is either under control of four heat

shock elements (4xHSE), four proteasome-associated control elements (4xPACE) or four pleiotropic drug response elements (4xPDRE). I transformed the yeast strains with plasmids carrying either of the reporters and induced depletion for 16 hours. Afterwards, I harvested the cells and measured YFP intensity in a 96-well microplate reader. Treatment at 37°C or expression of a synthetic ‘clogger’ construct, consisting of the MTS of cytochrome b₂ fused to dihydrofolate reductase (DHFR) served as positive controls. Unfortunately, loss of either contact site or both does not trigger a response to mitochondrial stress as observed by the YFP reporter assay (Fig. 23A).

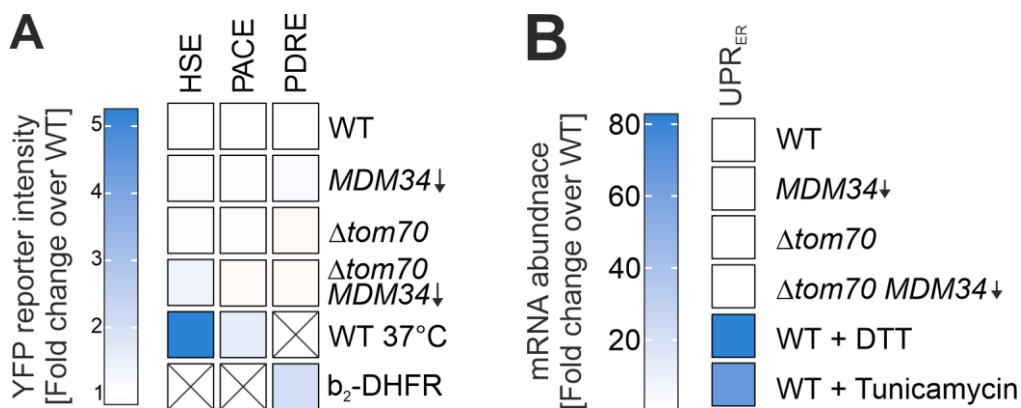


Fig. 23 Morphological rearrangements of mitochondria do not trigger major stress response pathways. **A.** Cells of the indicated strains were grown in galactose media in the presence of ATc for 16 hours. Afterwards they were harvested and YFP intensity was measured. Cells contained YFP reporters under control of the heat shock element (HSE), the proteasome-associated control element (PACE), or the pleiotropic drug response element (PDRE). Shown is the fold change in YFP intensity over wild type for 3 biological replicates (HSE and PACE) and one replicate for PDRE. **B** Cells were grown as described in A. Afterwards RNA was extracted the levels of spliced *HAC1* were measured with RT qPCR. Shown is the fold change in spliced *HAC1* mRNA abundance over wild type for 3 biological replicates.

To check for induction of the UPR, I employed RT qPCR to measure the levels of spliced *HAC1* compared to *ACT1*. Here treatment for one hour with either DTT or tunicamycin served as positive controls. As above cells were grown in liquid media and induced for 16 hours. Afterwards the cells were lysed, RNA was extracted and the mRNA levels were determined via RT qPCR. Again, induction of the UPR was not observed either (Fig. 23B). Thus, the structural abnormalities seen upon loss of ERMES are not accompanied by a ‘classical’ stress response, however it is likely that some type of signal is transmitted to the nucleus and this in turn triggers a response by a yet unknown mechanism.

In summary, these findings suggest that indeed Tom70 and ERMES have overlapping functions in their role as constituents of MCSs and furthermore are parallel axes within the ER-SURF pathway. ER-membrane contact sites might even be relevant for the intracellular sorting of proteins and therefore the identity of organellar membranes.

3.10 Identifying a core set of ER-SURF clients using affinity purification of ER and mitochondria

Due to the considerable membrane mixing, in conditions where MCSs are disturbed, during classical fractionation procedures I decided to employ a strategy to purify ER and mitochondria using affinity purification based on an established technique [122], in order to assess whether mitochondrial precursors would strand on the ER upon loss of contact sites.

This method is based on the expression of membrane proteins on the target organelle with a tandem affinity tag (referred to as bait-tag from here on after), consisting of a myc epitope followed by a 3C protease cleavage site fused to a FLAG epitope. Thus, I used Tom20, the major receptor of the TOM complex, for the mitochondrial membrane, Sec63, main constituent of the SEC translocon on the ER, and Rtn1, responsible for the tubular structure of the ER, for the ER membrane. I genomically tagged these with the bait-tag in wild type and $\Delta tom70$ cells and transformed the generated strains with either an empty vector or the *MDM34*↓ plasmid. In addition, I transformed wild type and $\Delta tom70$ cells without a bait-tag with the same plasmids to serve as negative controls. I grew all strains in minimal galactose-containing media inducing depletion for 16 hours with ATc. Then the cells were harvested, lysed and subjected to crude subcellular fractionation via differential centrifugation. The last pellet fraction (containing ER and mitochondria) was used for immunoprecipitation against the FLAG epitope. Afterwards, the organelles were released by addition of 3C protease and reisolated via centrifugation. The obtained fraction was then lysed, digested with Trypsin and subjected to LC-MS/MS (Fig. 24A).

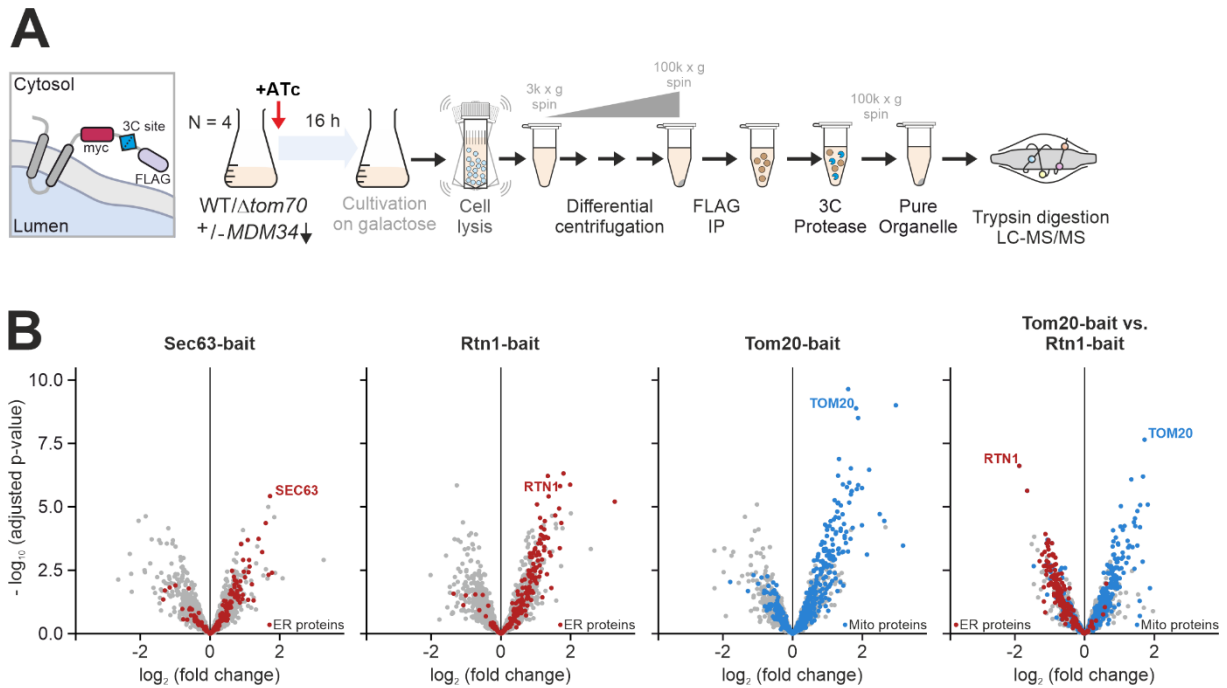


Fig. 24 ER and mitochondria can be isolated via affinity purification. A. Schematic depiction of the bait-tag and workflow of the proteomic analysis of wild type and $\Delta tom70$ with a bait-tag on either Tom20, Rtn1 or Sec63 and each with an empty vector or the $MDM34\downarrow$ plasmid. **B.** Comparison of the proteomes of wild type cells with no bait-tag and empty vector to wild type cells with a bait-tag on the indicated protein with an empty vector (first three plots). Comparison of the proteomes of wild type cells with Tom20-bait and empty vector to wild type cells with Rtn1-bait with an empty vector (last plot on the right). Mitochondrial proteins [5] were indicated in blue. ER proteins were indicated in red [117].

Preliminary analysis of the data obtained for the wild type condition showed that Sec63-bait and Rtn1-bait pull down many ER proteins, albeit that Rtn1-bait led to an even stronger enrichment. By the same token, Tom20-bait pulled down many mitochondrial proteins. Comparison of Tom20-bait and Rtn1-bait showed a clear separation between ER and mitochondria, implying that the two membranes can be separated using this purification approach (Fig. 24B).

Next, I wanted to know if mitochondrial proteins change their distribution between ER and mitochondria in response to depletion of ERMES. Therefore, I performed a correlation analysis looking at the Tom20 versus the Rtn1 pulldown in wild type compared to $MDM34$ knockdown. Specifically, I was interested in proteins that would be enriched in the Tom20 pulldown only in wild type conditions ($\log_{2}FC$ in wild type > 0.75) but not in the knockdown condition ($\log_{2}FC$ in $MDM34\downarrow$ between -0.75 and 0.75), because this implies a shift in distribution from most of the protein in/on mitochondria in the former case to the protein being more present on the ER in the latter case. Additionally, I excluded proteins that were too similar in enrichment in both cases ($|\log_{2}FC$ wild type $- \log_{2}FC$ $MDM34\downarrow$ < 0.5).

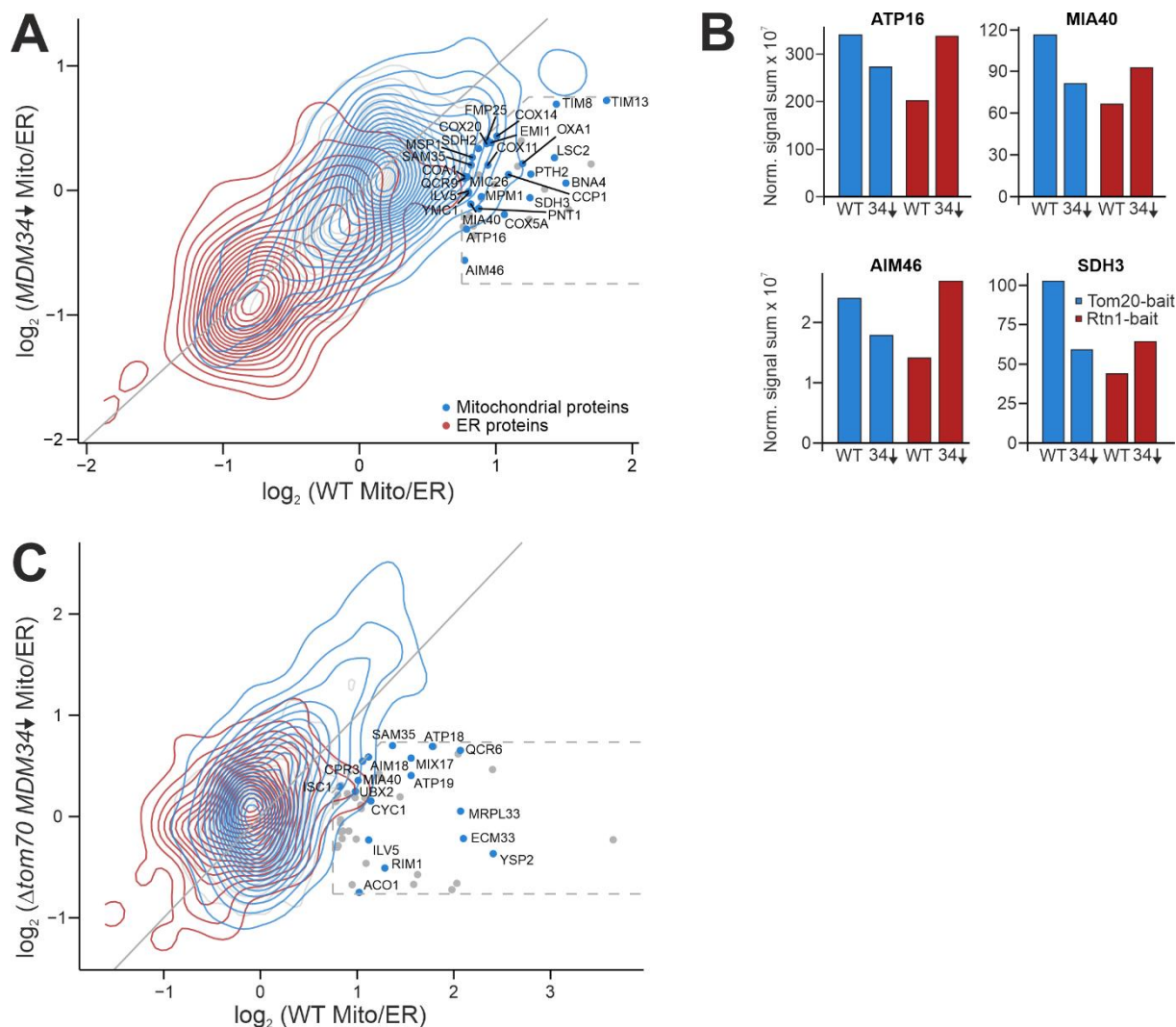


Fig. 25 A subset of mitochondrial proteins accumulate on the ER in the absence of contact sites. **A.** Correlation analysis showing the log₂ fold changes of the Rtn1 and Tom20 affinity purification samples from wild type (x-axis) and *MDM34* knockdown (y-axis) cells. Data points were represented as 2 dimensional densities and only points in the target area were indicated for better visibility. Mitochondrial proteins [5] were indicated in blue. ER proteins were indicated in red [117] and all other proteins were indicated in grey. **B.** Normalized signal intensities for specified proteins in either wild type or *MDM34* knockdown cells for Tom20 or Rtn1 pulldowns. **C.** Correlation analysis of Sec63 versus Tom20 pulldown for wild type (x-axis) and double mutant (y-axis).

The correlation analysis revealed a subpopulation of proteins that met the established criteria among which was Oxa1, the model substrate of ER-SURF (Fig. 25A). This was an indication that this approach indeed allowed for the identification of ER-SURF substrates. Moreover, the correlation analysis also demonstrated that ER and mitochondria are separable through immunoprecipitation and that most proteins behave rather similarly in both conditions. Looking closer at the target set and analyzing the normalized signal intensity many of the proteins showed the expected shift in intensity from mitochondria to ER when Mdm34 is absent (Fig. 25B). However, some proteins only showed a reduction in the mitochondrial signal and no increase in the ER signal, which still put them in the target set (data not shown). I reasoned that this might be due to their possible degradation by the ERAD machinery, which would create a

similarly balanced system akin to the classical routing of precursor proteins and the competition between import and degradation in the cytosol [93,120,123,124]. I applied the same correlation analysis to wild type versus $\Delta tom70$ and also wild type versus the double mutant. Looking at the comparison with the double mutant the separation between mitochondria and ER was almost completely lost like the phenomenon observed for the highly purified mitochondria (Fig. 25C, Fig. 21B). This argues in favor of the idea that ER mitochondria contact sites determine the molecular identity of the respective organelle.

Using the results of the correlation analysis and further expanding it to all mitochondria versus ER pulldowns I was able to compile a list of 84 putative ER-SURF clients. All putative ER-SURF clients are listed in Tab. 1. The list contained the mostly membrane proteins (~ 75 %) further buttressing the relevance of ER-SURF for hydrophobic membrane proteins.

Tab. 1 Set of putative ER-SURF clients. Given are the systematic and standard name as well as the mitochondrial sub localizations and protein type [5,125,126]. Sub localizations were abbreviated as follows: OMM for outer mitochondrial membrane, IMS for inter membrane space and IMM for inner mitochondrial membrane.

Systematic Name	Standard Name	Sub localization	Type
YBR078W	ECM33	IMM	Membrane
YOL077W-A	ATP19	IMM	Membrane
YHR199C	AIM46	IMM	Membrane
YKL141W	SDH3	IMM	Membrane
YNL052W	COX5A	IMM	Membrane
YOR266W	PNT1	IMM	Membrane
YKL195W	MIA40	IMM	Membrane
YPR058W	YMC1	IMM	Membrane
YPL132W	COX11	IMM	Membrane
YGR235C	MIC26	IMM	Membrane
YDR231C	COX20	IMM	Membrane
YLR077W	FMP25	IMM	Membrane
YEL024W	RIP1	IMM	Membrane
YMR157C	AIM36	IMM	Membrane
YNR018W	RCF2	IMM	Membrane
YER141W	COX15	IMM	Membrane
YML030W	RCF1	IMM	Membrane
YML081C-A	ATP18	IMM	Membrane
YDL004W	ATP16	IMM	Membrane
YER154W	OXA1	IMM	Membrane
YGR183C	QCR9	IMM	Membrane
YIL157C	COA1	IMM	Membrane
YDR512C	EMI1	IMM	Membrane
YML129C	COX14	IMM	Membrane
YLL041C	SDH2	IMM	Membrane
YJR095W	SFC1	IMM	Membrane
YGR147C	NAT2	IMM	Membrane
YJL054W	TIM54	IMM	Membrane
YOR211C	MGM1	IMM	Membrane

YDR316W	OMS1	IMM	Membrane
YMR089C	YTA12	IMM	Membrane
YOR222W	ODC2	IMM	Membrane
YPL063W	TIM50	IMM	Membrane
YLR008C	PAM18	IMM	Membrane
YDL174C	DLD1	IMM	Membrane
YGR231C	PHB2	IMM	Membrane
YBR262C	MIC12	IMM	Membrane
YKR016W	MIC60	IMM	Membrane
YNL100W	MIC27	IMM	Membrane
YOL027C	MDM38	IMM	Membrane
YBL030C	PET9	IMM	Membrane
YDL067C	COX9	IMM	Membrane
YMR302C	YME2	IMM	Membrane
YFR033C	QCR6	IMM	Membrane
YOR271C	FSF1	IMM	Membrane
YGR181W	TIM13	IMS	Soluble
YKR066C	CCP1	IMS	Soluble
YBR091C	TIM12	IMS	Soluble
YMR002W	MIX17	IMS	Soluble
YJL066C	MPM1	IMS	Soluble
YJR135W-A	TIM8	IMS	Soluble
YOR090C	PTC5	IMS	Soluble
YMR145C	NDE1	IMS	Membrane
YJR048W	CYC1	IMS	Soluble
YLR355C	ILV5	Matrix	Soluble
YDL202W	MRPL11	Matrix	Soluble
YCR028C-A	RIM1	Matrix	Soluble
YMR286W	MRPL33	Matrix	Soluble
YGR244C	LSC2	Matrix	Soluble
YKL192C	ACP1	Matrix	Soluble
YOR020C	HSP10	Matrix	Soluble
YPL215W	CBP3	Matrix	Soluble

YLR304C	ACO1	Matrix	Soluble
YML078W	CPR3	Matrix	Soluble
YHR083W	SAM35	OMM	Membrane
YHR198C	AIM18	OMM	Membrane
YML013W	UBX2	OMM	Membrane
YBL057C	PTH2	OMM	Membrane
YGR028W	MSP1	OMM	Membrane
YNL026W	SAM50	OMM	Membrane
YER019W	ISC1	OMM	Membrane
YER004W	FMP52	OMM	Membrane
YBL098W	BNA4	OMM	Membrane
YPL186C	UIP4	OMM	Membrane
YOR045W	TOM6	OMM	Membrane
YBR179C	FZO1	OMM	Membrane
YNL131W	TOM22	OMM	Membrane
YIL065C	FIS1	OMM	Membrane
YPR133W-A	TOM5	OMM	Membrane
YNL070W	TOM7	OMM	Membrane
YMR203W	TOM40	OMM	Membrane
YKL027W	TCD2	OMM	Membrane
YDR326C	YSP2	unknown	Soluble
YLR305C	STT4	unknown	Soluble

Altogether I could show that ER and mitochondria can be purified via affinity purification and moreover the obtained fractions could be used in tandem with mass spectrometry to probe the mis-localization of a subpopulation of mitochondrial proteins. In turn, I was able to generate a set of proteins that might use the ER-SURF pathway for their biogenesis.

3.11 Hydrophobic transmembrane segments determine the contact site dependence of mitochondrial proteins

Having established a preliminary set of proteins that depend on the ER-SURF route, I further wanted to investigate the determinants of ER-SURF dependence. The sorting of tail-anchored proteins, which are present on both ER and mitochondrial membranes, is mainly determined by

the hydrophobicity of their transmembrane domain [127,128]. Thus, I assumed that a similar mechanism might determine the route mitochondrial precursors take.

For further analysis, I focused on proteins of the inner mitochondrial membrane since they make up the largest group of ER-SURF clients. I analyzed the hydrophobicity of the inner membrane proteins of ER-SURF in comparison to all other inner membrane proteins of the mitochondria. Therefore, I calculated the scaled local hydrophobicity over a 21 amino acid window [129] representing the typical length of a transmembrane segment.

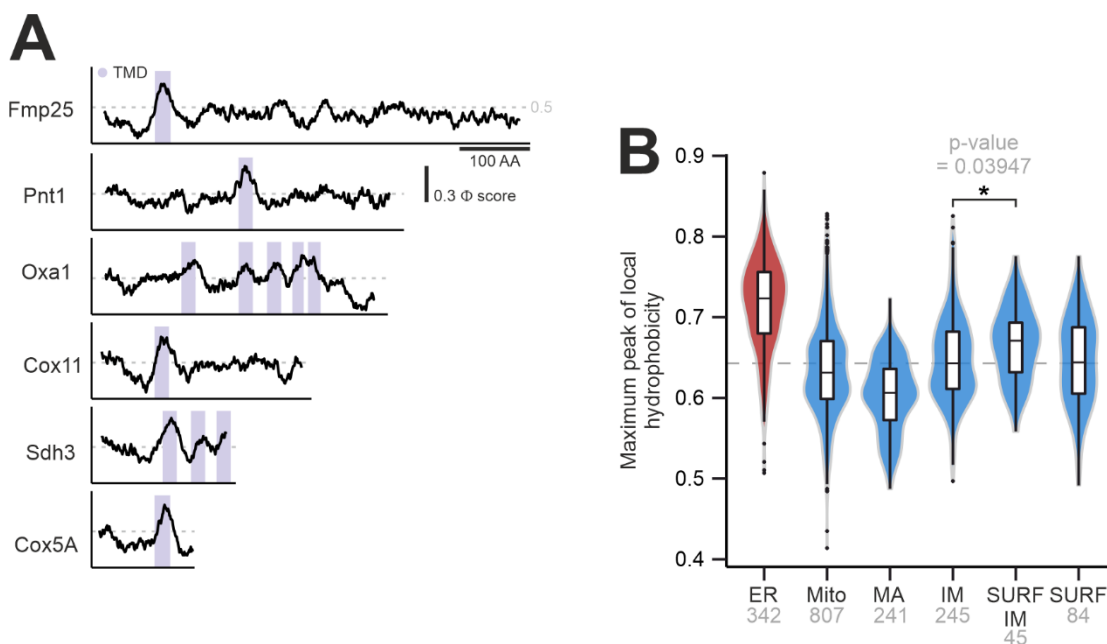


Fig. 26 Inner membrane proteins of ER-SURF have very hydrophobic transmembrane domains. A. Hydrophobicity profiles of several Mdm34-dependent inner membrane proteins. Hydrophobicity (Φ) scores were calculated from a 21-residue window [129]. Transmembrane domains (TMD) are highlighted. AA, amino acid residues. **B.** The violin plots show the distribution of the peak in hydrophobicity of proteins in the indicated subpopulation. The hydrophobicity was calculated as described in A and the peak value for each protein extracted. Statistical difference was calculated with a Kolmogorov-Smirnov test comparing the indicated subpopulations with all other mitochondrial proteins. Statistical significance was assigned as follows: p-value < 0.05 = *, p-value < 0.01 = **, p-value < 0.005 = ***.

Looking at the hydrophobicity distribution plotted over the length of the protein many proteins showed a high peak of hydrophobicity in their transmembrane domains (Fig. 26A). Next, I compared the distribution in peak local hydrophobicity between the ER-SURF groups and all other mitochondrial proteins. No difference was observed comparing all ER-SURF clients with all other mitochondrial proteins, however just looking at the subclass of inner membrane proteins revealed a significant upward shift in the distribution of ER-SURF proteins (Fig. 26B) arguing in favor of the idea that similar to tail-anchored proteins ER-SURF dependence is at least in part determined by hydrophobicity.

Next, I wanted to test the direct dependence of precursor import on Mdm34 and Tom70. Hence, I prepared semi-intact cells from wild type and $\Delta tom70$ each harboring an empty vector or the $MDM34\downarrow$ plasmid that have been depleted for ERMES for 16 hours. I incubated these with several radiolabeled substrates and quantified the import into mitochondria of these semi-intact cells in comparison to wild type.

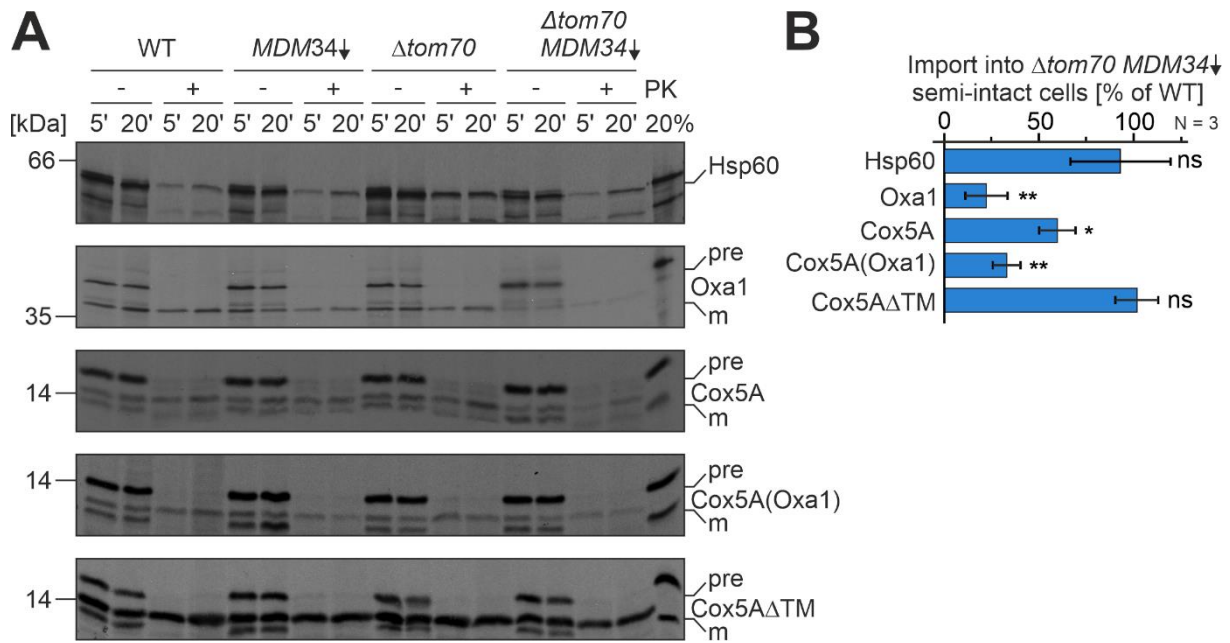


Fig. 27 Oxa1 and Cox5A are dependent on Tom70 and ERMES in the context of ER-SURF. **A** Radiolabeled lysates were synthesized in reticulocyte lysate in the presence of ^{35}S methionine and incubated with semi-intact cells obtained from the indicated strains. After 5 and 20 minutes, the cells were isolated, treated without or with proteinase K (PK) for 30 min on ice and subjected to SDS-PAGE, western blotting and autoradiography. 20% of the radioactive protein used per import reaction was loaded for comparison. **B** Quantification of the import of the indicated proteins into semi-intact cells of wild type and double mutant of three biological replicates ($n = 3$). Statistical difference was calculated with a student's t-test. Statistical significance was assigned as follows: p-value $< 0.05 = *$.

As shown in Fig. 27A loss of ERMES or Tom70 did not impair the import of any of the chosen substrates, again reflecting the redundant functions of the two contact sites. In contrast, loss of both severely impacted the import capacity for Oxa1 and Cox5A. Deleting the single transmembrane segment of Cox5A, yielding a soluble matrix protein, fully restored the import capacity in the double mutant. Generating a chimera of Cox5A with the second transmembrane domain of Oxa1 instead of the native transmembrane segment, yielding Cox5A(Oxa1) [130], once again restored the dependency on the contact sites. The import of the control protein Hsp60 was unperturbed in all tested conditions (Fig. 27A-B). These findings confirm that a single hydrophobic stretch can determine the dependence of precursor proteins on membrane contact sites and in turn on ER-SURF.

To test the relevance of membrane contact sites in a more physiological condition I decided to again use the Oxa1 overexpression approach (Fig. 5A). To this end, I transformed the strains with the Oxa1 overexpression plasmid. Next, I induced the depletion of ERMES for 8 hours and subsequently added galactose to induce expression of Oxa1. After 4 more hours of growth cells were harvested, lysed and subjected to SDS-PAGE.

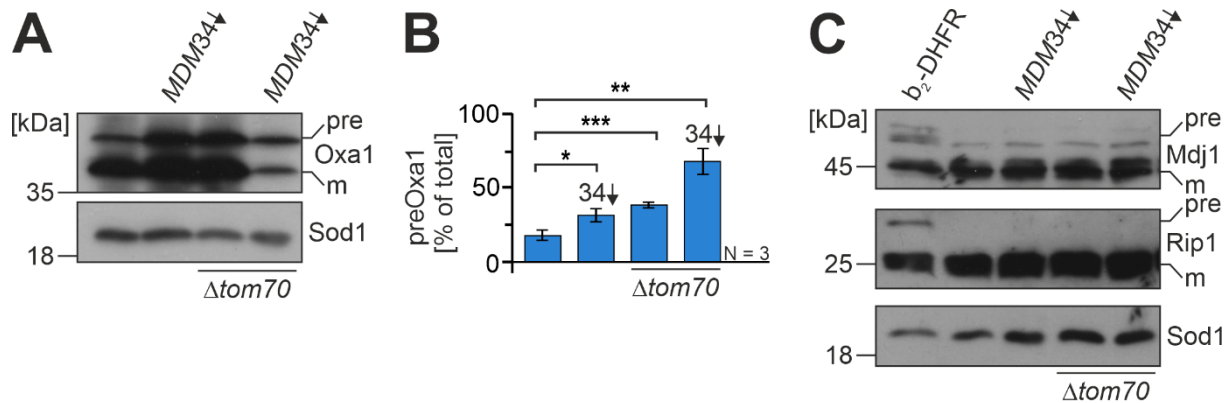


Fig. 28 Membrane contact sites are important for the biogenesis of Oxa1. **A** Western blot analysis of cells carrying an Oxa1 overexpression plasmid. Cells of the indicated strains were grown in lactate medium with ATc for 8 hours and shifted to lactate medium that contains ATc and 0.5% galactose for 4 hours to induce expression. Cells were harvested, lysed and subjected to SDS-PAGE. The precursor (pre) and mature (m) species of Oxa1 are indicated. Shown is the relative amount of precursor Oxa1 in relation to the total amount of Oxa1 (precursor + total). **B** Plotted are mean values and standard deviations of three biological replicates. Statistical difference was calculated with a student's t-test. Statistical significance was assigned as follows: p-value < 0.05 = *, p-value < 0.01 = **, p-value < 0.005 = ***. **C** Western blotting analysis of steady-state precursor formation of Rip1 and Mdj1. Cells were treated as described in A. Cells that express b₂-DHFR were used as a positive control.

Upon loss of the ERMES or Tom70 contact site a marked and significant increase of the Oxa1 precursor form was observed. In the absence of both contact a large accumulation of precursor Oxa1 was apparent concomitant with a strong synthetic defect in Oxa1 biogenesis (Fig. 28A-B). Following this result, I wondered whether the observed defect could be explained by a compromised or clogged import machinery. To this end I measured protein steady-state levels of Mdj1 and Rip1, which show precursor accumulation in conditions of a compromised import [92,131]. As a positive control, I expressed the b₂-DHFR fusion construct. Western blotting analysis revealed that loss of contact sites does not lead to precursor accumulation of either Rip1 or Mdj1 (Fig. 28C). Thus, these data show that contact sites are relevant for the biogenesis of hydrophobic inner membrane proteins *in vivo*.

All in all, I demonstrated that one determinant for contact site dependence is hydrophobicity of a given transmembrane segment. Moreover, I could show that *in vitro* and *in vivo* contact sites are relevant for the biogenesis of inner membrane proteins and that this effect is unrelated to a disturbed import mechanism.

In this study, I could demonstrate that ERMES is critical for the ER-SURF pathway and works in parallel to Tom70 and Djp1. Loss of one or both contact sites leads to a strong abatement of mitochondrial proteins concomitant with growth impairments on respiratory media. The immunoprecipitation of organelles coupled with mass spectrometry identified 84 putative ER-SURF clients, which are predominantly membrane proteins. Moreover, ER-facilitated import of mitochondrial proteins seems to be dependent on the hydrophobicity of a given transmembrane domain.

4. DISCUSSION

The aim of this work was to investigate whether membrane contact sites might be involved in the ER-SURF pathway. Indeed, I could demonstrate that ERMES as well as the contact site formed by Tom70 are vital for ER-SURF. Moreover, I could expand the client spectrum of the ER facilitated import and gain insight into a possible mechanism that leads to the association of mitochondrial proteins with the ER. In the following, I want to discuss limitations of this work as well as alternative hypotheses. Furthermore, I want to examine possible mechanisms and the relevance of ER-SURF for protein sorting and cellular proteostasis.

4.1 CRISPRi as an effective tool to interrogate the role of MCSs in protein biogenesis

The use of the CRISPR-mediated depletion of *MDM34* was crucial in unraveling the involvement of ER-SURF within the scope of this study. Upon induction of the system, *MDM34* was depleted rapidly and efficiently, which was also reflected on the protein level (Fig. 12, Fig. 15). These observations are consistent with the findings of *Smith et al.* [107]. However, looking at the persistence of the knockdown, a recovery of the *MDM34* mRNA levels was apparent (Fig. 12). This recovery seemed to coincide with the metabolic reprogramming during the diauxic shift and an increase in the tetracycline concentration was necessary to partly suppress this recovery (Fig. 13). Moreover, the mass spectrometric analysis of whole cells showed only a mild depletion of Mdm34 (Fig. 19). This observation might arise due to several reasons. Firstly, during the long induction time in the experimental setup, the knockdown efficiency might have diminished. In contrast, the occurring ratio compression, when using TMT labels and multiplexing complex samples in a mass spectrometer [132], led to an underestimation in the difference of the measured peptide/protein intensities. Due to these counteracting effects, it is hard to judge to what extent Mdm34 was depleted using CRISPRi over longer periods of time. However, a marked difference in the mitochondrial proteome was observed implying that ERMES was lost to a sufficient extent to elicit a response, which is also reflected in the synthetic defect when depleting Mdm34 in a deletion background of *TOM70* (Fig. 18, Fig. 19).

The efficiency of CRISPRi is mainly determined by: (1) the distance (-300 to -100 bp) of the gRNA target sequence to the transcriptional start site (TSS), (2) the presence of a protospacer adjacent motif (NGG for Cas9 from *S. pyogenes*) in the target area, (3) the nucleosome occupancy and (4) chromatin accessibility [107]. However, I could demonstrate that the knockdown was not persistent in the case of *MDM34* and seemed to be linked to metabolic

rewiring (Fig. 13). Moreover, Mdm34 was not fully depleted and a small pool remained, which might be incompatible for specific applications and needs to be considered when adapting this technique to other targets. It is also conceivable that depletion of a given mRNA might be counteracted by increased translation. Another aspect is the timing of the depletion. This approach takes a minimum of 6 to 8 hours to diminish the protein amount (Fig. 15). In comparison to degron-mediated depletion, this approach is slower [133], which might be incompatible with certain experimental setups. One major advantage of this system is that all components are encoded on one plasmid (Fig. 12). In contrast, other approaches to create conditional mutants require genomic alterations, e.g., in temperature-sensitive mutants, DAmP (decreased abundance by mRNA perturbation) mutants or for degron mediated depletion [133–135]. This makes it easy to employ this system and test many different conditions and genomic backgrounds. However, since major determinants of this system’s efficiency are epigenetic, it is crucial to validate the knockdown efficiency when switching between strain backgrounds. The ease of creating a knockdown plasmid as well as its application make this system well suited to study essential genes, synthetic negative interactions as well as circumvent the generation of suppressor mutations.

4.2 ER-SURF is dependent on the presence of ER-mitochondria contact sites

In this thesis, I could establish ERMES and Tom70 as components of the ER-SURF pathway. I could show that the import of hydrophobic inner membrane proteins is affected upon loss of both contact sites (Fig. 27), that the biogenesis of Oxa1 is impaired *in vivo* (Fig. 28) and that a specific subclass of mitochondrial proteins is enriched on the ER surface (Fig. 25). Nevertheless, several questions remain about the transfer of proteins from the ER to mitochondria.

Does ERMES have an active role in protein transfer? The expression of a synthetic tether construct was not sufficient to rescue the import defect observed when Mdm34 is not present (Fig. 10), implying that proximity alone might not be enough to facilitate transfer of preproteins to mitochondria. This might also be due to the fact that the chimera tether is not dynamic, does not provide the proper distance or the GFP barrel between the two membranes poses too large an obstacle for a precursor protein. Since ERMES components do not contain any typical protein interacting domains that would allow for the handling of a wide range of substrates [136,137] it seems unlikely that ERMES directly contacts precursors that come from the ER. However, it might also be the case that ERMES associates with additional proteins that aid in the transfer or pose as an assembly platform for the transfer “machinery”. Indeed, *Hansen et*

al., could show that depletion of Cdc48, one of the main protein extractors from mitochondria and ER, markedly increased the accumulation of Oxa1 on the ER surface, which indicates that Cdc48 might be required for the extraction and degradation of Oxa1 or alternatively that Cdc48 can extract Oxa1 and allows for its retargeting in the context of ER-SURF [32]. Surprisingly, one of the proteins that was more abundant upon depletion of Tom70 and ERMES was Der1 (Fig. 19), whose role in ERAD-L is well-established [10]. This raises the question why Der1, involved in the degradation of luminal ER proteins, might be upregulated in conditions where mitochondrial proteins accumulate on the ER surface? One tempting hypothesis is that Der1 aids in the release of such stranded proteins, due to its membrane thinning properties [138], since Der1 works in concert with Usa1, Hrd1, Der3, Ubx2 and many more components [10], none of which are upregulated in the same manner. However, mass spectrometry only reflects abundance, meaning that it is not possible not conclude whether Der1 is less degraded or stronger translated. To this end a transcriptomic analysis would be required, which would shed light on the transcriptional regulation and allow to infer whether the changes on the proteome are due to transcriptional effects or due to degradation.

How are proteins brought to and retrieved from ERMES? The *in vitro* import assays indicate that ERMES works in parallel to Djp1 (Fig. 5, Fig. 7) and in parallel to Tom70 (Fig. 18, Fig. 27) implying that the former forms one arm of ER-SURF and the latter two a second arm. Tom70 and Djp1 are well suited to handle a broad substrate range due to their intrinsic nature as an import receptor at TOM and as an Hsp40 protein respectively [73,139]. It is conceivable that a redundant pathway would work in a similar fashion with similar properties. Ydj1, similar to Djp1, is in part localized to the ER through a farnesyl anchor [140], interacts with Tom20 and is crucial for the targeting of mitochondrial proteins [65]. It has been implicated playing a role in the targeting of the β -barrel proteins and signal anchored proteins of the outer membrane [67,141]. This substrate spectrum would cover most of the outer membrane proteins identified here as ER-SURF clients (Tab. 1) and complement that of Djp1. These properties make Ydj1 an interesting candidate, however till now there is no indication that Ydj1 interacts with any ERMES subunit nor that it localizes to membrane contact sites in general.

Which determinants are crucial for ER-SURF targeting? ER-SURF was initially established as a pathway mainly for hydrophobic inner membrane proteins of mitochondria [32]. Using affinity-purified organelles in tandem with mass spectrometry I could, for the first time, compile a set of putative client proteins of ER-SURF (Fig. 25) and indeed most of these proteins were residents of the inner membrane (Tab. 1). Moreover, looking at the maximum peak in local

hydrophobicity it turned out that ER-SURF clients on average, exhibit higher peaks than other inner membrane proteins. This suggests that hydrophobicity is a key factor in the route precursors take towards mitochondria (Fig. 26). This idea was further validated by showing that the dependence of Cox5A on contact sites was directly related to the presence or absence of a transmembrane domain (Fig. 27). Nevertheless, highly hydrophobic carrier proteins which reside in the inner membrane and are very abundant were not found among the ER-SURF clients indicating that hydrophobicity might not be the only determinant. Although, the fact that carriers were not in the substrate list might be due to the limitation of solubilizing and keeping hydrophobic proteins stable in solution for mass spectrometric measurements, leading to poor quantification of peptides generated from such proteins [142]. Shakya and colleagues could show that upon treatment of cells with CCCP a certain group of mitochondrial proteins, including carrier proteins Mir1, Oac1 and Dic1, associate with the ER membrane [56]. It remains unclear however if this effect is due to precursor overaccumulation or whether carrier proteins are true clients of ER-SURF.

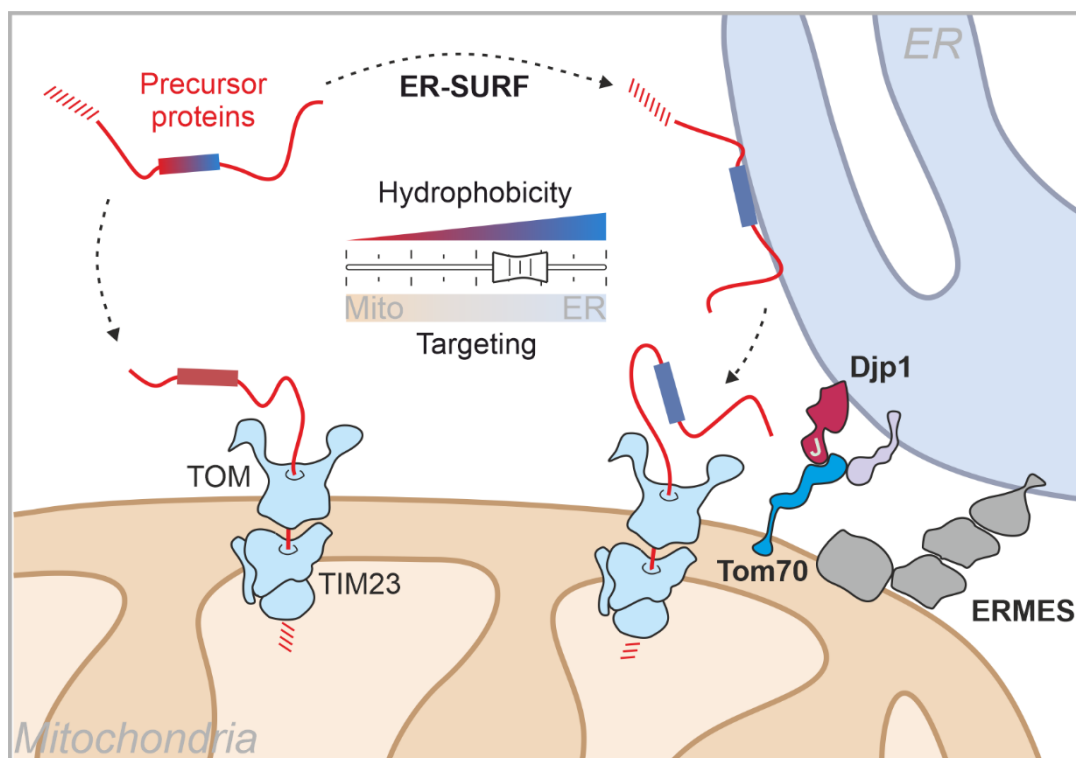


Fig. 29 Proposed model of ER-SURF routing. Mitochondrial membrane proteins, especially of the inner membrane can associate with the ER surface. This is caused by very hydrophobic transmembrane segments. However, the stranded proteins can be retargeted towards mitochondria via two redundant routes: ERMES and Djp1/Tom70.

Taken together these findings show that mitochondrial membrane proteins, depending on the hydrophobicity of their transmembrane domain, are targeted to the ER either by erroneous recognition by SRP, by binding of Get3 or by yet unknown mechanisms. Afterwards, these proteins can take one of two routes for retargeting either via the Djp1/Tom70 axis or via the ERMES axis and subsequently be productively imported into mitochondria (Fig. 29).

4.3 Protein trafficking via ER-SURF is independent of lipid transfer at MCSs

Membrane contact sites were initially identified in an effort to uncover the lipid transport between ER and mitochondria, given that the latter is not part of the endomembrane system. Indeed, extensive work has shown that ERMES transports lipids between the two organelles. Although it was debated what type of lipid species ERMES transports, there is good evidence that it is mainly phosphatidylserine (PS) and to a lesser extent phosphatidylethanolamine (PE). Hence, an altered lipid composition was observed when ERMES was lost [22,23,143,144].

One argument that may be raised is that the observed effects upon loss of ERMES are indirectly caused by an altered lipid composition of these cells. This in turn could lead to an impaired import or destabilize membrane proteins explaining accumulation on the ER membrane in the former case and decreased abundance in the latter. Decreased levels of PE and cardiolipin have been shown to affect the import efficiency of mitochondrial precursor proteins and the stability of the import complexes [145–148]. However, the import experiments with the *MDM34* deletion clearly show that there is no import impairment on the mitochondrial level (Fig. 8). Moreover, the double deletion of *MDM34* and *DJPI* only affects Oxa1 and Coq2 and not Hsp60 and MrpIL15 in the semi-intact cell assay further demonstrating that the import machinery per se is intact (Fig. 7, Fig. 9). By the same token, import experiments with the depletion model only affect Oxa1 and Cox5A, whereas Hsp60 and Cox5A Δ TM show normal import (Fig. 27). The initial experiments were conducted with deletions of *MDM34*, which turned out to be suppressor mutants. The suppressor mutant of ERMES did not exhibit any growth defects (Fig. 11) or a disturbed mitochondrial morphology (data not shown) indicating that the observed import defects were independent of an altered lipid composition of mitochondria. A recently developed approach of mass tagging of lipids *in vivo* could, for the first time, demonstrate the lipid transport activity of ERMES in a cellular context. The authors of this study demonstrated that loss of ERMES partly abolishes lipid flux between ER and mitochondria, however, the overall lipid composition of mitochondria was hardly changed. Only disruption of ERMES and vCLAMP (the contact site between mitochondria and the vacuole), which in part is formed by Mcp1 and Vps13, markedly changed the lipid composition of mitochondria [149].

Taken together these findings indicate that the observed import defects are a direct consequence of loss of ERMES. Nevertheless, a partial lipid borne effect cannot be excluded especially in the depletion model. A lipidomic approach would be necessary to elucidate any changes in mitochondrial lipids, however proteomic analysis of isolated mitochondria and affinity-purified mitochondria showed considerable “contamination” with ER proteins (Fig. 21, Fig. 25). Thus, any purified mitochondrial fraction contains ER which in turn would bias the lipidomic analysis making it hard to draw any conclusions about changes to the mitochondrial lipidome.

Another alternative hypothesis to the one presented here is that precursor overaccumulation in the cytosol leads to random association of mitochondrial proteins with the ER, as observed by expression of the b₂-DHFR fusion protein or upon depletion of the membrane potential with CCCP [119,120]. However, also in this case the import experiments demonstrate that the import machinery is unaffected by loss of contact sites between ER and mitochondria. Moreover, characteristic precursor accumulation for Rip1 and Mdj1 was not observed in conditions where ERMES and or the Tom70 contact sites were absent (Fig. 28). The YFP reporter assay revealed that loss of membrane contact sites does not trigger a response for HSE, PACE or PDRE (Fig. 23), which are signature response pathways to precursor overaccumulation in the cytosol [93,119]. *Knöringer et al.* could show that expression of the ‘clogger’ protein leads to induction of the unfolded protein response on the ER [121], which also was not the case for loss of contact sites (Fig. 23). Hence, it is unlikely that the observed phenotypes are caused by precursor overaccumulation in the cytosol.

4.4 The ER as a productive partner in mitochondrial protein biogenesis

Why have cells evolved a pathway such as ER-SURF? Proteins of mitochondria and ER are targeted to their cognate organelle by similar concepts (N-terminal signals, internal signals or TA proteins) [46]. The two organelles share major components of quality control pathways e.g., Cdc48 and Ubx2 [150]. Moreover, protein dislocases (Msp1 and Spf1) are present on the ER as well as mitochondria to aid in sorting tail-anchored proteins to their proper destination [95–97]. It seems that under the given conditions a pathway, such as ER-SURF, that facilitates these targeting and quality control mechanisms seems feasible.

In the case of carrier proteins, ER-SURF might pose as a protective mechanism for the cytosolic proteostasis. Due to their hydrophobic nature and aggregation propensity carrier proteins pose a large burden on the cytosolic chaperone network [60,77,151]. Therefore, it is conceivable that the cell actively tries to distribute such proteins onto the ER, a large membrane system in the

cell, which yields several benefits: (1) preventing aggregation, (2) increasing the chaperone capacity of the cytosol and (3) allow for targeting and import into mitochondria. Xiao and colleagues could already show that carrier proteins are transported to the ER in a Get3 mediated fashion preventing their aggregation in conditions where the mitochondrial membrane potential is low and import is not possible [60].

ER-SURF might also be relevant for proteins that are dually localized. Ubx2 which is present on both membranes and involved in MAD and ERAD [10,92], was also among the putative ER-SURF clients (Tab. 1). Psd1, a protein of the inner membrane, is also found on the ER [152,153]. Although, it was not identified as a client, similar to Oxa1 it can be recognized by SRP and presumably be targeted to the ER [57] and moreover be subject to ER-SURF. ER facilitated transport might serve as a gatekeeper for such proteins and thereby regulate their distribution between the two membranes.

Although Djp1 and ERMES are not conserved in higher eukaryotes, a paralog of Mmm1, can be found in higher eukaryotes which also forms contacts between ER and mitochondria, called PDZD8 [154,155]. Loss or mutation of this protein is associated with altered mitochondrial morphology, disrupted calcium homeostasis, neurological disorders and cognitive impairments [154,156–158]. Moreover, a recent study in mammalian cells has shown that BCL2, which is a negative regulator of apoptosis, is transferred from the ER to mitochondria at membrane contact sites in a Tom20 mediated fashion [159]. These findings imply that the players of ER-SURF might not be conserved but the pathway in itself might be.

In summation, the results of this study could further our understanding of the ER-SURF pathway demonstrating that membrane contact sites are vital players in this context. I could uncover a possible targeting mechanism akin to the sorting mechanism of tail-anchored proteins. Moreover, I was able to establish a set of proteins that use ER-SURF. However, many questions still remain, regarding the mechanistic details, the client spectrum as well as the conservation of this pathway.

5. OUTLOOK

The findings of this study clearly establish ER-mitochondria contact sites as critical components in the ER-SURF pathway. Nevertheless, many aspects remain elusive.

To exclude any lipid-borne effects, when contact sites are impaired, a lipidomic analysis would be most informative. However, the problem of obtaining pure mitochondria remains. However, mutants of ERMES components that do not transport any lipids have been characterized [160]. Expressing such a mutant from a plasmid, while depleting the genomic version using CRISPRi, would create intact ERMES complexes that cannot transport lipids. This in turn should rescue the import defect into semi-intact cells showing that protein transport is independent of lipid transport. A similar approach would be to overexpress the dominant suppressor mutant of Vps13 (D716H) [106], which would also permit to dissect the lipid transport activity from the protein transfer.

Since depletion of contact sites leads to marked changes of the whole cell proteome it would be interesting to see whether the changes are caused by degradation or by translation. Thus, a transcriptomic approach would be well suited to answer this question and by extension shed light on primary and secondary effects upon loss of ER-mitochondria contact sites.

The ER-SURF set identified here was based on mass spectrometric analysis and would need to be validated. Therefore, testing more putative candidates in the semi-intact import could be one approach. However, this assay has several limitations: (1) It is an *in vitro* import assay, which does not necessarily reflect the situation *in vivo*. (2) The cytosol is partially washed out, which might contain important factors for association of proteins to the ER. (3) The assay shows a high variance between biological replicates and is strictly dependent on the quality of the obtained semi-intact cells. Another option would be to check protein-protein interaction of ER-SURF clients with the ER surface *in vivo*. One common way would be to use split GFP. Appending the 11th β -sheet to a client protein, expressing β -sheets 1-10 either on the ER surface with a tail-anchor sequence or in the client's cognate sub compartment and afterwards measuring and comparing GFP intensity [121]. This would give quantitative insight into the association of any protein with the ER. Additionally, microscopic analysis would indicate if the fully formed GFP shows the proper localization. One disadvantage of this approach is that the binding of the two GFP parts is irreversible. This could trap clients on the ER preventing proper release and thereby leading to overestimation of the ER-associated fraction. Thus, an alternative split fluorescent detection system would be the splitFAST, which additionally is also reversible

[161]. Such an assay would also allow not only to validate but also expand the clients of ER-SURF e.g., carriers for which it was already shown that they can associate with the ER. A more sensitive approach would be the BirA Avi-tag system, which was used to dissect the client spectrum of Sec61 and the alternative translocon in the ER Ssh1 [162]. It makes use of the fact that BirA specifically and efficiently biotinylates the Avi-tag in its vicinity. This system might provide the necessary specificity to check whether Djpl1/Tom70 have the same client spectrum to ERMES or whether they differ.

Another major question is how mitochondrial proteins end up on the ER. One approach to address this question would be to repeat the affinity purification of organelles followed by mass spectrometry using mutants of the signal recognition particle, mutants in Ssb1/Ssb2 or mutants of Cdc48. In case of an SRP mutant, one would expect fewer mitochondrial proteins on the ER if SRP is indeed one targeting factor. For Ssb1/Ssb2 and Ccd48 one would expect more mitochondrial proteins on the ER because the former fine tunes SRP in selecting only ER proteins, and the latter is responsible for extraction of proteins. Mutants of ERAD, especially Der1, would also be a good candidate. If upon perturbation of ERAD mitochondrial proteins accumulate on the ER, which is likely, then this would imply a competition for substrates of ER-SURF. Moreover, afterwards checking the import into semi-intact cells could determine the role of Der1 in protein transfer if import in such a mutant is disturbed for any given client.

It seems likely that more players take part in the transfer process of clients from ER to mitochondria. To get a better picture of proteins involved, a proximity labeling approach seems feasible [163,164]. This could allow for the identification of additional extractors, transfer proteins or even receptors on the mitochondrial surface.

Although, with this work, I could demonstrate the involvement of ERMES and Tom 70 contact sites in the transfer of precursor proteins from ER to mitochondria further research is required until a holistic picture of ER-SURF can emerge.

6. MATERIALS AND METHODS

6.1 Genetic Methods

6.1.1 *E. coli* strains

For plasmid purification and isolation, the *Escherichia coli* (*E. coli*) strain MH1 and DH5 α were used [165,166]. The strains are described in Tab. 2.

Tab. 2 Bacterial strains used in this study. Listed are the used *E. coli* strains with genotype and their references.

Strain	Genotype	Reference
MH1	MC1061 derivative; araD139, lacX74, galU, galK, hsr, hsm+, strA	[166]
DH5 α	K12 derivative; F- ϕ 80dlacZ Δ M15, Δ (lacZYAargF)U169, deoR, recA1, endA1, hsdR17(rk- mk+), phoA, supE44, λ -, thi-1, gyrA96, relA1	[165]

6.1.2 Transformation of chemo-competent *E. coli* cells

50 μ l chemically competent *E. coli* cells were transformed for the amplification of plasmid DNA. Therefore, the cells were thawed slowly on ice and 5 μ l of a ligation or 2 μ l plasmid DNA were added. The mixture was incubated on ice for 10 min, subjected to heat shock treatment at 42°C for 1 min and cooled down on ice for 2 min. Next, 800 μ l LB medium was added to the cells, followed by incubation for 30 min at 37°C and 450 rpm. Transformed cells were plated onto LB agar plates containing 100 μ g/ml ampicillin and incubated overnight at 37°C.

6.1.3 *S. cerevisiae* strains, plasmids and primers

Saccharomyces cerevisiae (*S. cerevisiae*) Strains are stored in glycerol stocks and were plated onto agar plates. Cultures were inoculated from plates in liquid media and cultivated shaking at 130 rpm and 30°C. The strains and plasmids used in this study are shown in Tab. 3, Tab. 4 and Tab. 5.

Tab. 3 Overview of *S. cerevisiae* strains used in this study. Listed are the wild type background strains and strains generated via homologous recombination with their genotype and references.

Strain	Genotype	Reference
YPH499 (WT)	MATa ura3-52 lys2-801 ade2-101 trp1- Δ 63 his3- Δ 200 leu2- Δ 1	[167]
Δ djp1	YPH499 <i>DJP1::NatNT2</i>	

$\Delta mdm34$	YPH499 <i>MDM34::KanMX</i>	This study
$\Delta djp1\Delta mdm34$	YPH499 <i>DJP1::NatNT2 MDM34::KanMX</i>	This study
Mdm34-HA	YPH499 <i>MDM34::6xHA-NatMX</i>	This study
$\Delta tom70$	YPH499 <i>TOM70::KanMX</i>	This study
$\Delta lam6$	YPH499 <i>LAM6::KanMX</i>	This study
Rtn1-bait	YPH499 <i>RTN1::MYC-3Csite-FLAG-KanMX</i>	This study
Sec63-bait	YPH499 <i>SEC63::MYC-3Csite-FLAG-KanMX</i>	This study
Tom20-bait	YPH499 <i>TOM20::MYC-3Csite-FLAG-KanMX</i>	This study
$\Delta tom70$ Rtn1-bait	YPH499 <i>TOM70::NatMX RTN1::MYC-3Csite-FLAG-KanMX</i>	This study
$\Delta tom70$ Sec63-bait	YPH499 <i>TOM70::NatMX SEC63::MYC-3Csite-FLAG-KanMX</i>	This study
$\Delta tom70$ Tom20-bait	YPH499 <i>TOM70::NatMX TOM20::MYC-3Csite-FLAG-KanMX</i>	This study

Tab. 4 Overview of *S. cerevisiae* strains obtained by transformation. Listed are the strains used in this study with their genotype and references.

Strain	Plasmid	Reference
WT + Oxa1-HA	pYX223-Oxa1-HA	This study
$\Delta djp1$ + Oxa1-HA	pYX223-Oxa1-HA	This study
$\Delta mdm34$ + Oxa1-HA	pYX223-Oxa1-HA	This study
WT + p415	p415	This study
$\Delta djp1\Delta mdm34$ + p415	p415	This study
WT + Tether	p415-GPD-Chimera	This study
$\Delta djp1\Delta mdm34$ + Tether	p415-GPD-Chimera	This study
WT + CRISPRi EV	pKR366	This study
WT + CRISPRi <i>MDM34</i>	pKR366- <i>MDM34</i>	This study
WT + CRISPRi EV + mtNeonGreen	pKR366, pRS303-Su9-mNeonGreen	This study
WT + CRISPRi <i>MDM34</i> + mtNeonGreen	pKR366- <i>MDM34</i> , pRS303-Su9-mNeonGreen	This study
Mdm34-HA + CRISPRi <i>MDM34</i>	pKR366- <i>MDM34</i>	This study
$\Delta tom70$ + CRISPRi EV	pKR366	This study

$\Delta tom70$ + CRISPRi <i>MDM34</i>	pKR366- <i>MDM34</i>	This study
$\Delta djp1$ + CRISPRi EV	pKR366	This study
$\Delta djp1$ + CRISPRi <i>MDM34</i>	pKR366- <i>MDM34</i>	This study
$\Delta lam6$ + CRISPRi EV	pKR366	This study
$\Delta lam6$ + CRISPRi <i>MDM34</i>	pKR366- <i>MDM34</i>	This study
WT + CRISPRi EV + Oxa1-HA	pKR366, pYX223-Oxa1-HA	This study
WT + CRISPRi <i>MDM34</i> + Oxa1-HA	pKR366- <i>MDM34</i> , pYX223-Oxa1-HA	This study
$\Delta tom70$ + CRISPRi EV + Oxa1-HA	pKR366, pYX223-Oxa1-HA	This study
$\Delta tom70$ + CRISPRi <i>MDM34</i> + Oxa1-HA	pKR366- <i>MDM34</i> , pYX223-Oxa1-HA	This study
WT + b ₂ -DHFR	pYX233-b ₂ -DHFR	This study
WT + CRISPRi EV + HSE-YFP	pKR366, pNH605-HSE-YFP	This study
WT + CRISPRi <i>MDM34</i> + HSE-YFP	pKR366- <i>MDM34</i> , pNH605-HSE-YFP	This study
$\Delta tom70$ + CRISPRi EV + HSE-YFP	pKR366, pNH605-HSE-YFP	This study
$\Delta tom70$ + CRISPRi <i>MDM34</i> + HSE-YFP	pKR366- <i>MDM34</i> , pNH605-HSE-YFP	This study
WT + CRISPRi EV + PACE-YFP	pKR366, pNH605-PACE-YFP	This study
WT + CRISPRi <i>MDM34</i> + PACE-YFP	pKR366- <i>MDM34</i> , pNH605-PACE-YFP	This study
$\Delta tom70$ + CRISPRi EV + PACE-YFP	pKR366, pNH605-PACE-YFP	This study
$\Delta tom70$ + CRISPRi <i>MDM34</i> + PACE-YFP	pKR366- <i>MDM34</i> , pNH605-PACE-YFP	This study
WT + CRISPRi EV + PDRE-YFP	pKR366, pNH605-PDRE-YFP	This study
WT + CRISPRi <i>MDM34</i> + PDRE-YFP	pKR366- <i>MDM34</i> , pNH605-PDRE-YFP	This study
$\Delta tom70$ + CRISPRi EV + PDRE-YFP	pKR366, pNH605-PDRE-YFP	This study
$\Delta tom70$ + CRISPRi <i>MDM34</i> + PDRE-YFP	pKR366- <i>MDM34</i> , pNH605-PDRE-YFP	This study
Rtn1-bait + CRISPRi EV	pKR366	This study
Rtn1-bait + CRISPRi <i>MDM34</i>	pKR366- <i>MDM34</i>	This study
$\Delta tom70$ Rtn1-bait + CRISPRi EV	pKR366	This study

$\Delta tom70$ Rtn1-bait + CRISPRi <i>MDM34</i>	pKR366- <i>MDM34</i>	This study
Sec63-bait + CRISPRi EV	pKR366	This study
Sec63-bait + CRISPRi <i>MDM34</i>	pKR366- <i>MDM34</i>	This study
$\Delta tom70$ Sec63-bait + CRISPRi EV	pKR366	This study
$\Delta tom70$ Sec63-bait + CRISPRi <i>MDM34</i>	pKR366- <i>MDM34</i>	This study
Tom20-bait + CRISPRi EV	pKR366	This study
Tom20-bait + CRISPRi <i>MDM34</i>	pKR366- <i>MDM34</i>	This study
$\Delta tom70$ Tom20-bait + CRISPRi EV	pKR366	This study
$\Delta tom70$ Tom20-bait + CRISPRi <i>MDM34</i>	pKR366- <i>MDM34</i>	This study

Tab. 5 Yeast plasmids used in this study. Listed below are the plasmids used in this thesis. The selection marker for yeast as well as the yeast origin are given.

Plasmid	Description	Reference
pYX223-Oxa1-HA	2 μ , HIS3, AmpR, <i>pGAL1</i> , Oxa1-HA	[32]
p415	CEN/ARS, LEU2, AmpR, <i>pGPD</i> , <i>tCYC1</i>	[168]
p415-GPD-Chimera	p415 Tom70 _{TMD} -GFP-Ubc6 _{TA}	[16]
pKR366	CEN/ARS, URA3, AmpR, <i>pTEF</i> NLS-dCas9-NLS-Mxi1, <i>pGPM1</i> TetR, <i>pRPR1</i> -gRNA	[77,107]
pKR366- <i>MDM34</i>	pKR366 <i>pRPR1-MDM34</i> gRNA	This study
pRS303-mtNeonGreen	INT, HIS3, AmpR, <i>pTEF2</i> Su9-mNeonGreen	[169]
pYX233-b ₂ -DHFR	2 μ , TRP1, AmpR, <i>pGAL1</i> , b ₂ -DHFR	[119]
pNH605-HSE-YFP	INT, HIS3, AmpR, <i>pCYC1</i> -4xHSE-YFP	[119]
pNH605-PACE-YFP	INT, HIS3, AmpR, <i>pCYC1</i> -4xPACE-YFP	[119]
pNH605-PDRE-YFP	INT, HIS3, AmpR, <i>pCYC1</i> -4xPDRE-YFP	This study
pYM17	AmpR, 6xHA-NatMX for genomic tagging	[170]
pJR2	AmpR, MYC-3Csite-FLAG-KanMX for genomic tagging	[122]
pGEM4-Oxa1	pSP6, Oxa1, AmpR	Herrmann Lab
pGEM4-Hsp60	pSP6, Hsp60, AmpR	[32]
pGEM4-Coq2	pSP6, Coq2, AmpR	[32]
pGEM4-MrpL15	pSP6, MrpL15, AmpR	Herrmann Lab
pGEM4-Cox5A	pSP6, Cox5A, AmpR	[130]
pGEM4-Cox5A(Oxa1)	pSP6, Cox5A(Oxa1), AmpR	[130]

pGEM4-Cox5A(Δ TM)	pSP6, Cox5A(Δ TM), AmpR	[130]
---------------------------	---------------------------------	-------

6.1.4 *S. cerevisiae* transformation

S. cerevisiae cells were grown to exponential phase and 1.5 ml culture was harvested by centrifugation for 1 min at 12,000 g. The cell pellet was washed with 1 ml ddH₂O. The cells were resuspended with 1 ml of 0.1 M lithium acetate and incubated for 10 min at 30°C and 1,000 rpm. After centrifugation (1 min at 12,000g), the cell pellet was resuspended in 74 μ l ddH₂O, 5 μ l salmon sperm DNA (ssDNA, denatured at 96°C for 10 min and cooled down), 5 μ l 100 ng/ μ l plasmid DNA, 36 μ l 1M lithium acetate (final concentration 0.1 M) and 240 μ l 50% (w/v) polyethylene glycol (PEG) 4000. The mixture was vortexed for 20 sec and incubated for 30 min at 30°C, followed by a heat shock for 25 min at 42°C. Afterwards, the cells were pelleted and resuspended in 90 μ l sterile ddH₂O. The suspension was plated on selective media. For homologous recombination with antibiotic cassettes, the cells were first plated onto YPD and incubated overnight and the next day replica plated onto YPD with an antibiotic.

6.2 Molecular Biology Methods

6.2.1 Isolation of plasmid DNA from *E. coli*

Plasmid DNA was isolated from *E. coli* cells either in small (Mini-prep) or large scale (Midi-prep). For small scale isolation of plasmids, 5 ml selective LB_{Amp} were inoculated with a single bacterial colony and incubated overnight. To isolate plasmid DNA, 2 ml of culture were harvested, and the DNA was extracted using the NucleoSpin Plasmid-Kit (Macherey-Nagel) according to manufacturer's instructions.

For large scale isolation, 200 ml selective LB media were inoculated with bacteria. The cells were cultured overnight before plasmid DNA of the whole culture was isolated using the *PureYield*TM Plasmid Midiprep System (Promega) according to manufacturer's instructions.

6.2.2 Determination of DNA concentration

To determine the DNA concentration and purity the Spectrophotometer/Fluorometer DS-11 FX+ (DeNovix) was used. After calibration with 1 μ l of water, 1 μ l of DNA was used for the measurement.

6.2.3 Polymerase Chain Reaction

DNA amplification for homologous recombination or plasmid construction was achieved by polymerase chain reaction (PCR). One reaction had a volume of 50 μ l containing 100 ng

template DNA, 0.5 μ M of each primer, 0.2 mM dNTPs (deoxyriboNucleoside Triphosphates), 1 U Q5® High-Fidelity (HF) polymerase and 1x Q5® reaction buffer. Tab. 6 displays the PCR program for the amplification of DNA and Tab. 7 shows the primers used in this study. The elongation time was determined by the insert length and the polymerase used (Q5: 1 kbp/15 sec).

Tab. 6 PCR cyclor program. Protocol for DNA amplification by standard PCR.

Temperature [°C]	Time [sec]	Cycle Number	Reaction
98	30		Initial denaturation of DNA and nuclease inactivation
98	10	35x	DNA denaturation
56-63	30		Primer annealing
72	15-30 sec/kb		Elongation
72	5		Final elongation
4	∞		Cooling

Tab. 7 Primers used in this study. Listed below are the names, sequences as well as a short description. of the primers used in this thesis. f, forward primer; r, reverse primer.

Primer	Sequence	Description
Act1 f	AGAGTTGCCCCAGAAGAACC	qPCR SYBR Green
Act1 r	CGACGTGAGTAACACCATCACC	qPCR SYBR Green
Tfc1 f	TGAGAGAGCTCTTCGCTAGACGTCCA	qPCR SYBR Green
Tfc1 r	TCCACTGAACTTCTGGGGTCTATACCA	qPCR SYBR Green
Mdm34 f	CCACAACCAAAGTCATCAACC	qPCR SYBR Green
Mdm34 r	GTCGTCGTTGCTGTTACTC	qPCR SYBR Green
Act1 f	CTCCTCGTGCTGTCTTCC	qPCR Taqman
Act1 r	TGGTGACAATACCGTGTTCA	qPCR Taqman
Act1 Probe	6FAM-TCGTCGGTAGACCAAGACACCAAGGT-BHQ1	qPCR Taqman
Hac1i f	ACAATTCAATTGATCTTGACAATTGG	qPCR Taqman
Hac1i r	TCAATTCAAATGAATTCAAACCTGAC	qPCR Taqman
Hac1i Probe	6FAM-CGTAATCCAGAAGCGCA-BHQ1	qPCR Taqman

Mdm34 gRNA f	aggGAGACCAATTAGAAGAGTCA	gRNA for pKR366
Mdm34 gRNA r	aacTGACTCTTCTAATTGGTCTC	gRNA for pKR366
Mdm34 HA f	CTTCAAATAACTGGAAATGGGGCATGGAGG ATAGCCCCCACCATATCATCGTACGCTGC AGGTCGAC	genomic tagging of <i>MDM34</i> with HA
Mdm34 HA r	GGAGAGTATGTATTTGTGTAGTTATGTACTT AGATATGTAACCTTAATTTAATCGATGAATTC GAGCTCG	genomic tagging of <i>MDM34</i> with HA
Sec63 bait f	GATATCGATACGGATACAGAAGCTGAAGAT GATGAATCACCAGAAGGTGGAGAACAAAA GTTG	genomic tagging of <i>SEC63</i> with bait
Sec63 bait r	CGTCTAAGAGCTAAAATGAAAACTATACT AATCACTTATATCTAGAATTCGAGCTCGTTT AAAC	genomic tagging of <i>SEC63</i> with bait
Rtn1 bait f	TGAAGAAAAGTACAAAAAAGTTGCAAAATG AATTGGAAAAAACAACGCTGGTGGAGAA CAAAA	genomic tagging of <i>RTN1</i> with bait
Rtn1 bait r	GAGACAAAAGTTAGCTATTCTTGTTTGAAA TGAAAAAAGCACTCAGAATTCGAGC TCGTTTAAAC	genomic tagging of <i>RTN1</i> with bait
Tom20 bait f	GAAGCAAGGCCGAATCTGATGCGGTTGCTG AAGCTAACGATATCGATGACGGTGGAGAAC AAAA	genomic tagging of <i>TOM20</i> with bait
Tom20 bait r	AGTAAAAGAAACAAAAACGGAGAAAAAAA GCAAGCAAATGTTACTCTCAGAATTCGAG CTCGTTTAAAC	genomic tagging of <i>TOM20</i> with bait

Colony PCR was used for the verification of successful homologous recombination. Therefore, one colony of yeast was mixed with 20 µl of 0.2 % SDS and boiled for 10 min at 96°C. Afterwards, cell debris and intact cells were pelleted using a small table-top centrifuge for 30

seconds. 1 μ l of the supernatant was added as template DNA to the PCR reaction described in Tab. 8 using the Q5[®] HF polymerase. The PCR program is described above in Tab. 6.

Tab. 8 Colony PCR. Listed are the reagents and their amounts used for performing a colony PCR.

Component	Volume
H ₂ O	32.5 μ l
5x Q5 [®] reaction buffer	10 μ l
dNTPs	1 μ l
Primer forward (10 μ M)	2.5 μ l
Primer reverse (10 μ M)	2.5 μ l
Q5 [®] polymerase	0.5 μ l
Total	49 μ l

6.2.4 Restriction digest of DNA

For plasmid verification or to prepare insert DNA and vectors for ligation, restriction digestion was performed. The 50 μ l reaction mix contained 2.5 μ l of a specific restriction enzyme, specific restriction buffer and 2 μ g of DNA. To avoid self-ligation of the vector the digest reaction of the plasmid DNA also contained 1 μ l calf intestine alkaline phosphatase (CIP). The reaction mixture was incubated for 15 min at 37°C, analyzed by agarose gel electrophoresis or directly purified using the Monarch[®] PCR & DNA Cleanup Kit (NEB) according to manufacturer's instructions.

6.2.5 Ligation of DNA fragments

Insert fragments were ligated into vector plasmid DNA in a 20 μ l reaction volume. Therefore 50 ng vector DNA, a 3-fold molar excess of insert DNA to vector, 2 μ l T4 DNA ligase, 2 μ l 10x ligase reaction buffer were added together. The reaction was performed at room temperature (RT) for 2 h. 10 μ l of the ligation reaction was used for the transformation of *E. coli* cells. Single colonies were analyzed via restriction digestion.

6.2.6 Agarose gel electrophoresis

Agarose gel electrophoresis was used both for analytic (test of successful ligation) and preparative purposes (isolation of DNA fragments). To cast the gel matrix 1% agarose (w/v) was completely dissolved in TAE buffer (40 mM Tris, 1.14% acetic acid, 10 mM EDTA pH 8.0) by heating the solution in the microwave. After cooling down the agarose solution 0.5 μ g/ml ethidium bromide was added to visualize DNA under ultraviolet light. Prior to loading, samples were supplemented with 6x purple loading dye (NEB). The electrophoresis was

performed in 1x TAE buffer at 10 V/cm. The separation of DNA fragments was analyzed under ultraviolet light. To isolate DNA fragment of interest (for preparative purposes) the respective DNA band was cut out using a scalpel and purified with Monarch® PCR & DNA Cleanup Kit (NEB) according to manufacturer's instructions.

6.2.7 Analysis of mRNA levels by qRT-PCR

For total RNA extraction yeast strains were cultivated in synthetic media to mid-log phase. 4 OD₆₀₀ of cells were harvested and RNA was extracted using the RNeasy Mini Kit (Qiagen) in conjunction with the RNase-Free DNase Set (Qiagen) according to the manufacturer's instructions. Yield and purity of the obtained RNA was determined with a Spectrophotometer/Fluorometer DS-11 FX+ (DeNovix). 500 ng RNA were reverse transcribed into cDNA using the qScript cDNA Synthesis Kit (Quanta Biosciences) according to the manufacturer's instructions. To measure relative mRNA levels, the iTaq Universal SYBR Green Supermix (BioRad) was used with 2 µl of a 1:10 dilution of cDNA sample. For assessment of *HAC1_{spliced}* mRNA the Luna Universal Probe One-Step RT-qPCR Kit (NEB) was used with 2 µl of a 50 ng/ µl RNA sample. Measurements were performed in technical triplicates with the CFX96 Touch Real-Time PCR Detection System (BioRad). Calculations of the relative mRNA expressions were conducted following the 2- $\Delta\Delta$ Ct method [171]. For normalization, the housekeeping genes *TFC1* or *ACT1* were used due to their stability [172]. See Tab. 7 for primer sequences.

6.3 Cell Biology Methods

6.3.1 *E. coli* – cultivation media

E. coli cells were grown on LB-medium or LB-plates. 1% bacto-tryptone, 0.5% yeast extract and 1% sodium chloride were used for liquid culture. The pH was adjusted to 7.5 with NaOH and 100 µg/ml ampicillin (Amp), 30 µg/ml kanamycin (Kan) or 25 µg/ml chloramphenicol (Cam) were used for plasmid selection. For agar plates, LB medium was supplemented with 2% bacto-agar (w/v) and autoclaved.

6.3.2 *S. cerevisiae* – cultivation media

Yeast cells were grown in non-selective YP-media, containing 1% yeast extract and 2% peptone. The pH was adjusted to 5.5 with HCl and the media was supplemented with 2% of the respective carbon source (D, glucose; Gal, galactose, G, glycerol). For YP-plates, 2% agar, 1% yeast extract and 2% peptone (pH adjusted to 5.5 with HCl) were autoclaved and subsequently

supplemented with 2% of the respective carbon source. For selection, 100 µg/ml G418, cloNAT or hygromycin b were added.

Cells harboring plasmids were cultured in selective media (S-medium) or selective lactic acid-based (SLac-medium). For this purpose, 1,7 g/l yeast nitrogen base, 5 g/l ammonium sulfate were mixed with drop-out mix lacking auxotrophic markers and 2% of the respective carbon source. For SLac medium, 1,7 g/l yeast nitrogen base, 5 g/l ammonium sulfate and 2,2% lactic acid (90%(v/v)) were mixed with drop-out mix lacking auxotrophic markers and could be supplemented with 0.5% galactose to induce protein expression from a GAL-promotor. In table 7, the components of the 20x drop-out mix are listed. For plates containing selective media, ½ volume consisting of water supplemented with 2% (w/v) agar was autoclaved. The agar-solution was mixed with S-medium or SLac-medium respectively to 1 volume and poured into petri dishes.

6.3.3. Dropout-Mix

The dropout-mix contains all amino acids. For plasmid selection individual amino acids were left out. The composition of the dropout-mix is listed in Tab. 9.

Tab. 9 Composition of the dropout-mix. Depending on the selection marker, amino acids were left out.

Amino acids/Nucleobase	Amount (mg/l)
L-adenine hemi sulfate salt	400
L-Arginine	400
L-Histidine HCl Monohydrate	400
L-Isoleucine	600
L-Leucin	2000
L-Lysin HCl	600
L-Methionine	400
L-Phenylalanine	1000
L-Threonine	400
L-Tryptophan	400
L-Tyrosine	400
L-Uracil	400
L-Valine	3000

6.3.4 Growth Assays

For spot analysis, the respective yeast strains were grown in liquid media. Yeast cells equivalent to 0.5 OD₆₀₀ were harvested at the exponential phase. The cells were washed in sterile water and 3 µl of ten-fold serial dilutions were spotted on the respective media followed by incubation at 30°C. Pictures were taken after different days of the incubation.

Growth curves were performed in a 96-well plate, using the automated ELx808™ Absorbance Microplate Reader (BioTek®). The growth curves started at 0.1 OD₆₀₀ and the OD₆₀₀ was measured every 10 min for 72 h at 30°C. The mean of technical triplicates was calculated and plotted in R.

6.3.5 YFP reporter assay

The PACE-YFP, HSE-YFP and PDRE-YFP reporter genes were integrated into the *LEU2* locus of the yeast genome. Cells were induced by addition of 960 ng/ml ATc for 16 h in galactose-containing media. As positive controls the empty vector sample shifted to 37°C for 16 h (PACE and HSE) and 4 h induction of b₂-DHFR (PDRE) were used. 4 OD₆₀₀ of cells were harvested by centrifugation (12,000 g, 5 min, RT) and resuspended in 400 µl H₂O. 100 µl of the cell suspension were transferred to flat-bottomed black 96-well imaging plates (BD Falcon, Heidelberg, Germany) in technical triplicates. Cells were sedimented by gentle spinning (30 g, 5 min, RT) and fluorescence (excitation 497 nm, emission 540 nm) was measured using a ClarioStar Fluorescence plate reader (BMG-Labtech, Offenburg, Germany). The corresponding wild-type strain not expressing YFP was used for background subtraction of autofluorescence. Fluorescence intensities were normalized to the value obtained from the wild-type empty vector control in each of three independent biological replicates.

6.3.6 Isolation of mitochondria

For the isolation of mitochondria, cells were grown in rich or selective galactose media to mid-log phase. Cultures for CRISPRi samples were additionally treated with ATc (960 ng/ml final) for 16 h. Cells were harvested (2,000 g, 5 min, RT) in exponential phase. After a washing step, cells were treated for 10 min with 2 ml per g wet weight MP1 buffer (100 mM DTT, 10 mM Tris pH unadjusted) at 30°C. After washing with 1.2 M sorbitol, yeast cells were resuspended in 6.7 ml per g wet weight MP2 buffer (20 mM KPi buffer pH 7.4, 1.2 M sorbitol, 3 mg per g wet weight zymolyase 20T from Seikagaku Biobusiness) and incubated for 1 h at 30°C. Spheroplasts were collected via centrifugation at 4°C and resuspended in ice-cold homogenization buffer (13.4 ml/g wet weight) (10 mM Tris pH 7.4, 1 mM EDTA pH 8, 0.2% fatty acids free bovine serum albumin (BSA), 1 mM PMSF, 0.6 M sorbitol). Spheroplasts were

disrupted by 10 strokes with a cooled glass potter. Cell debris was removed via centrifugation at 1,500 g for 5 min. The supernatant was centrifuged for 12 min at 12,000 g for 10 min to collect mitochondria. Mitochondria were resuspended in 1 ml of ice-cold SH-buffer (0.6 M sorbitol, 20 mM Hepes pH 7.4). The mitochondria were diluted to a protein concentration of 10 mg/ml.

6.3.7 Preparation of semi-intact cells

Cells were grown to mid-log phase. 250 OD₆₀₀ of cells were harvested by centrifugation (700 g, 7 min, room temperature). The cell pellet was resuspended in 25 ml SP1 buffer (10 mM DTT, 100 mM Tris pH unadjusted) and incubated for 10 min at 30°C in a shaker. Cells were pelleted (1,000 g, 5 min, room temperature), resuspended in 6 ml SP2 buffer (0.6 M sorbitol, 1x YP, 0.2% glucose, 50 mM KPi pH 7.4, 3 mg/g wet weight zymolyase) and incubated at 30°C for 30-60 min. Spheroblasts were collected, resuspended in 40 ml of SP3 buffer (1x YP, 1% glucose, 0.7 M sorbitol) and incubated for 20 min at 30°C shaking. After centrifugation (1,000 g, 5 min, 4°C), spheroblasts were washed two times with 20 ml of ice-cold permeabilization buffer (20 mM Hepes pH 6.8, 150 mM KOAc, 2 mM Mg-Acetate, 0.4 M sorbitol). The pellet was resuspended in 1 ml permeabilization buffer containing 0.5 mM EGTA and 100 µl aliquots were slowly frozen over liquid nitrogen for 30 min. A detailed procedure with pictures of how cells should be slowly frozen was published before [102].

6.3.8 Fluorescence microscopy

For microscopy cells were grown to mid log phase and 1 OD was harvested via centrifugation. Cell pellets were resuspended in 30 µl of PBS. 3-5 µl were pipetted onto a glass slide and covered with a cover slip. Manual microscopy was performed using a Leica Dmi8 Thunder Imager. Images were acquired using an HC PL APO100x/1,44 Oil UV objective with Immersion Oil Type A 518 F. For excitation of mNeongreen 510 nm was used. All mitochondrial images were taken as Z-stacks. Image analysis was done with the LAS X software and further processing of images was performed in Fiji/ImageJ.

For timelapse imaging first a glass slide with an agar pad had to be prepared. Therefore, synthetic liquid media supplemented with 2 % galactose was mixed with 1.5 % (w/v) agarose, boiled in a microwave and 180 µl was pipetted into a single cavity slide (42410010 Karl Hecht Assistant). The mixture was flattened by pressing a second glass slide on top of the hot mixture, orthogonal to the cavity slide. Just before adding cells onto the agar pad the upper glass slide was removed. Cells were grown and harvested as above but resuspended in liquid minimal

media. 3-5 μ l were pipetted onto the agar pad and covered with a cover slip. Images were taken every 5 min while the microscope incubation chamber was heated to 30°C

6.3.9 Electron microscopy and immuno-electron microscopy

Aliquots of semi-intact cells were thawed on ice and fixed in 2% glutaraldehyde, 3% formaldehyde over night at 4°C. The samples were processed as described [173]. Sections were quenched with 50 mM glycine in PBS for 15 min and washed with PBS 3x for 10 min. Grids were blocked with PBST + 2% BSA for 15 min and labelled with monoclonal mouse anti-porin antibodies (16G9E6BC4, cat # 459500, Thermo Fisher) in a 1:100 dilution in PBST-BSA. A secondary goat anti-mouse IgG 10 nm gold conjugated antibody (BBInternational SKU#. BA GAM40) 1:100 in PBST-BSA for 2 h was used. Sections were washed 5x 5 min in PBS, fixed with 1% glutaraldehyde in PBS for 5 min and washed in H₂O. Proteins were visualized using 2% uranyl acetate stain for 10 min and lead citrate (Reynold's) for 1 min. Sections were analyzed in a Philips CM100 electron microscope.

6.4 Protein Biochemistry Methods

6.4.1 Whole cell lysates

For whole cell lysates, yeast strains were cultivated in liquid media to mid-log phase. 2 OD₆₀₀ were harvested by centrifugation (12,000 g, 5 min) and resuspended in 100 μ l reducing loading buffer. Cells were transferred to screw-cap tubes containing 1 mm glass beads. Cell lysis was performed using a FastPrep-24 5G homogenizer (MP Biomedicals, Heidelberg, Germany) with 3 cycles of 30 s, speed 8.0 m/s, 120 s breaks, glass beads). Lysates were boiled at 96°C for 3 min and stored at -20°C until further use. Equal amounts were resolved via SDS-PAGE.

6.4.2 SDS-polyacrylamide gel electrophoresis (SDS-PAGE)

Sodiumdodecylsulfate polyacrylamide gel electrophoresis (SDS-PAGE) allows the separation of proteins by size. In this method, proteins are denatured and negatively charged through the detergent SDS. This allows the migration through an electric field which is put on a gel matrix of polyacrylamide. The network of acrylamide fibers leads to a slow migration of unfolded and large proteins whereas small or partially folded proteins (for example folded because of preserved disulfide bridges) run faster through the gel. In this study, a self-made vertical one-dimensional gel system was used in this study. For the standard gel system, glass plates with a size of 160 x 180 mm and spacers with 1 mm thickness were sealed using a base gel, on top of which first the separation gel and then the stacking gel was placed. The concentration of acrylamide and bis-acrylamide in the separation gel depends on the molecular size of the

proteins of interest. The composition of the gels is represented in Tab. 10. Prior to loading, samples were supplemented with reducing sample (Laemmli) buffer (50 mM Tris-HCl pH 6.8, 10% glycerin, 2% SDS, 0.01% bromophenol blue, 100 mM DTT). To determine the protein size the unstained marker from peQLab was used. The electrophoresis was conducted at 25 mA for 2 - 4 h in SDS running buffer (25 mM Tris-HCl pH 8.3, 190 mM glycine, 0.1% SDS).

Tab. 10 Gel composition for SDS-PAGE. Composition of the running, stacking and base gel.

Gel	Composition
Running gel	16% acrylamide 0.11% bisacrylamide 375 mM Tris-HCl pH 8.8 0.1% SDS 0.1% ammonium persulfate (APS) 0.03%N,N,N',N'-Tetramethylethylenediamine (TEMED)
Stacking gel	5% acrylamide 0.03% bisacrylamide 60 mM Tris-HCl pH 6.8 0.1% SDS 0.05% ammonium persulfate (APS) 0.1%N,N,N',N'-Tetramethylethylenediamine (TEMED)
Base gel	20% acrylamide 0.13% bisacrylamide 375 mM Tris-HCl pH 8.8 0.1% SDS 0.05% ammonium persulfate (APS) 0.1%N,N,N',N'-Tetramethylethylenediamine (TEMED)

6.4.3 Transfer of proteins to a nitrocellulose membrane (Western Blot)

Proteins separated by SDS-PAGE were transferred from a gel onto a nitrocellulose membrane using a semi-dry blotting method [174]. Therefore, the SDS-gel was placed onto a nitrocellulose membrane. It was covered with two Whatman papers below and one Whatman paper on top of it. The stack was soaked in blotting buffer (20 mM Tris, 150 mM glycine, 0.08% SDS, 20% methanol), arranged in this order on the anode transfer module and covered with the cathode transfer module. The transfer of proteins from the gel onto the membrane was performed for

1.5 h at 1.3 mA/cm². To detect proteins on the nitrocellulose membrane, it was stained with Ponceau S solution (0.2% (w/v) Ponceau S, 3% (w/v) acetic acid) for 5 min.

6.4.4 Protein import into mitochondria

The TNT® Quick Coupled Transcription/Translation Kit from Promega was for synthesis of ³⁵S-methionine labeled proteins in reticulocyte lysate. 50 µg mitochondria were taken in import buffer (500 mM sorbitol, 50 mM Hepes pH 7.4, 80 mM KCl, 10 mM Mg(OAc)₂ and 2 mM KH₂PO₄), 2 mM ATP and 2 mM NADH and incubated for 10 min at 30°C. The import reaction was started by addition of 1% (v/v) reticulocyte lysate. Samples were taken after the indicated time points and the reaction was stopped by a 1:10 dilution in ice-cold SH buffer supplemented with 100 µg/ml proteinase K. The samples were incubated on ice for 30 min to remove precursors which were not imported. The protease treatment was stopped by addition of 2 mM PMSF. The samples were centrifuged 15 min at 25,000 g and 4°C. The mitochondria were washed with 500 µl SH/KCl-buffer (0.6 M sorbitol, 20 mM HEPES/KOH pH 7.4, 150 mM KCl) and 2 mM PMSF. The mitochondria were reisolated by centrifugation for 15 min at 25,000 g and 4°C, resuspended in sample buffer and resolved via SDS-PAGE.

6.4.5 Import into semi-intact cells

Semi-intact cells were thawed on ice and the OD₆₀₀ was measured in 1.2 M sorbitol. Semi-intact cells of an OD₆₀₀ 0.2 were used per reaction. Semi-intact cells were added to a mixture of B88 buffer, 2 mM ATP, 2 mM NADH, 5 mM creatine phosphate and 100 µg/ml creatine phosphatase. Radiolabeled lysate was added, and the mixture was first incubated for 10 min on ice to allow the cells to take up the lysate before the suspensions were shifted to 30°C for 5 and 20 min to allow the import of proteins into mitochondria. The import reactions were stopped by a 1:10 dilution in ice-cold B88 buffer containing 2 mM CCCP, with or without 100 µg/ml proteinase K. After an incubation of 30 min on ice, 2 mM PMSF was added. Semi-intact cells were reisolated by centrifugation (4,000 g, 5 min, 4°C), washed with B88, 2 mM PMSF and pelleted by centrifugation (10 min, 16,000 g, 4°C). Finally, the pellet was resuspended in sample buffer and resolved via SDS-PAGE.

6.4.6 Radioactive *in vivo* labelling of mitochondrial translation products

Cells were grown in galactose media lacking methionine to exponential phase in the presence of ATc for 16 hours. Afterwards cells were harvested, washed twice with synthetic galactose media without amino acids and finally resuspended in the same medium. The reaction was supplemented with 6µl amino acid mix (2 mg/ml) and additional 12 µl tyrosine (1 mg /ml). Then 3.8 µl cycloheximide (10 mg/ml) was added, to stop cytosolic translation, and the samples

were incubated for 10 minutes at 30°C. 1 µl of ³⁵S-methionine was added to the cell suspension and the reaction was further incubated for 15 minutes at 30°C. The reaction was quenched by addition of 10 µl of cold methionine and 7 µl cysteine and the cells were lysed by addition of 50 µl of rödel mix (0.3 M NaOH, 1% β-mercaptoethanol and 3 mM PMSF). The lysis was carried out for 10 minutes on ice and subsequently TCA was added to the samples to a final concentration of 12%. Proteins were precipitated with TCA and analyzed by SDS-PAGE and autoradiography.

6.4.7 TCA precipitation of proteins

Trichloroacetic acid (TCA) was used for protein precipitation. Therefore, samples were supplemented with 72% (w/v) TCA to a final concentration of TCA of 12%. The samples were incubated at -80°C for 2 h or at -20°C overnight. Afterwards they were thawed slowly on ice and the precipitated proteins pelleted for 20 min at 30000 x g and 4°C. The protein pellet was washed with 1 ml of ice-cold Acetone 100%. After a second centrifugation (20 min at 30000 x g and 4°C) the pellet was dried at 30°C and resuspended in reducing sample buffer.

6.4.8 Autoradiography

Radioactive proteins can be detected by autoradiography. Therefore, the dried cellulose membrane was exposed to an imaging plate (Fujifilm). For quantification the films were scanned in a grey-scale 8-bit format and the quantification was performed using the ImageQuant software.

6.4.9 Sample preparation and mass-spectrometric identification of proteins

For the quantitative comparison of proteomes of *Atom70* and WT cells, carrying the CRISPRi EV or CRISPRi *MDM34*, were induced for 8 h and 24 h with ATc. 10 OD₆₀₀ of cells were harvested at each time point by centrifugation (12,000 g, 5 min) and snap-frozen in liquid nitrogen and stored at -80°C. Cells lysates were prepared in lysis buffer (50 mM Tris pH 7.5, 2% (w/v) SDS, Tablets mini EDTA-free protease inhibitor (Roche)) using a FastPrep-24 5G homogenizer (MP Biomedicals, Heidelberg, Germany) with 3 cycles of 30 s, speed 8.0 m/s, 120 s breaks, glass beads). Lysates were boiled for 5 min at 96°C and centrifuged (16,000 g, 2 min, 4°C). Protein concentrations were determined using the Pierce BCA Protein Assay (Thermo Scientific, #23225). 20 µg of each lysate were subjected to an in-solution tryptic digest using a modified version of the Single-Pot Solid-Phase-enhanced Sample Preparation (SP3) protocol. Here, lysates were added to Sera-Mag Beads (Thermo Scientific, #4515-2105-050250, 6515-2105-050250) in 10 µl 15% formic acid and 30 µl of ethanol. Binding of proteins was achieved by shaking for 15 min at room temperature. SDS was removed by 4 subsequent

washes with 200 μ l of 70% ethanol. Proteins were digested with 0.4 μ g of sequencing grade modified trypsin (Promega, #V5111) in 40 μ l Hepes/NaOH, pH 8.4 in the presence of 1.25 mM TCEP and 5 mM chloroacetamide (Sigma-Aldrich, #C0267) overnight at room temperature. Beads were separated, washed with 10 μ l of an aqueous solution of 2% DMSO and the combined eluates were dried down. In total three biological replicates were prepared (n=3). Peptides were reconstituted in 10 μ l of H₂O and reacted with 80 μ g of TMT10plex (Thermo Scientific, #90111) label reagent dissolved in 4 μ l of acetonitrile for 1 h at room temperature. Excess TMT reagent was quenched by the addition of 4 μ l of an aqueous solution of 5% hydroxylamine (Sigma, #438227). Peptides were mixed to achieve a 1:1 ratio across all TMT-channels. Mixed peptides were desalted on home-made StageTips containing Empore C₁₈ disks [175] and subjected to an SCX fractionation on StageTips into 3 fractions, followed by additional cleanup on C₁₈ StageTips. The resulting fractions were then analyzed by LC-MS/MS on a Q Exactive HF (Thermo Scientific) as previously described.

For mass spectrometry of sucrose-purified mitochondria, first crude mitochondria were prepared as described above from either WT or $\Delta tom70$ harboring an empty vector or a knockdown vector. In total four/three biological replicates were prepared for WT (n=4) and $\Delta tom70$ (n=3) respectively. For purification a four-step sucrose gradient was poured into SW41 rotor tubes. The gradient consisted of 1.5 ml 60 % sucrose, 4 ml 32 % sucrose, 1.5 ml 23 % sucrose and 1.5 ml 15 % sucrose (w/v) in EM buffer (20 mM MOPS-KOH pH 7.2, 1 mM EDTA). 5 mg of crude mitochondria were loaded onto the gradient and centrifuged at 134,000 g for 1 hour at 2°C. The pure mitochondria were collected from the 32 % / 60 % interface and diluted with 2 volumes of SEM buffer (20 mM MOPS-KOH pH 7.2, 1 mM EDTA, 0.6 M sorbitol). Afterwards mitochondria were reisolated at 15,000 g for 15 min at 2°C. This pellet was resuspended in SEM and the protein concentration was determined with the Bradford assay [176]. 100 μ g of pure mitochondria were lysed in 100 μ l lysis buffer (50 mM Tris pH 7.5, 2% (w/v) SDS, Tablets mini EDTA-free protease inhibitor (Roche)) by boiling for 10 min at 96°C. Protein concentrations were determined using the Pierce BCA Protein Assay (Thermo Scientific, #23225). 20 μ g of each lysate were subjected to an in-solution tryptic digest using a modified version of the Single-Pot Solid-Phase-enhanced Sample Preparation (SP3) protocol. Here, lysates were added to Sera-Mag Beads (Thermo Scientific, #4515-2105-050250, 6515-2105-050250) in 10 μ l 15% formic acid and 30 μ l of ethanol. Binding of proteins was achieved by shaking for 15 min at room temperature. SDS was removed by 4 subsequent washes with 200 μ l of 70% ethanol. Proteins were digested with 0.4 μ g of sequencing grade modified trypsin (Promega, #V5111) in 40 μ l Hepes/NaOH, pH 8.4 in the presence of 1.25 mM TCEP and 5

mM chloroacetamide (Sigma-Aldrich, #C0267) overnight at room temperature. Beads were separated, washed with 10 μ l of an aqueous solution of 2% DMSO and the combined eluates were dried down. Peptides were reconstituted in 20 μ l of H₂O, acidified to pH <2 with Tri-fluoroacetic acid and desalted with 3x C₁₈ StageTips. Samples were dried down in speed-vac and resolubilized in 9 μ l buffer A (0.1 % formic acid in MS grade water) and 1 μ l buffer A* (2 % acetonitrile, 0.1 % tri-fluoroacetic acid in MS grade water). The samples were analyzed by LC-MS/MS on a Q Exactive HF(Thermo Scientific) as previously described [177].

For IP mass spectrometry of purified organelles, a modified protocol from Reinhard et al., was used [122]. WT and $\Delta tom70$ strains carrying a genomic bait-tag on Rtn1, Sec63, Tom20 or no tag, and in turn each harboring an empty vector or a knockdown vector were grown in galactose medium containing ATc to induce repression of *MDM34*. For each strain biological quadruplicates (n=4) were prepared (64 samples in total). After 16 h 100 OD₆₀₀ cells were harvested by centrifugation (5,000 g for 5 min) and resuspended in 1 ml SEH buffer (20 mM HEPES pH 7.4, 1 mM EDTA, 0.6 M Sorbitol, 1x cOmplete™ Tablets mini EDTA-free protease inhibitor [Roche]). Resuspended yeast cells were transferred into screw cap tubes containing 500 μ l glass beads. Cell lysates were prepared using a FastPrep-24 5G homogenizer (MP Biomedicals, Heidelberg, Germany) with 10 cycles of 15 s, speed 5.0 m/s, 45 s breaks. Afterwards lysates were subjected to a subcellular fractionation via differential centrifugation. Samples were centrifuged for 5 min at 3,300 g, for 20 min at 12,000 g, and for 1 hour at 100,000 g. After each step the pellet was discarded and only the last pellet (P100), containing heavy membranes, was collected, resuspended in 100 μ l SEH buffer, snap-frozen in liquid N₂ and stored at -80°C until further use. 900 μ l of IP buffer (20 mM HEPES pH 7.4, 1 mM EDTA, 100 mM NaCl) was added to P100 prior to the IP. Diluted samples were mixed with 50 μ l of Pierce Anti-DYKDDDDK Magnetic Agarose from Thermo. The beads were equilibrated by washing 200 μ l of beads slurry once with 1 ml PBS pH 7.4 and twice with 1 ml of wash buffer (20 mM HEPES pH 7.4, 1 mM EDTA, 75 mM NaCl). Samples were bound to Anti-DYKDDDDK beads for 2 hours at 4°C tumbling end-over-end. IP Samples were briefly centrifuged (1 min at 2,500 g) and supernatant was discarded by using a magnetic rack. Beads were washed 3x with 1 ml wash buffer and finally 400 μ l elution buffer (PBS pH 7.4, 0.5 mM EDTA, 0.03 mg/ml HRV-3C protease [Sigma-Aldrich #SAE0045]) was added onto the beads. Organelles were eluted for 2 hours at 4°C tumbling end-over-end, the beads were separated with a magnetic rack and eluted organelles were transferred to a fresh microtube. Afterwards intact organelles were pelleted via centrifugation for 2 hours at 200,000 g and the resulting pellet was resuspended in 35 μ l lysis buffer (6 M GdmCl, 10 mM TCEP, 40 mM CAA, 100 mM Tris pH 8.5). Organelles were lysed

by boiling for 10 min at 96°C. For protein digestion first lysed samples were diluted 1:10 with digestion buffer (10% ACN, 25 mM Tris pH 8.5), next Trypsin and LysC were added in a 1:50 ratio and the reaction was incubated overnight at 37°C. The next day fresh Trypsin was added in a 1:100 ratio for 30 min at 37°C. pH of samples was adjusted to pH <2 with tri-fluoroacetic acid. Desalting/reversed-Phase cleanup with 3x SDB-RPS StageTips. Samples were dried down in speed-vac and resolubilized in 12 µl buffer A⁺⁺ (0.1 % formic acid, 0.01 % tri-fluoroacetic acid in MS grade water). The samples were analyzed by LC-MS/MS on a Q Exactive HF(Thermo Scientific) as previously described [177].

Briefly, peptides were separated using an Easy-nLC 1200 system (Thermo Scientific) coupled to a Q Exactive HF mass spectrometer via a Nanospray-Flex ion source. The analytical column (50 cm, 75 µm inner diameter (NewObjective) packed in-house with C18 resin ReproSilPur 120, 1.9 µm diameter Dr. Maisch) was operated at a constant flow rate of 250 nl/min. A 3 h gradient was used to elute peptides (Solvent A: aqueous 0.1% formic acid; Solvent B: 80 % acetonitrile, 0.1% formic acid). Peptides were analyzed in positive ion mode applying with a spray voltage of 2.3 kV and a capillary temperature of 250°C. For TMT labelled peptides MS spectra were acquired in profile mode with a mass range of 375–1.400 m/z using a resolution of 120,000 [maximum fill time of 80 ms or a maximum of 3e6 ions (automatic gain control, AGC)]. Fragmentation was triggered for the top 15 peaks with charge 2–8 on the MS scan (data-dependent acquisition) with a 30 s dynamic exclusion window (normalized collision energy was 32). Precursors were isolated with a 0.7 m/z window and MS/MS spectra were acquired in profile mode with a resolution of 60,000 (maximum fill time of 100 ms, AGC target of 1e5 ions, fixed first mass 100 m/z).

For label-free peptides MS spectra were acquired in profile mode a mass range of 300–1650 m/z using a resolution of 60,000 [maximum fill time of 20 ms or a maximum of 3e6 ions (automatic gain control, AGC)]. Fragmentation was triggered for the top 15 peaks with charge 2–8 on the MS scan (data-dependent acquisition) with a 20 s dynamic exclusion window (normalized collision energy was 28). Precursors were isolated with a 1.4 m/z window and MS/MS spectra were acquired in profile mode with a mass range of 200 to 2000 m/z and a resolution of 15,000, maximum fill time of 80 ms, AGC target of 1e5 ions.

6.4.10 Analysis of mass spectrometry data

Peptide and protein identification and quantification was done using the MaxQuant software (version 1.6.10.43) [178–180] and a *Saccharomyces cerevisiae* proteome database obtained from Uniprot. For TMT labelled peptides, 10plex TMT was chosen in Reporter ion MS2

quantification, up to 2 tryptic miss-cleavages were allowed, protein N-terminal acetylation and Met oxidation were specified as variable modifications and Cys carbamidomethylation as fixed modification. The “Requantify” and “Second Peptides” options were deactivated. False discovery rate was set at 1% for peptides, proteins and sites, minimal peptide length was 7 amino acids. For label-free data, the LFQ normalization algorithm and second peptides was enabled. Match between run was applied within each group of replicates. False discovery rate was set at 1% for peptides, proteins and sites, minimal peptide length was 7 amino acids.

The output files of MaxQuant were processed using the R programming language. Only proteins that were quantified with at least two unique peptides were considered for the analysis. Moreover, only proteins that were identified in at least two out of three MS runs per replicate were kept. A total of 3,550 proteins for the whole cell proteome, a total of 1,624 proteins for the pure mitochondria and a total of 3,045 for the organelle-IP passed the quality control filters. Raw signal sums were cleaned for batch effects using limma [181] and further normalized using variance stabilization normalization [182]. Proteins were tested for differential expression using the limma package for the indicated comparison of strains. A reference list of yeast mitochondrial proteins was used [5].

6.5 Immunology Methods

6.5.1 Immune decoration of cellulose membranes

Proteins transferred onto a nitrocellulose membrane were visualized by immunodecoration with specific antibodies. After staining the membrane with Ponceau S, it was incubated for 30 min at RT with 5% (w/v) milk in TBS buffer (10 mM Tris/HCl pH 7.5, 150 mM NaCl) to block non-specific protein binding sites. Then, the blocking solution was replaced by a solution containing the specific primary antibody (1:125 to 1:10,000 in 5% milk in TBS, prepared by immunization in rabbits). The membrane was incubated in this solution overnight at 4°C, washed three times (each 5 min) with TBS, followed by incubation with the secondary antibody (goat anti-rabbit) coupled to horseradish peroxidase (1: 10,000 in 5% milk in TBS, BioRad) for 1 h at RT. After the washing procedure with TBS, the membrane was coated with 1:1 mix of ECL solutions (ECL 1: 100 mM Tris/HCl pH 8.5, 0.044% (w/v) luminol, 0.0066% p-coumaric acid; ECL 2: 100 mM Tris/HCl pH 8.5, 0.03% H₂O₂). Luminescence signals were detected on Super RX Medical X-Ray Films (Fuji) using the Optimax Type TR-developer (MS Laborgeräte). For the horseradish peroxidase coupled HA-antibody no secondary antibody was needed and the films could be exposed directly after the washing of the primary antibody.

6.5.2 Antibodies

If not differently described antibodies were raised in rabbits using recombinant purified proteins. The secondary antibody was ordered from BioRad (Goat Anti-Rabbit IgG (H+L)) - HRP Conjugate, #172- 1019, Goat Anti-Mouse IgG (H+L)-HRP Conjugate, #172-1011). The horseradish-peroxidase coupled HA antibody was ordered from Roche (Anti-HA-Peroxidase, High Affinity (3F10)). The commonly used antibodies in this thesis are listed in Tab. 11.

Tab. 11 Antibodies. List of antibodies and their dilutions used in this study.

Name	Dilution	Reference
α Sod1	1:1,000	[183]
α HA	1:500	Roche #12 013 819 001
α Djp1	1:2,000	[32]
α MrpL40	1:2,000	[184]
α Rip1	1:750	Thomas Becker (University of Freiburg, Germany)
α Mdj1	1:125	

REFERENCES

- [1] J. Choi, J. Park, D. Kim et al., “Fungal secretome database: integrated platform for annotation of fungal secretomes,” *BMC genomics*, vol. 11, p. 105, 2010.
- [2] E. Wallin and G. von Heijne, “Genome-wide analysis of integral membrane proteins from eubacterial, archaean, and eukaryotic organisms,” *Protein science : a publication of the Protein Society*, vol. 7, no. 4, pp. 1029–1038, 1998.
- [3] W. A. Prinz, A. Toulmay, and T. Balla, “The functional universe of membrane contact sites,” *Nature Reviews Molecular Cell Biology*, vol. 21, no. 1, pp. 7–24, 2020.
- [4] N. Pfanner, B. Warscheid, and N. Wiedemann, “Mitochondrial proteins: from biogenesis to functional networks,” *Nature Reviews Molecular Cell Biology*, vol. 20, no. 5, pp. 267–284, 2019.
- [5] M. Morgenstern, S. B. Stiller, P. Lübbert et al., “Definition of a High-Confidence Mitochondrial Proteome at Quantitative Scale,” *Cell reports*, vol. 19, no. 13, pp. 2836–2852, 2017.
- [6] J. M. Herrmann and Y. Bykov, “Protein translocation in mitochondria: Sorting out the Toms, Tims, Pams, Sams and Mia,” *FEBS Letters*, vol. 597, no. 12, pp. 1553–1554, 2023.
- [7] L. Krämer, C. Groh, and J. M. Herrmann, “The proteasome: friend and foe of mitochondrial biogenesis,” *FEBS Letters*, vol. 595, no. 8, pp. 1223–1238, 2021.
- [8] Y. Araiso, A. Tsutsumi, J. Qiu et al., “Structure of the mitochondrial import gate reveals distinct preprotein paths,” *Nature*, vol. 575, no. 7782, pp. 395–401, 2019.
- [9] N. Aviram and M. Schuldiner, “Targeting and translocation of proteins to the endoplasmic reticulum at a glance,” *Journal of Cell Science*, vol. 130, no. 24, pp. 4079–4085, 2017.
- [10] N. Berner, K.-R. Reutter, and D. H. Wolf, “Protein Quality Control of the Endoplasmic Reticulum and Ubiquitin-Proteasome-Triggered Degradation of Aberrant Proteins: Yeast Pioneers the Path,” *Annual review of biochemistry*, vol. 87, pp. 751–782, 2018.
- [11] S. Itskanov, K. M. Kuo, J. C. Gumbart et al., “Stepwise gating of the Sec61 protein-conducting channel by Sec63 and Sec62,” *Nature Structural & Molecular Biology*, vol. 28, no. 2, pp. 162–172, 2021.
- [12] L. Scorrano, M. A. de Matteis, S. Emr et al., “Coming together to define membrane contact sites,” *Nature Communications*, vol. 10, no. 1, p. 1287, 2019.

- [13] I. G. Castro, S. P. Shortill, S. K. Dziurdzik et al., “Systematic analysis of membrane contact sites in *Saccharomyces cerevisiae* uncovers modulators of cellular lipid distribution,” *eLife*, vol. 11, 2022.
- [14] N. Shai, E. Yifrach, C. W. T. van Roermund et al., “Systematic mapping of contact sites reveals tethers and a function for the peroxisome-mitochondria contact,” *Nature Communications*, vol. 9, no. 1, p. 1761, 2018.
- [15] M. R. Wozny, A. Di Luca, D. R. Morado et al., “Supramolecular architecture of the ER-mitochondria encounter structure in its native environment,”
- [16] B. Kornmann, E. Currie, S. R. Collins et al., “An ER-mitochondria tethering complex revealed by a synthetic biology screen,” *Science (New York, N.Y.)*, vol. 325, no. 5939, pp. 477–481, 2009.
- [17] B. Kornmann, C. Osman, and P. Walter, “The conserved GTPase Gem1 regulates endoplasmic reticulum-mitochondria connections,” *Proceedings of the National Academy of Sciences*, vol. 108, no. 34, pp. 14151–14156, 2011.
- [18] Y. Kakimoto, S. Tashiro, R. Kojima et al., “Visualizing multiple inter-organelle contact sites using the organelle-targeted split-GFP system,” *Scientific Reports*, vol. 8, no. 1, p. 6175, 2018.
- [19] D. A. Stroud, S. Oeljeklaus, S. Wiese et al., “Composition and topology of the endoplasmic reticulum-mitochondria encounter structure,” *Journal of molecular biology*, vol. 413, no. 4, pp. 743–750, 2011.
- [20] K. Yamano, S. Tanaka-Yamano, and T. Endo, “Tom7 regulates Mdm10-mediated assembly of the mitochondrial import channel protein Tom40,” *The Journal of biological chemistry*, vol. 285, no. 53, pp. 41222–41231, 2010.
- [21] C. Meisinger, N. Wiedemann, M. Rissler et al., “Mitochondrial protein sorting: differentiation of beta-barrel assembly by Tom7-mediated segregation of Mdm10,” *Journal of Biological Chemistry*, vol. 281, no. 32, pp. 22819–22826, 2006.
- [22] R. Kojima, T. Endo, and Y. Tamura, “A phospholipid transfer function of ER-mitochondria encounter structure revealed in vitro,” *Scientific Reports*, vol. 6, no. 1, p. 30777, 2016.
- [23] Y. Tamura, R. Kojima, and T. Endo, “Advanced In Vitro Assay System to Measure Phosphatidylserine and Phosphatidylethanolamine Transport at ER/Mitochondria Interface,” *Methods in molecular biology (Clifton, N.J.)*, vol. 1949, pp. 57–67, 2019.

- [24] A. M. English, M.-H. Schuler, T. Xiao et al., “ER-mitochondria contacts promote mitochondrial-derived compartment biogenesis,” *Journal of Cell Biology*, vol. 219, no. 12, 2020.
- [25] P. S. Tirrell, K. N. Nguyen, K. Luby-Phelps et al., “MICOS subcomplexes assemble independently on the mitochondrial inner membrane in proximity to ER contact sites,” *Journal of Cell Biology*, vol. 219, no. 11, 2020.
- [26] M. Eisenberg-Bord, H. S. Tsui, D. Antunes et al., “The Endoplasmic Reticulum-Mitochondria Encounter Structure Complex Coordinates Coenzyme Q Biosynthesis,” *Contact (Thousand Oaks (Ventura County, Calif.))*, vol. 2, 2515256418825409, 2019.
- [27] A. E. Hobbs, M. Srinivasan, J. M. McCaffery et al., “Mmm1p, a mitochondrial outer membrane protein, is connected to mitochondrial DNA (mtDNA) nucleoids and required for mtDNA stability,” *The Journal of cell biology*, vol. 152, no. 2, pp. 401–410, 2001.
- [28] S. Meeusen and J. Nunnari, “Evidence for a two membrane-spanning autonomous mitochondrial DNA replisome,” *The Journal of cell biology*, vol. 163, no. 3, pp. 503–510, 2003.
- [29] Y. Elbaz-Alon, M. Eisenberg-Bord, V. Shinder et al., “Lam6 Regulates the Extent of Contacts between Organelles,” *Cell reports*, vol. 12, no. 1, pp. 7–14, 2015.
- [30] A. Murley, R. D. Sarsam, A. Toulmay et al., “Ltc1 is an ER-localized sterol transporter and a component of ER-mitochondria and ER-vacuole contacts,” *The Journal of cell biology*, vol. 209, no. 4, pp. 539–548, 2015.
- [31] Ł. Opaliński, J. Song, C. Priesnitz et al., “Recruitment of Cytosolic J-Proteins by TOM Receptors Promotes Mitochondrial Protein Biogenesis,” *Cell reports*, vol. 25, no. 8, 2036-2043.e5, 2018.
- [32] K. G. Hansen, N. Aviram, J. Laborenz et al., “An ER surface retrieval pathway safeguards the import of mitochondrial membrane proteins in yeast,” *Science (New York, N.Y.)*, vol. 361, no. 6407, pp. 1118–1122, 2018.
- [33] S. Lahiri, J. T. Chao, S. Tavassoli et al., “A conserved endoplasmic reticulum membrane protein complex (EMC) facilitates phospholipid transfer from the ER to mitochondria,” *PLoS biology*, vol. 12, no. 10, e1001969, 2014.
- [34] M. J. Shurtleff, D. N. Itzhak, J. A. Hussmann et al., “The ER membrane protein complex interacts cotranslationally to enable biogenesis of multipass membrane proteins,” *eLife Sciences Publications, Ltd*, 29.05.2018.

- [35] M. Kunze and J. Berger, “The similarity between N-terminal targeting signals for protein import into different organelles and its evolutionary relevance,” *Frontiers in physiology*, vol. 6, p. 259, 2015.
- [36] N. Aviram, T. Ast, E. A. Costa et al., “The SND proteins constitute an alternative targeting route to the endoplasmic reticulum,” *Nature*, vol. 540, no. 7631, pp. 134–138, 2016.
- [37] M. R. Pool, “Targeting of Proteins for Translocation at the Endoplasmic Reticulum,” *International Journal of Molecular Sciences*, vol. 23, no. 7, 2022.
- [38] S. Haßdenteufel, M. Sicking, S. Schorr et al., “hSnd2 protein represents an alternative targeting factor to the endoplasmic reticulum in human cells,” *FEBS Letters*, vol. 591, no. 20, pp. 3211–3224, 2017.
- [39] A. Tripathi, E. C. Mandon, R. Gilmore et al., “Two alternative binding mechanisms connect the protein translocation Sec71-Sec72 complex with heat shock proteins,” *The Journal of biological chemistry*, vol. 292, no. 19, pp. 8007–8018, 2017.
- [40] M. Schuldiner, J. Metz, V. Schmid et al., “The GET complex mediates insertion of tail-anchored proteins into the ER membrane,” *Cell*, vol. 134, no. 4, pp. 634–645, 2008.
- [41] J. W. Chartron, C. J. M. Suloway, M. Zaslaver et al., “Structural characterization of the Get4/Get5 complex and its interaction with Get3,” *Proceedings of the National Academy of Sciences*, vol. 107, no. 27, pp. 12127–12132, 2010.
- [42] F. Wang, E. C. Brown, G. Mak et al., “A chaperone cascade sorts proteins for posttranslational membrane insertion into the endoplasmic reticulum,” *Molecular cell*, vol. 40, no. 1, pp. 159–171, 2010.
- [43] T. Pleiner, M. Hazu, G. Pinton Tomaleri et al., “A selectivity filter in the ER membrane protein complex limits protein misinsertion at the ER,” *Journal of Cell Biology*, vol. 222, no. 8, 2023.
- [44] A. Guna, N. Volkmar, J. C. Christianson et al., “The ER membrane protein complex is a transmembrane domain insertase,” *Science*, vol. 359, no. 6374, pp. 470–473, 2018.
- [45] P. J. Chitwood, S. Juskiewicz, A. Guna et al., “EMC Is Required to Initiate Accurate Membrane Protein Topogenesis,” *Cell*, vol. 175, no. 6, 1507-1519.e16, 2018.
- [46] B. Kizmaz and J. M. Herrmann, “Membrane insertases at a glance,” *Journal of Cell Science*, vol. 136, no. 13, 2023.
- [47] K. G. Hansen and J. M. Herrmann, “Transport of Proteins into Mitochondria,” *The Protein Journal*, vol. 38, no. 3, pp. 330–342, 2019.

- [48] C. C. Williams, C. H. Jan, and J. S. Weissman, “Targeting and plasticity of mitochondrial proteins revealed by proximity-specific ribosome profiling,” *Science*, vol. 346, no. 6210, pp. 748–751, 2014.
- [49] A. P. Gerber, D. Herschlag, and P. O. Brown, “Extensive association of functionally and cytologically related mRNAs with Puf family RNA-binding proteins in yeast,” *PLoS biology*, vol. 2, no. 3, E79, 2004.
- [50] Y. Saint-Georges, M. Garcia, T. Delaveau et al., “Yeast mitochondrial biogenesis: a role for the PUF RNA-binding protein Puf3p in mRNA localization,” *PloS one*, vol. 3, no. 6, e2293, 2008.
- [51] C. Lesnik, Y. Cohen, A. Atir-Lande et al., “OM14 is a mitochondrial receptor for cytosolic ribosomes that supports co-translational import into mitochondria,” *Nature Communications*, vol. 5, no. 1, p. 5711, 2014.
- [52] R. George, P. Walsh, T. Beddoe et al., “The nascent polypeptide-associated complex (NAC) promotes interaction of ribosomes with the mitochondrial surface in vivo,” *FEBS Letters*, vol. 516, 1-3, pp. 213–216, 2002.
- [53] V. Zara, A. Ferramosca, P. Robitaille-Foucher et al., “Mitochondrial carrier protein biogenesis: role of the chaperones Hsc70 and Hsp90,” *Biochemical Journal*, vol. 419, no. 2, pp. 369–375, 2009.
- [54] H. Murakami, D. Pain, and G. Blobel, “70-kD heat shock-related protein is one of at least two distinct cytosolic factors stimulating protein import into mitochondria,” *Journal of Cell Biology*, vol. 107, 6 Pt 1, pp. 2051–2057, 1988.
- [55] J. C. Young, N. J. Hoogenraad, and F. U. Hartl, “Molecular chaperones Hsp90 and Hsp70 deliver preproteins to the mitochondrial import receptor Tom70,” *Cell*, vol. 112, no. 1, pp. 41–50, 2003.
- [56] V. P. Shakya, W. A. Barbeau, T. Xiao et al., “A nuclear-based quality control pathway for non-imported mitochondrial proteins,” *eLife*, vol. 10, 2021.
- [57] F. Willmund, M. del Alamo, S. Pechmann et al., “The cotranslational function of ribosome-associated Hsp70 in eukaryotic protein homeostasis,” *Cell*, vol. 152, 1-2, pp. 196–209, 2013.
- [58] C. H. Jan, C. C. Williams, and J. S. Weissman, “Principles of ER cotranslational translocation revealed by proximity-specific ribosome profiling,” *Science*, vol. 346, no. 6210, p. 1257521, 2014.

- [59] D. G. Vitali, M. Sinzel, E. P. Bulthuis et al., “The GET pathway can increase the risk of mitochondrial outer membrane proteins to be mistargeted to the ER,” *Journal of Cell Science*, vol. 131, no. 10, 2018.
- [60] T. Xiao, V. P. Shakya, and A. L. Hughes, “ER targeting of non-imported mitochondrial carrier proteins is dependent on the GET pathway,” *Life Science Alliance*, vol. 4, no. 3, e202000918, 2021.
- [61] K. Döring, N. Ahmed, T. Riemer et al., “Profiling Ssb-Nascent Chain Interactions Reveals Principles of Hsp70-Assisted Folding,” *Cell*, vol. 170, no. 2, 298–311.e20, 2017.
- [62] A. J. Caplan and M. G. Douglas, “Characterization of YDJ1: a yeast homologue of the bacterial dnaJ protein,” *Journal of Cell Biology*, vol. 114, no. 4, pp. 609–621, 1991.
- [63] C. Sahi, J. Kominek, T. Ziegelhoffer et al., “Sequential duplications of an ancient member of the DnaJ-family expanded the functional chaperone network in the eukaryotic cytosol,” *Molecular biology and evolution*, vol. 30, no. 5, pp. 985–998, 2013.
- [64] J. Becker, W. Walter, W. Yan et al., “Functional interaction of cytosolic hsp70 and a DnaJ-related protein, Ydj1p, in protein translocation in vivo,” *Molecular and Cellular Biology*, vol. 16, no. 8, pp. 4378–4386, 1996.
- [65] A. J. Caplan, D. M. Cyr, and M. G. Douglas, “YDJ1p facilitates polypeptide translocation across different intracellular membranes by a conserved mechanism,” *Cell*, vol. 71, no. 7, pp. 1143–1155, 1992.
- [66] H. Hoseini, S. Pandey, T. Jores et al., “The cytosolic cochaperone Sti1 is relevant for mitochondrial biogenesis and morphology,” *The FEBS journal*, vol. 283, no. 18, pp. 3338–3352, 2016.
- [67] T. Jores, J. Lawatscheck, V. Beke et al., “Cytosolic Hsp70 and Hsp40 chaperones enable the biogenesis of mitochondrial β -barrel proteins,” *Journal of Cell Biology*, vol. 217, no. 9, pp. 3091–3108, 2018.
- [68] F.-N. Vögtle, S. Wortelkamp, R. P. Zahedi et al., “Global analysis of the mitochondrial N-proteome identifies a processing peptidase critical for protein stability,” *Cell*, vol. 139, no. 2, pp. 428–439, 2009.
- [69] S. G. Garg and S. B. Gould, “The Role of Charge in Protein Targeting Evolution,” *Trends in cell biology*, vol. 26, no. 12, pp. 894–905, 2016.
- [70] G. von Heijne, “Mitochondrial targeting sequences may form amphiphilic helices,” *The EMBO journal*, vol. 5, no. 6, pp. 1335–1342, 1986.
- [71] T. Shiota, K. Imai, J. Qiu et al., “Molecular architecture of the active mitochondrial protein gate,” *Science*, vol. 349, no. 6255, pp. 1544–1548, 2015.

- [72] D. Mokranjac, “How to get to the other side of the mitochondrial inner membrane - the protein import motor,” *Biological chemistry*, vol. 401, 6-7, pp. 723–736, 2020.
- [73] N. Wiedemann and N. Pfanner, “Mitochondrial Machineries for Protein Import and Assembly,” *Annual review of biochemistry*, vol. 86, pp. 685–714, 2017.
- [74] S. Im Sim, Y. Chen, D. L. Lynch et al., “Structural basis of mitochondrial protein import by the TIM23 complex,” *Nature*, 2023.
- [75] L. F. Fielden, J. D. Busch, S. G. Merkt et al., “Central role of Tim17 in mitochondrial presequence protein translocation,” *Nature*, pp. 1–8, 2023.
- [76] P. Horten, L. Colina-Tenorio, and H. Rampelt, “Biogenesis of Mitochondrial Metabolite Carriers,” *Biomolecules*, vol. 10, no. 7, 2020.
- [77] S. Backes, Y. S. Bykov, T. Flohr et al., “The chaperone-binding activity of the mitochondrial surface receptor Tom70 protects the cytosol against mitoprotein-induced stress,” *Cell reports*, vol. 35, no. 1, p. 108936, 2021.
- [78] C. M. Koehler, E. Jarosch, K. Tokatlidis et al., “Import of mitochondrial carriers mediated by essential proteins of the intermembrane space,” *Science (New York, N.Y.)*, vol. 279, no. 5349, pp. 369–373, 1998.
- [79] C. Sirrenberg, M. F. Bauer, B. Guiard et al., “Import of carrier proteins into the mitochondrial inner membrane mediated by Tim22,” *Nature*, vol. 384, no. 6609, pp. 582–585, 1996.
- [80] N. Mesecke, N. Terziyska, C. Kozany et al., “A disulfide relay system in the intermembrane space of mitochondria that mediates protein import,” *Cell*, vol. 121, no. 7, pp. 1059–1069, 2005.
- [81] R. Edwards, S. Gerlich, and K. Tokatlidis, “The biogenesis of mitochondrial intermembrane space proteins,” *Biological chemistry*, vol. 401, 6-7, pp. 737–747, 2020.
- [82] T. Jores, A. Klinger, L. E. Groß et al., “Characterization of the targeting signal in mitochondrial β -barrel proteins,” *Nature Communications*, vol. 7, no. 1, p. 12036, 2016.
- [83] H. Takeda, A. Tsutsumi, T. Nishizawa et al., “Mitochondrial sorting and assembly machinery operates by β -barrel switching,” *Nature*, vol. 590, no. 7844, pp. 163–169, 2021.
- [84] H. Takeda, J. V. Busto, C. Lindau et al., “A multipoint guidance mechanism for β -barrel folding on the SAM complex,” *Nature structural & molecular biology*, vol. 30, no. 2, pp. 176–187, 2023.
- [85] K. A. Diederichs, X. Ni, S. E. Rollauer et al., “Structural insight into mitochondrial β -barrel outer membrane protein biogenesis,” *Nature Communications*, vol. 11, no. 1, p. 3290, 2020.

- [86] L. Drwesh and D. Rapaport, “Biogenesis pathways of α -helical mitochondrial outer membrane proteins,” *Biological chemistry*, vol. 401, 6-7, pp. 677–686, 2020.
- [87] L. Drwesh, B. Heim, M. Graf et al., “A network of cytosolic (co)chaperones promotes the biogenesis of mitochondrial signal-anchored outer membrane proteins,” *eLife*, vol. 11, 2022.
- [88] T. Becker, L.-S. Wenz, V. Krüger et al., “The mitochondrial import protein Mim1 promotes biogenesis of multispinning outer membrane proteins,” *Journal of Cell Biology*, vol. 194, no. 3, pp. 387–395, 2011.
- [89] K. N. Doan, A. Grevel, C. U. Mårtensson et al., “The Mitochondrial Import Complex MIM Functions as Main Translocase for α -Helical Outer Membrane Proteins,” *Cell reports*, vol. 31, no. 4, p. 107567, 2020.
- [90] O. Neuber, E. Jarosch, C. Volkwein et al., “Ubx2 links the Cdc48 complex to ER-associated protein degradation,” *Nature cell biology*, vol. 7, no. 10, pp. 993–998, 2005.
- [91] N. O. Bodnar, K. H. Kim, Z. Ji et al., “Structure of the Cdc48 ATPase with its ubiquitin-binding cofactor Ufd1-Npl4,” *Nature Structural & Molecular Biology*, vol. 25, no. 7, pp. 616–622, 2018.
- [92] C. U. Mårtensson, C. Priesnitz, J. Song et al., “Mitochondrial protein translocation-associated degradation,” *Nature*, vol. 569, no. 7758, pp. 679–683, 2019.
- [93] H. Weidberg and A. Amon, “MitoCPR-A surveillance pathway that protects mitochondria in response to protein import stress,” *Science (New York, N.Y.)*, vol. 360, no. 6385, 2018.
- [94] V. Okreglak and P. Walter, “The conserved AAA-ATPase Msp1 confers organelle specificity to tail-anchored proteins,” *Proceedings of the National Academy of Sciences*, vol. 111, no. 22, pp. 8019–8024, 2014.
- [95] Y.-C. Chen, G. K. E. Umanah, N. Dephoure et al., “Msp1/ATAD1 maintains mitochondrial function by facilitating the degradation of mislocalized tail-anchored proteins,” *The EMBO journal*, vol. 33, no. 14, pp. 1548–1564, 2014.
- [96] S. Matsumoto, K. Nakatsukasa, C. Kakuta et al., “Msp1 Clears Mistargeted Proteins by Facilitating Their Transfer from Mitochondria to the ER,” *Molecular cell*, vol. 76, no. 1, 191-205.e10, 2019.
- [97] M. J. McKenna, S. Im Sim, A. Ordureau et al., “The endoplasmic reticulum P5A-ATPase is a transmembrane helix dislocase,” *Science*, vol. 369, no. 6511, 2020.
- [98] Q. Qin, T. Zhao, W. Zou et al., “An Endoplasmic Reticulum ATPase Safeguards Endoplasmic Reticulum Identity by Removing Ectopically Localized Mitochondrial Proteins,” *Cell reports*, vol. 33, no. 6, p. 108363, 2020.

- [99] Y. S. Bykov, D. Rapaport, J. M. Herrmann et al., “Cytosolic Events in the Biogenesis of Mitochondrial Proteins,” *Trends in Biochemical Sciences*, vol. 45, no. 8, pp. 650–667, 2020.
- [100] T. Becker, J. Song, and N. Pfanner, “Versatility of Preprotein Transfer from the Cytosol to Mitochondria,” *Trends in cell biology*, vol. 29, no. 7, pp. 534–548, 2019.
- [101] C. Meisinger, S. Pfannschmidt, M. Rissler et al., “The morphology proteins Mdm12/Mmm1 function in the major beta-barrel assembly pathway of mitochondria,” *The EMBO journal*, vol. 26, no. 9, pp. 2229–2239, 2007.
- [102] J. Laborenz, K. Hansen, C. Prescianotto-Baschong et al., “In vitro import experiments with semi-intact cells suggest a role of the Sec61 paralog Ssh1 in mitochondrial biogenesis,” *Biological chemistry*, vol. 400, no. 9, pp. 1229–1240, 2019.
- [103] S. M. Burgess, M. Delannoy, and R. E. Jensen, “MMM1 encodes a mitochondrial outer membrane protein essential for establishing and maintaining the structure of yeast mitochondria,” *The Journal of cell biology*, vol. 126, no. 6, pp. 1375–1391, 1994.
- [104] K. H. Berger, L. F. Sogo, and M. P. Yaffe, “Mdm12p, a component required for mitochondrial inheritance that is conserved between budding and fission yeast,” *The Journal of cell biology*, vol. 136, no. 3, pp. 545–553, 1997.
- [105] M. J. Youngman, A. E. A. Hobbs, S. M. Burgess et al., “Mmm2p, a mitochondrial outer membrane protein required for yeast mitochondrial shape and maintenance of mtDNA nucleoids,” *The Journal of cell biology*, vol. 164, no. 5, pp. 677–688, 2004.
- [106] A. B. Lang, A. T. John Peter, P. Walter et al., “ER-mitochondrial junctions can be bypassed by dominant mutations in the endosomal protein Vps13,” *The Journal of cell biology*, vol. 210, no. 6, pp. 883–890, 2015.
- [107] J. D. Smith, S. Suresh, U. Schlecht et al., “Quantitative CRISPR interference screens in yeast identify chemical-genetic interactions and new rules for guide RNA design,” *Genome biology*, vol. 17, p. 45, 2016.
- [108] J. P. Murphy, E. Stepanova, R. A. Everley et al., “Comprehensive Temporal Protein Dynamics during the Diauxic Shift in *Saccharomyces cerevisiae*,” *Molecular & cellular proteomics : MCP*, vol. 14, no. 9, pp. 2454–2465, 2015.
- [109] F. Di Bartolomeo, C. Malina, K. Campbell et al., “Absolute yeast mitochondrial proteome quantification reveals trade-off between biosynthesis and energy generation during diauxic shift,” *Proceedings of the National Academy of Sciences*, vol. 117, no. 13, pp. 7524–7535, 2020.

- [110] B. M. DUGGAR, “Aureomycin; a product of the continuing search for new antibiotics,” *Annals of the New York Academy of Sciences*, vol. 51, Art. 2, pp. 177–181, 1948.
- [111] A. C. FINLAY and G. L. HOBBY, “Terramycin, a new antibiotic,” *Science (New York, N.Y.)*, vol. 111, no. 2874, p. 85, 1950.
- [112] G. D. Clark-Walker and A. W. Linnane, “In vivo differentiation of yeast cytoplasmic and mitochondrial protein synthesis with antibiotics,” *Biochemical and biophysical research communications*, vol. 25, no. 1, pp. 8–13, 1966.
- [113] N. Moullan, L. Mouchiroud, X. Wang et al., “Tetracyclines Disturb Mitochondrial Function across Eukaryotic Models: A Call for Caution in Biomedical Research,” *Cell reports*, vol. 10, no. 10, pp. 1681–1691, 2015.
- [114] K. S. Dimmer, S. Fritz, F. Fuchs et al., “Genetic basis of mitochondrial function and morphology in *Saccharomyces cerevisiae*,” *Molecular biology of the cell*, vol. 13, no. 3, pp. 847–853, 2002.
- [115] L. F. Sogo and M. P. Yaffe, “Regulation of mitochondrial morphology and inheritance by Mdm10p, a protein of the mitochondrial outer membrane,” *The Journal of cell biology*, vol. 126, no. 6, pp. 1361–1373, 1994.
- [116] M. Costanzo, B. VanderSluis, E. N. Koch et al., “A global genetic interaction network maps a wiring diagram of cellular function,” *Science (New York, N.Y.)*, vol. 353, no. 6306, 2016.
- [117] E. Wiederhold, L. M. Veenhoff, B. Poolman et al., “Proteomics of *Saccharomyces cerevisiae* Organelles,” *Molecular & cellular proteomics : MCP*, vol. 9, no. 3, pp. 431–445, 2010.
- [118] A. Sickmann, J. Reinders, Y. Wagner et al., “The proteome of *Saccharomyces cerevisiae* mitochondria,” *Proceedings of the National Academy of Sciences of the United States of America*, vol. 100, no. 23, pp. 13207–13212, 2003.
- [119] F. Boos, L. Krämer, C. Groh et al., “Mitochondrial protein-induced stress triggers a global adaptive transcriptional programme,” *Nature cell biology*, vol. 21, no. 4, pp. 442–451, 2019.
- [120] L. Wrobel, U. Topf, P. Bragoszewski et al., “Mistargeted mitochondrial proteins activate a proteostatic response in the cytosol,” *Nature*, vol. 524, no. 7566, pp. 485–488, 2015.
- [121] K. Knöringer, C. Groh, L. Krämer et al., “The unfolded protein response of the endoplasmic reticulum supports mitochondrial biogenesis by buffering nonimported proteins,” *Molecular biology of the cell*, vol. 34, no. 10, ar95, 2023.

- [122] J. Reinhard, L. Starke, C. Klose et al., *A new technology for isolating organellar membranes provides fingerprints of lipid bilayer stress*, 2022.
- [123] L. Krämer, N. Dalheimer, M. Räschele et al., “MitoStores: Chaperone-controlled protein granules store mitochondrial precursors in the cytosol,”
- [124] P. Bragoszewski, A. Gornicka, M. E. Sztolsztener et al., “The ubiquitin-proteasome system regulates mitochondrial intermembrane space proteins,” *Molecular and Cellular Biology*, vol. 33, no. 11, pp. 2136–2148, 2013.
- [125] U. Schulte, F. den Brave, A. Haupt et al., “Mitochondrial complexome reveals quality-control pathways of protein import,” *Nature*, vol. 614, no. 7946, pp. 153–159, 2023.
- [126] F.-N. Vögtle, J. M. Burkhart, H. Gonczarowska-Jorge et al., “Landscape of submitochondrial protein distribution,” *Nature Communications*, vol. 8, no. 1, p. 290, 2017.
- [127] F. Wang, A. Whynot, M. Tung et al., “The mechanism of tail-anchored protein insertion into the ER membrane,” *Molecular cell*, vol. 43, no. 5, pp. 738–750, 2011.
- [128] P. Leznicki and S. High, “SGTA antagonizes BAG6-mediated protein triage,” *Proceedings of the National Academy of Sciences*, vol. 109, no. 47, pp. 19214–19219, 2012.
- [129] J. Kyte and R. F. Doolittle, “A simple method for displaying the hydropathic character of a protein,” *Journal of molecular biology*, vol. 157, no. 1, pp. 105–132, 1982.
- [130] S. Meier, W. Neupert, and J. M. Herrmann, “Proline residues of transmembrane domains determine the sorting of inner membrane proteins in mitochondria,” *The Journal of cell biology*, vol. 170, no. 6, pp. 881–888, 2005.
- [131] D. Poveda-Huertes, S. Matic, A. Marada et al., “An Early mtUPR: Redistribution of the Nuclear Transcription Factor Rox1 to Mitochondria Protects against Intramitochondrial Proteotoxic Aggregates,” *Molecular cell*, vol. 77, no. 1, 180-188.e9, 2020.
- [132] L. Ting, R. Rad, S. P. Gygi et al., “MS3 eliminates ratio distortion in isobaric multiplexed quantitative proteomics,” *Nature methods*, vol. 8, no. 11, pp. 937–940, 2011.
- [133] K. Nishimura, T. Fukagawa, H. Takisawa et al., “An auxin-based degron system for the rapid depletion of proteins in nonplant cells,” *Nature Methods*, vol. 6, no. 12, pp. 917–922, 2009.
- [134] S. Ben-Aroya, X. Pan, J. D. Boeke et al., “Making temperature-sensitive mutants,” *Methods in enzymology*, vol. 470, pp. 181–204, 2010.

- [135] D. K. Breslow, D. M. Cameron, S. R. Collins et al., “A comprehensive strategy enabling high-resolution functional analysis of the yeast genome,” *Nature Methods*, vol. 5, no. 8, pp. 711–718, 2008.
- [136] K. O. Kopec, V. Alva, and A. N. Lupas, “Homology of SMP domains to the TULIP superfamily of lipid-binding proteins provides a structural basis for lipid exchange between ER and mitochondria,” *Bioinformatics (Oxford, England)*, vol. 26, no. 16, pp. 1927–1931, 2010.
- [137] A. P. AhYoung, J. Jiang, J. Zhang et al., “Conserved SMP domains of the ERMES complex bind phospholipids and mediate tether assembly,” *Proceedings of the National Academy of Sciences*, vol. 112, no. 25, E3179-88, 2015.
- [138] X. Wu, M. Siggel, S. Ovchinnikov et al., “Structural basis of ER-associated protein degradation mediated by the Hrd1 ubiquitin ligase complex,” *Science*, vol. 368, no. 6489, 2020.
- [139] C. Sahi and E. A. Craig, “Network of general and specialty J protein chaperones of the yeast cytosol,” *Proceedings of the National Academy of Sciences of the United States of America*, vol. 104, no. 17, pp. 7163–7168, 2007.
- [140] A. J. Caplan, J. Tsai, P. J. Casey et al., “Farnesylation of YDJ1p is required for function at elevated growth temperatures in *Saccharomyces cerevisiae*,” *Journal of Biological Chemistry*, vol. 267, no. 26, pp. 18890–18895, 1992.
- [141] H. Yamamoto, K. Fukui, H. Takahashi et al., “Roles of Tom70 in import of presequence-containing mitochondrial proteins,” *The Journal of biological chemistry*, vol. 284, no. 46, pp. 31635–31646, 2009.
- [142] J. Carroll, M. C. Altman, I. M. Fearnley et al., “Identification of membrane proteins by tandem mass spectrometry of protein ions,” *Proceedings of the National Academy of Sciences of the United States of America*, vol. 104, no. 36, pp. 14330–14335, 2007.
- [143] T. T. Nguyen, A. Lewandowska, J.-Y. Choi et al., “Gem1 and ERMES do not directly affect phosphatidylserine transport from ER to mitochondria or mitochondrial inheritance,” *Traffic (Copenhagen, Denmark)*, vol. 13, no. 6, pp. 880–890, 2012.
- [144] C. Voss, S. Lahiri, B. P. Young et al., “ER-shaping proteins facilitate lipid exchange between the ER and mitochondria in *S. cerevisiae*,” *Journal of Cell Science*, vol. 125, Pt 20, pp. 4791–4799, 2012.
- [145] T. Becker, S. E. Horvath, L. Böttinger et al., “Role of phosphatidylethanolamine in the biogenesis of mitochondrial outer membrane proteins,” *The Journal of biological chemistry*, vol. 288, no. 23, pp. 16451–16459, 2013.

- [146] M.-H. Schuler, F. Di Bartolomeo, L. Böttinger et al., “Phosphatidylcholine affects the role of the sorting and assembly machinery in the biogenesis of mitochondrial β -barrel proteins,” *The Journal of biological chemistry*, vol. 290, no. 44, pp. 26523–26532, 2015.
- [147] Y. Tamura, T. Endo, M. Iijima et al., “Ups1p and Ups2p antagonistically regulate cardiolipin metabolism in mitochondria,” *Journal of Cell Biology*, vol. 185, no. 6, pp. 1029–1045, 2009.
- [148] K. Malhotra, A. Modak, S. Nangia et al., “Cardiolipin mediates membrane and channel interactions of the mitochondrial TIM23 protein import complex receptor Tim50,” *Science advances*, vol. 3, no. 9, e1700532, 2017.
- [149] A. T. John Peter, C. Petrunger, M. Peter et al., “METALIC reveals interorganelle lipid flux in live cells by enzymatic mass tagging,” *Nature cell biology*, vol. 24, no. 6, pp. 996–1004, 2022.
- [150] C. Koch, M. Schuldiner, and J. M. Herrmann, “ER-SURF: Riding the Endoplasmic Reticulum Surface to Mitochondria,” *International Journal of Molecular Sciences*, vol. 22, no. 17, p. 9655, 2021.
- [151] Y. Liu, X. Wang, L. P. Coyne et al., “Mitochondrial carrier protein overloading and misfolding induce aggresomes and proteostatic adaptations in the cytosol,” *Molecular biology of the cell*, vol. 30, no. 11, pp. 1272–1284, 2019.
- [152] J. R. Friedman, M. Kannan, A. Toulmay et al., “Lipid Homeostasis Is Maintained by Dual Targeting of the Mitochondrial PE Biosynthesis Enzyme to the ER,” *Developmental cell*, vol. 44, no. 2, 261-270.e6, 2018.
- [153] M. O. Gok, N. O. Speer, W. M. Henne et al., “ER-localized phosphatidylethanolamine synthase plays a conserved role in lipid droplet formation,” *Molecular biology of the cell*, vol. 33, no. 1, ar11, 2022.
- [154] Y. Hirabayashi, S.-K. Kwon, H. Paek et al., “ER-mitochondria tethering by PDZD8 regulates Ca²⁺ dynamics in mammalian neurons,” *Science*, vol. 358, no. 6363, pp. 623–630, 2017.
- [155] J. G. Wideman, D. L. Balacco, T. Fieblinger et al., “PDZD8 is not the 'functional ortholog' of Mmm1, it is a paralog,” *F1000Research*, vol. 7, p. 1088, 2018.
- [156] A. H. Al-Amri, P. Armstrong, M. Amici et al., “PDZD8 Disruption Causes Cognitive Impairment in Humans, Mice, and Fruit Flies,” *Biological psychiatry*, vol. 92, no. 4, pp. 323–334, 2022.

- [157] Y. Gao, J. Xiong, Q.-Z. Chu et al., “PDZD8-mediated lipid transfer at contacts between the ER and late endosomes/lysosomes is required for neurite outgrowth,” *Journal of Cell Science*, vol. 135, no. 5, 2022.
- [158] Y. Kurihara, K. Mitsunari, N. Mukae et al., “PDZD8-deficient mice manifest behavioral abnormalities related to emotion, cognition, and adaptation due to dyslipidemia in the brain,” *Molecular brain*, vol. 16, no. 1, p. 11, 2023.
- [159] L. Lalier, V. Mignard, M.-P. Joalland et al., “TOM20-mediated transfer of Bcl2 from ER to MAM and mitochondria upon induction of apoptosis,” *Cell Death & Disease*, vol. 12, no. 2, p. 182, 2021.
- [160] S. Kawano, Y. Tamura, R. Kojima et al., “Structure-function insights into direct lipid transfer between membranes by Mmm1-Mdm12 of ERMES,” *Journal of Cell Biology*, vol. 217, no. 3, pp. 959–974, 2018.
- [161] A. G. Tebo and A. Gautier, “A split fluorescent reporter with rapid and reversible complementation,” *Nature Communications*, vol. 10, no. 1, p. 2822, 2019.
- [162] N. Cohen, N. Aviram, and M. Schuldiner, “A systematic proximity ligation approach to studying protein-substrate specificity identifies the substrate spectrum of the Ssh1 translocon,” *The EMBO journal*, vol. 42, no. 11, e113385, 2023.
- [163] B. Singer-Krüger, T. Fröhlich, M. Franz-Wachtel et al., “APEX2-mediated proximity labeling resolves protein networks in *Saccharomyces cerevisiae* cells,” *The FEBS journal*, vol. 287, no. 2, pp. 325–344, 2020.
- [164] T. C. Branon, J. A. Bosch, A. D. Sanchez et al., “Efficient proximity labeling in living cells and organisms with TurboID,” *Nature biotechnology*, vol. 36, no. 9, pp. 880–887, 2018.
- [165] M. J. Casadaban and S. N. Cohen, “Analysis of gene control signals by DNA fusion and cloning in *Escherichia coli*,” *Journal of molecular biology*, vol. 138, no. 2, pp. 179–207, 1980.
- [166] M. Meselson and R. Yuan, “DNA restriction enzyme from *E. coli*,” *Nature*, vol. 217, no. 5134, pp. 1110–1114, 1968.
- [167] R. S. Sikorski and P. Hieter, “A system of shuttle vectors and yeast host strains designed for efficient manipulation of DNA in *Saccharomyces cerevisiae*,” *Genetics*, vol. 122, no. 1, pp. 19–27, 1989.
- [168] D. Mumberg, R. Müller, and M. Funk, “Yeast vectors for the controlled expression of heterologous proteins in different genetic backgrounds,” *Gene*, vol. 156, no. 1, pp. 119–122, 1995.

- [169] S. Lenhard, S. Gerlich, A. Khan et al., “The Orf9b protein of SARS-CoV-2 modulates mitochondrial protein biogenesis,” *Journal of Cell Biology*, vol. 222, no. 10, 2023.
- [170] C. Janke, M. M. Magiera, N. Rathfelder et al., “A versatile toolbox for PCR-based tagging of yeast genes: new fluorescent proteins, more markers and promoter substitution cassettes,” *Yeast (Chichester, England)*, vol. 21, no. 11, pp. 947–962, 2004.
- [171] K. J. Livak and T. D. Schmittgen, “Analysis of relative gene expression data using real-time quantitative PCR and the 2(-Delta Delta C(T)) Method,” *Methods (San Diego, Calif.)*, vol. 25, no. 4, pp. 402–408, 2001.
- [172] M.-A. Teste, M. Duquenne, J. M. François et al., “Validation of reference genes for quantitative expression analysis by real-time RT-PCR in *Saccharomyces cerevisiae*,” *BMC molecular biology*, vol. 10, p. 99, 2009.
- [173] C. Prescianotto-Baschong and H. Riezman, “Ordering of compartments in the yeast endocytic pathway,” *Traffic*, vol. 3, no. 1, pp. 37–49, 2002.
- [174] J. Kyhse-Andersen, “Electroblotting of multiple gels: a simple apparatus without buffer tank for rapid transfer of proteins from polyacrylamide to nitrocellulose,” *Journal of Biochemical and Biophysical Methods*, vol. 10, 3-4, pp. 203–209, 1984.
- [175] J. Rappsilber, M. Mann, and Y. Ishihama, “Protocol for micro-purification, enrichment, pre-fractionation and storage of peptides for proteomics using StageTips,” *Nature protocols*, vol. 2, no. 8, pp. 1896–1906, 2007.
- [176] M. M. Bradford, “A rapid and sensitive method for the quantitation of microgram quantities of protein utilizing the principle of protein-dye binding,” *Analytical biochemistry*, vol. 72, pp. 248–254, 1976.
- [177] S. Sridharan, N. Kurzawa, T. Werner et al., “Proteome-wide solubility and thermal stability profiling reveals distinct regulatory roles for ATP,” *Nature communications*, vol. 10, no. 1, p. 1155, 2019.
- [178] J. Cox and M. Mann, “MaxQuant enables high peptide identification rates, individualized p.p.b.-range mass accuracies and proteome-wide protein quantification,” *Nature biotechnology*, vol. 26, no. 12, pp. 1367–1372, 2008.
- [179] J. Cox, N. Neuhauser, A. Michalski et al., “Andromeda: a peptide search engine integrated into the MaxQuant environment,” *Journal of proteome research*, vol. 10, no. 4, pp. 1794–1805, 2011.
- [180] S. Tyanova, T. Temu, and J. Cox, “The MaxQuant computational platform for mass spectrometry-based shotgun proteomics,” *Nature protocols*, vol. 11, no. 12, pp. 2301–2319, 2016.

- [181] M. E. Ritchie, B. Phipson, Di Wu et al., “limma powers differential expression analyses for RNA-sequencing and microarray studies,” *Nucleic acids research*, vol. 43, no. 7, e47, 2015.
- [182] W. Huber, A. von Heydebreck, H. Sültmann et al., “Variance stabilization applied to microarray data calibration and to the quantification of differential expression,” *Bioinformatics (Oxford, England)*, 18 Suppl 1, S96-104, 2002.
- [183] C. Klöppel, C. Michels, J. Zimmer et al., “In yeast redistribution of Sod1 to the mitochondrial intermembrane space provides protection against respiration derived oxidative stress,” *Biochemical and biophysical research communications*, vol. 403, no. 1, pp. 114–119, 2010.
- [184] S. Longen, M. W. Woellhaf, C. Petrunaro et al., “The disulfide relay of the intermembrane space oxidizes the ribosomal subunit mrp10 on its transit into the mitochondrial matrix,” *Developmental cell*, vol. 28, no. 1, pp. 30–42, 2014.

ABBREVIATIONS

°C	Grade Celsius
μg	Microgram
μl	Microliter
μM	Micromolar
AAA+	ATPases Associated with diverse cellular Activities
Amp	Ampicillin
ATc	Anhydrotetracycline
ATP	Adenosine triphosphate
CCCP	Carbonylcyanid-m-chlorophenylhydrazon
CIP	Calf intestine alkaline phosphatase
dCas9	Catalytically dead Cas9
DMSO	Dimethyl sulfoxide
DNA	Deoxyribonucleic acid
DTT	Dithiothreitol
<i>E. coli</i>	<i>Escherichia coli</i>
ECL	Enhanced chemiluminescence
EDTA	Ethylene diamine tetraacetate
ER	Endoplasmic reticulum
ERAD	ER-associated degradation
EtOH	Ethanol
g	Gravity of earth
GFP	Green fluorescent protein

GO	Gene Ontology
gRNA	guide ribonucleic acid
h	Hours
HA	Hemagglutinin
HEPES	4-(2-hydroxyethyl)-1-piperazine-ethane sulfonic acid
HF	High fidelity
HSE	Heat shock element
IM	Inner mitochondrial membrane
IMS	Intermembrane space
kDa	Kilodalton
LB	Lysogeny broth media
M	Molarity
MAD	Mitochondria-associated degradation
mg	Milligram
min	Minute
ml	Milliliter
mM	Millimolar
mtDNA	mitochondrial DNA
MTS	Matrix targeting signal
nm	Nanometer
OD ₆₀₀	Optical density at 600 nm
OM	Outer mitochondrial membrane
P	Pellet, aggregated fraction

PACE	Proteasome associated control element
PAGE	Polyacrylamide gel electrophoresis
PAM	Presequence translocase-associated motor
PCR	Polymerase chain reaction
PDRE	Pleiotropic drug response element
PEG	Polyethylene glycol
PK	Proteinase K
RNA	Ribonucleic acid
rpm	Revolutions per minute
RT	Room temperature
s	Seconds
S	Soluble fraction
SAM	Sorting and assembly machinery
<i>S. cerevisiae</i>	<i>Saccharomyces cerevisiae</i>
SDS	Sodium dodecyl sulfate
SS	Signal-sequence
T	Total
TA	Tail-anchored
TBS	Tris buffered saline
TCA	Trichloroacetic acid
TIM	Translocase of the inner membrane
TMD	Transmembrane domain
TMT	Tandem Mass Tag

TOM	Translocase of the outer membrane
Tris	Tris-(hydroxymethyl)-aminomethane
U	Units
UPR	Unfolded protein response
w/v	Weight per volume
WT	Wild type
YFP	Yellow fluorescent protein

ACKNOWLEDGMENTS

“I shall be telling this with a sigh Somewhere ages and ages hence: Two roads diverged in a wood, and I—I took the one less traveled by, And that has made all the difference.”

Robert Frost

Mein erster Dank gilt dir **Hannes**. Als ich mit meinem Projekt hier begonnen habe, hätten wir beide wohl nicht gedacht, was für eine interessante Story daraus werden würde. Aber du hast mir freie Hand gelassen Dinge auszuprobieren, mich wissenschaftlich auszutoben und hattest immer eine gute Idee parat, wenn ich mal nicht weiterwusste. Ich bin froh und gleichzeitig dankbar, dass du es mir ermöglicht hast, meine Doktorarbeit in diesem Labor zu machen!

Lieber **Jan**, vielen Dank, dass du das Zweitgutachten meiner Arbeit übernommen hast.

Lieber **Timo**, dir möchte ich als Vorsitzender meiner Promotionskommission danken.

Ein großer Dank gilt auch **Markus**. Du hattest einen großen Anteil daran, dass diese Arbeit so spannend geworden ist. Die AG Zellbio kann manchmal sehr fordernd sein, aber du warst immer interessiert an unseren Ideen, hast uns bei der Planung und Umsetzung unserer MS Experimente geholfen und so auch in meinem Projekt. Mit dir war die Zusammenarbeit einfach, einfach.

Liebe **Simone, Connie, Andrea, Sabine** und **Vera**, ihr seid die gute Seele der AG Zellbio und gleichzeitig auch der Kern, der den Laden am Laufen hält. Ihr habt eine Atmosphäre im Labor geschaffen, in der es einfach angenehm war zu arbeiten. Ob es das morgendliche „Guten Morgen Christian!“ von Connie war oder das fast täglich Pläuschchen das ich mit Simone gehalten habe - es hat mir immer den Tag versüßt. Auch Sabine, Vera und Andrea standen mir immer mit Rat und Tat zur Seite und waren auch hin und wieder für ein Kaffeekränzchen zu haben. Ich bin euch sehr dankbar für all das - keiner verkörpert die Zellbio Familie wie ihr!

Tamara & Lea ihr wart meine Weggefährten und mit euch hat es einfach Spaß gemacht! Vielen Dank für eure Unterstützung, euren Rat und eure Ideen. Ich konnte nicht nur mit wissenschaftlichen Fragen zu euch kommen, sondern mit euch konnte man immer Quatsch machen, lachen, oder prokrastinieren. **Tamara** deine positive und verrückte Art haben richtig Schwung ins Labor gebracht und ich bin froh, so einen Menschen als Freund gewonnen zu haben. Ich danke dir für all die Teepausen, all die Späße, die wir uns erlaubt haben, im und auch außerhalb des Labors. **Lea** mit dir habe ich vor vielen Jahren mein Studium begonnen und zusammen haben wir im Studium alles erlebt. Nun gehen wir beide auf die Ziellinie zu,

vielleicht nicht so wie wir uns das einst vorgestellt hatten, aber doch gemeinsam! Ich habe dir viel zu verdanken - mehr als ich hier in ein paar Worten schreiben könnte, deshalb einfach nur Danke!

Lena es gibt so viel, wofür ich dir gerne danken würde, aber ich will mich kurzhalten. Zunächst mal danke fürs Korrekturlesen. Ich habe unsere gemeinsamen Eskapaden im Labor, unsere Scrubs/Brooklyn 99 Abende und all die Zeit, die ich mit dir verbringen durfte, genossen. Aber viel mehr noch möchte ich dir für all deine Unterstützung in Guten als auch in schwierigen Zeiten danken 😊!

Janina dich kennen die meisten Leute im Labor nur noch als meine „Labor Mutti“. Du hattest einen großen Anteil daran, dass ich zu dem Wissenschaftler geworden bin, der ich jetzt bin. Auch wenn ich manchmal das Gefühl hatte, dass ich dich mit der nächsten „Quick Question“ auf die Palme bringe, hast du dir immer Zeit für mich genommen. Und nicht nur in Sachen Wissenschaft konnte ich auf dich zählen, sondern bei allem, was mir auf dem Herzen lag. Du warst und bist für mich ein Vorbild, Danke!

Carina du warst mein Ansprechpartner in Sachen R, auch wenn es die banalsten Sachen waren hattest du immer ein offenes Ohr. Aber viel schöner fand ich es, jemanden im Labor zu wissen mit dem ich im Dialekt schwätzen konnte, auch wenn du dabei Saarländisch gesprochen hast und ich Pfälzisch, was die meisten im Labor sehr amüsant fanden.

Katharina du warst lange Zeit meine stille Weggefährtin im Labor 451 und ich fand es super. Ich habe zwar mit vielen Leuten Teepausen gemacht, aber wir waren die Begründer dieser Tradition. Ob es im Labor war oder an einem lauen Sommerabend am Vogelwoog - du warst immer für einen Spaß zu haben!

A big thanks goes to **Azkiya** and **Nikita**. I really enjoyed our discussion about our different cultures, about good food and sometimes even very philosophical topics. In particular I was amazed about the Urdu and Hindi language and how these two have indistinguishably sounding letters that are apparently different 😂.

Anna-Lena & Svenja auch euch möchte ich danken. Auch wenn ich nie wirklich eurer Betreuer war, habe ich mich doch immer etwas verantwortlich für euch gefühlt. **Anna-Lena** deine offene und empathische Art sind eine Bereicherung für das Labor und ich glaube die AG Zellbio wird sich daran auch in Zukunft noch erfreuen. **Svenja** du warst auch eins meiner „Teepausenopfer“, die herhalten musste, wenn ich mal nix schaffen wollte. Auch hast du, ob

du wolltest oder nicht, viele Teile dieser Arbeit Korrekturgelesen. Es hat Spaß gemacht, euch beide zu “betreuen”.

I also want to thank my former Master students **Caro, Ahmed** and **Pavel**. I enjoyed supervising all of you although each of you posed a different “challenge” for me. I learned a lot from all of you and hope that you did also learn from me. Be reassured that if you ever need help you can count on me.

Auch möchte ich **Büsra, Saskia, Katja, Anna, Sandra, Steffen** und allen weiteren Mitgliedern der Zellbio Familie danken. Es hat immer Spaß gemacht, sich mit euch auszutauschen, jeder hat einem geholfen und es war einfach eine tolle Atmosphäre im Labor.

Ein großer Dank gilt auch meiner **Familie**. Ihr habt mich stets unterstützt und stets bestärkt in dem, was ich tue. Ich weiß, dass ihr hart gearbeitet und viele Opfer gebracht habt, um mir dieses Privileg zu ermöglichen und dafür bin ich zutiefst dankbar!

Annika dein Optimismus und deine positive Art waren mir ein immenser Rückhalt in einer turbulenten Zeit. Ich bin endlich am Ziel und du hattest einen nicht unwichtigen Beitrag daran. Danke für alles!

CURRICULUM VITAE

Christian Koch

Place of birth Neustadt/Weinstraße, Germany

Education

- Since 11/2019 **PhD Studies**, University of Kaiserslautern
Cell Biology
Supervisor: Prof. Dr. Johannes Herrmann
“The ER-SURF pathway uses ER-mitochondria contact sites for protein targeting to mitochondria”
- 10/2017 – 09/2019 **Master of Science**, University of Kaiserslautern
Molecular Cell Biology
Cell Biology
Supervisor: Prof. Dr. Johannes Herrmann
“The relevance of the ER mitochondria encounter structure for the biogenesis of mitochondrial proteins”
- 10/2014 – 08/2017 **Bachelor of Science**, University of Kaiserslautern
Biowissenschaften
Cell Biology
Supervisor: Prof. Dr. Johannes Herrmann
“Die zytosolische Acetyltransferase NatA beeinflusst die Funktion der Mitochondrien”
- 08/2006 – 08/2014 **Allgemeine Hochschulreife**,
Käthe-Kollwitz-Gymnasium, Neustadt/Weinstraße
Secondary school diploma qualifying for university admission

Other scientific training

2019 – present

Supervision, University of Kaiserslautern

Cell Biology

Supervision of practical courses, bachelor and master student.

02/2019

Scientific Assistant, University of Kaiserslautern

Molecular Genetics